THERMAL ASPERITY ESTIMATION AND CANCELLATION FOR PERPENDICULAR MAGNETIC RECORDING SYSTEMS

YUPIN SUPPAKHUN

A THESIS SUBMITTED IN PARTIAL FULFILLMENT

OF THE REQUIREMENT FOR THE DEGREE OF

DOCTOR OF ENGINEERING IN ELECTRICAL ENGINEERING

FACULTY OF ENGINEERING

KING MONGKUT'S INSTITUTE OF TECHNOLOGY LADKRABANG

2011

KMITL-2011-EN-D-018-161

THERMAL ASPERITY ESTIMATION AND CANCELLATION FOR PERPENDICULAR MAGNETIC RECORDING SYSTEMS

YUPIN SUPPAKHUN

A THESIS SUBMITTED IN PARTIAL FULFILLMENT

OF THE REQUIREMENT FOR THE DEGREE OF

DOCTOR OF ENGINEERING IN ELECTRICAL ENGINEERING

FACULTY OF ENGINEERING

KING MONGKUT'S INSTITUTE OF TECHNOLOGY LADKRABANG

2011

KMITL-2011-EN-D-018-161

หัวข้อวิทยานิพนธ์	การประมาณและการหักล้างสัญญาณขรุขระเชิงความร้อนสำหรับช่องสัญญาณการบันทึกเชิงแม่เหล็กแนวตั้ง
นักศึกษา	นางยุพิน สรรพคุณ
รหัสประจำตัว	49060001
ปริญญา	วิศวกรรมศาสตรดุษฎีบัณฑิต
สาขาวิชา	วิศวกรรมไฟฟ้า
พ.ศ.	2554
อาจารย์ที่ปรึกษาวิทยานิพนธ์	รศ. ดร. พรชัย ทรัพย์นิธิ
อาจารย์ที่ปรึกษาวิทยานิพนธ์ร่วม	

บทคัดย่อ

ในวิทยานิพนธ์เล่มนี้ ได้นำเสนอวิธีการใหม่ในการประมาณและลดผลกระทบของสัญญาณขรุขระเชิงความร้อน สำหรับช่องสัญญาณการบันทึกเชิงแม่เหล็กแนวตั้ง บนพื้นฐานของสภาวะโครงข่าย (state trellis) จากนั้นได้ทำการเปรียบเทียบสมรรถนะของระบบที่ได้นำเสนอในการประมาณและลดผลกระทบของสัญญาณขรุขระเชิงความร้อน กับระบบที่ไม่ได้รับการหักล้างและระบบที่ถูกนำเสนอโดย Matthew และคณะในการลดผลกระทบดังกล่าว ผลที่ได้จากการจำลองระบบได้แสดงให้เห็นว่า วิธีที่ได้นำเสนอสามารถเพิ่มสมรรถนะให้กับระบบได้มากกว่า นอกจากนั้น ยังได้ทำการจำลองระบบที่มีการรวมผลกระทบจากการไม่เป็นเชิงเส้นของสัญญาณจากหัวอ่าน GMR (Giant Magneto-Resistance) และการเลื่อนของเส้นเชื่อมฐาน (BLW: Base Line Wander) ซึ่งเกิดขึ้นบ่อยจากส่วนหน้าสุดที่เกี่ยวข้อง แต่ในที่นี้สัญญาณดังกล่าวไม่ได้รับการพิจารณาหักล้าง เนื่องจากการศึกษาวิจัยนี้มุ่งพิจารณาการลดผลกระทบจากสัญญาณขรุขระเชิงความร้อนเท่านั้น แต่อย่างไรก็ตามจากผลการจำลองเมื่อรวมผลกระทบดังกล่าวเข้าไปในระบบพบว่าวิธีการที่นำเสนอในการลดผลกระทบของสัญญาณขรุขระเชิงความร้อน สมรรถนะของระบบลดลงตามลำดับ แต่ถึงกระนั้นระบบที่นำเสนอยังคงให้สมรรถนะของระบบที่ดีกว่า เมื่อเทียบกับวิธีการที่ถูกนำเสนอโดย Matthew และคณะ

Thesis	Thermal Asperity Estimation and Cancellation for Perpendicular Magnetic Recording Systems
Student	Mrs. Yupin Suppakhun
Student ID.	49060001
Degree	Doctor of Engineering
Program	Electrical Engineering
Year	2011
Thesis Adviser	Assoc. Prof. Dr. Pornchai Supnithi
Thesis Co-adviser	

ABSTRACT

In this thesis, we propose a new method to estimate and reduce the effect of thermal asperity in the perpendicular magnetic recording channel with a state trellis. We compare the performance of the proposed method TA estimation and cancellation with the previously proposed by Matthew and et.al. From the simulation results, the proposed method provides nearly an order of magnitude improvement over of Matthew method and more than an order of magnitude reduction when compared with the system without TA canceller. Furthermore, the giant magneto resistive (GMR) nonlinearity and baseline wander (BLW) which often appear at the front end are also included in this work. However, this work mainly focuses on how to estimate and reduce the impact of TA, so that the GMR nonlinearity and BLW affects are not compensated. The results indicate the severe performance degradation of both of these effects. However, the proposed method still outperforms Matthew method slightly.

ACKNOWLEDGEMENTS

First of all, I would like to express my deepest gratitude to Assoc. Prof. Dr. Pornchai Supnithi, Prof. Yoshihiro Okamoto, Asst. Prof. Yasuaki Nakamura and Prof. Hisashi Osawa, Ehime University, for the advice and support. They have guided me through the last four years with skill and patience, and I am the better for it. Working with them has taught me the importance of attention to details, clarity of thought and expression. I would also like to express my sincere appreciation to Assoc. Prof. Narong Hemmakorn (retired) and Assoc. Prof. Nipha Leelaruji (retired) for all the support and the generosity.

I am extremely thankful to everyone in my family, especially my parents. They have always taught me to be patient, diligent, concentrated, and cheerful. Utmost regards are given to my beloved sister for their understanding and support. I am truly blessed with the great encouragement and support from my husband, Kampol, and my son, whom I cherished dearly.

I would also like to thank King Mongkut's University of Technology North Bangkok, ASEAN University Network/Southeast Asia Engineering Education Development Network (AUN SEED-NET) for its financial support during my doctoral study.

Special thanks are also given to Dr.Chanon, Dr.Wannaree and others in the Communications and Storage Research Group (CSRG) Laboratory at KMITL. We had many fruitful discussions which consequently shed light on many questions I encountered.

Yupin Suppakhun

TABLE OF CONTENTS

TABLE OF CONTENTS (cont.)

Page

TABLE OF CONTENTS (cont.)

Page

LIST OF TABLES

Table Page

LIST OF FIGURES

Figure Page

LIST OF TABLES (cont.)

Figure Page

LIST OF FIGURES (cont.)

Figure Page

LIST OF FIGURES (cont.)

Figure Page

CHAPTER 1

INTRODUCTION

1.1 Literature Review

In order to achieve reliable high-density magnetic recording, the architectures of read channel are designed to well suppress the noise and distortions found in the read-back signal. For perpendicular magnetic recording (PMR), an important source of distortions is thermal asperity (TA). This phenomenon occurs when the slider comes into contact or it is very close to the media. The induced heat thus causes a sharp increase and decay in the signal amplitude, which if not detected and corrected appropriately, the system performance will undoubtedly be degraded [1].

In previous works, a partial-response (PR) target with dc-full component was considered the best choice for a PMR system with the additive white Gaussian noise (AWGN) [2]. A common method to reduce the effect of TA is to implement a high-pass filter (HPF) in the system and adjust its cut-off frequency [3], [4]. In [5], Dorfman and Wolf proposed an approach for TA suppression in longitudinal magnetic recording (LMR) by using the filter before processing the samples in a Viterbi detector, where D is the delay operator which represents a delay of a bit interval T. Two Viterbi detectors are run in parallel, one for an extended partial response class-4 (EPR4) channel and the other for a partial response class-5 (PR5) channel equipped with the $(1-D)$ filter when TA occurs. However, this improvement in TA reductions reduces the overall performance of the system. Similarly, for PMR system, Ueno proposed a method to reduce error deterioration due to TA by switching from the PR targets with DC component to the PR targets without DC component [6], [7]. Both methods use two channels running in parallel to avoid impact when TA occurs. This approach requires increased detector complexity to account for the different equalization targets. Alternatively, the TA signal can be estimated and used for the cancellation. In [8], Mathew and Tjhia proposed a simple TA estimation method using a window average, the TA cancellation in the read-back signal can be made by a straightforward subtraction. Although, in practice, in addition to TA, GMR nonlinearity and BLW often appear at the front end [9], [10], in all these previous works, GMR nonlinearity and BLW effects are not considered in the system.

1.2 Motivation and objectives

Two parallel targets lead to an increased complexity [5]-[8], while the method in [8], although simple to detect, can be improved. Therefore, in this work, we evaluate the performance of the perpendicular magnetic recording system with the TA events. We aim to find the solution to reduce the effect of the thermal asperity based on class-1 PR (PR1) target and class-2 PR (PR2) target while the detector complexity does not increase. We propose a new method to estimate the TA by using the state trellis of the PR target with DC component in PMR system. Table 1.1 shows the read channel complexity of TA detection and cancellation between the proposed method and others. We can see that the proposed method using only one PR target with and without TA effects, while other proposed methods have changed the characteristic of the PR targets and different targets.

Table 1.1 Comparison of the complexity between the proposed method and others.

TA estimation and cancellation method	complexity	Type of PR target	
		with TA	without TA
Proposed Method	1 channel	DC-full	DC-full
Dorfman and Wolf [5]	2 channels	DC-attenuation	DC-full
H. Ueno [6]	2 channels	DC-free	DC-attenuation
P. Kovintavewat and S. Koonkarnkhai [7]	2 channels	DC-attenuation	DC-full
Mathew and Tjhia [8]	2 channels	DC-attenuation	DC-full

1.3 Concept of the Research

The trellis used in the viterbi detector should be exploited to better cancel the TA. For perpendicular magnetic recording (PMR), an important source of distortions is thermal asperity (TA) [11] and the partial response (PR) target with dc-full component was considered the best choice for a PMR system in the absence of disturbances other than an additive white Gaussian noise (AWGN). Thus, we will apply the relation of the data on the state trellis of the partial response (PR) target with dc-full component to estimate the TA and reduce its effects of PRML system in the PMR channel.

1.4 Scope of the Research

In this thesis, we propose a new method to estimate the TA and reduce its effects through the state trellis of the partial response (PR) target with dc-full component. In addition, the GMR nonlinearity and BLW effect are included. Via computer simulation, we will compare the performance of PRML system in PMR channel with Mathew's method and the proposed method to estimate and reduce the impact of TA.

1.5 Outline of the Thesis

In this thesis, Chapter 2 is devoted to the overview and background of magnetic recording systems. The basic ideas of partial-response channel are optimal for PMR and LMR system and the noise in perpendicular recording channels is introduced. Chapter 3 is devoted to a comprehensive theory of detection techniques. The partial-response signaling with maximum-likelihood (PRML) sequence estimation for magnetic recording. In Chapter 4, we describe the thermal asperity (TA) effects and review the previous works which detect and cancel the thermal asperity effects in the perpendicular magnetic recording system. After that, we propose a new method to estimate and reduce the TA through the state trellis of partial response (PR) targets. We also compared the BER performance of PRML system with the proposed TA canceller with that without the canceller. The system simulation and results are in Chapter 5. We compare the performance of the proposed method TA estimation and cancellation with the Mathew's method. Finally, Chapter 6 includes the conclusions of the thesis and possibilities for further research.

CHAPTER 2

MAGNETIC RECORDING SYSTEM

2.1 Introduction

The consumer demand for hard disk drives (HDDs), which have mainly been used as secondary memories for computers, is rapidly growing because recent strong growth of the information society. Demands for applications in other devices such as video camera recorders, car navigation systems, portable music players, and cellular phones are also emerging. At the same time, the remarkable increases in HDD recording density that are being achieved are enabling higher recording capacities and HDD downsizing. Currently HDD technology is based on perpendicular recording in which the medium magnetization is perpendicular to the disk plane. Perpendicular recording addresses this 'thermal' limit and allows continued advances in areal density. In conventional 'longitudinal' magnetic recording (LMR), the magnetization in the bits is directed circumferentially along the track direction [11] as shown in Fig. 2.1.

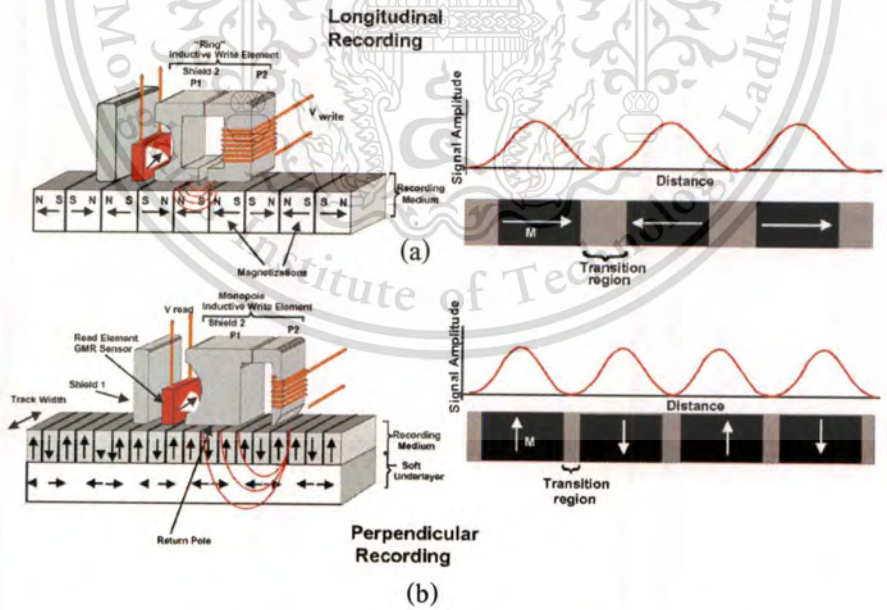

Figure 2.1 The physics of recording (a) longitudinal recording diagram and (b) Perpendicular recording diagram.

2.2 Basic Communication Channel Model for Magnetic Storage

Design and analysis of coding and signal processing techniques require a suitable communication channel model for magnetic storage systems. Such a model should correctly reflect the essential physics of the read and write processes of magnetic recording, and also provide a system-level description that allows convenient design, analysis and simulation of the communications and signal processing techniques under study.

Consider a general block diagram of a magnetic recording system for HDD as depicted in Figure 2.2. The message bits are encoded by the ECC encoder to protect information bits from random or burst noise. Currently, the Reed-Solomon (RS) code [4], [12] is a standard ECC in HDD. Then, the RS-encoded sequence is encoded again with the modulation encoder to control minimum and maximum distances between consecutive magnetic transitions [13]. The minimum distance constraint mitigates local medium noise and nonlinearity associated with crowded magnetic transitions, while the maximum distance constraint ensures that the signal arise enough in the read-back signal (the data sequences were not part of the d.c. component).

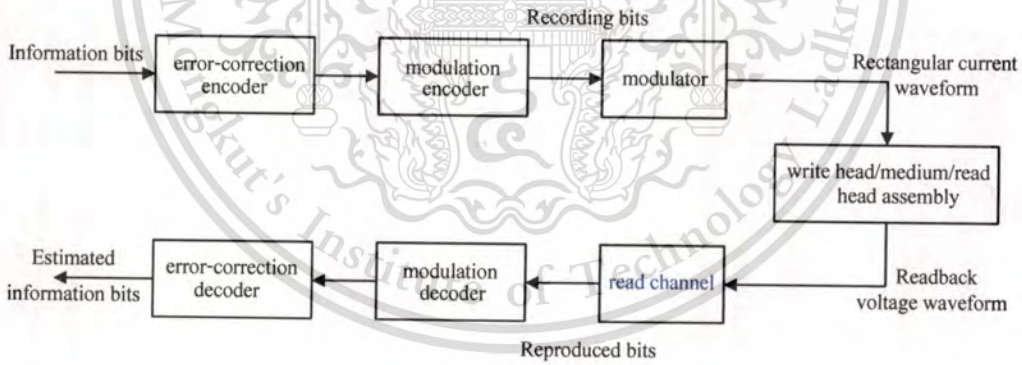

Figure 2.2 Simplified block diagram of a magnetic recording system/storage system.

The run-length limited (RLL) code [14] is often used for modulation encoding. The data sequence from the modulation encoder will be written in medium, called "recording bits". The modulated bit stream is converted into a rectangular current waveform (write current waveform) by the modulator and then stored in the medium in the form of a magnetization waveform.

During the read process, the data in the medium will be sensed by read head and then converted into the electrical signal. After preamplification, we obtain the read-back signal. The read-back voltage waveform will be created when the reading head has been moved through response to a written transition. The read-back is then passed through what is generally called the read channel in the data storage community. The read channel consists of a low pass filter (LPF), a sampler driven by a phase locked loop and an analog-to-digital converter, an equalizer and a symbol detector (in a broader definition, the read channel also includes the modulation encoder/decoder and, possibly, some auxiliary inner error correction or error detection encoder/decoder). The detected bit sequence is then sent to the modulation decoder and finally to the error correction decoder [15].

2.3 Write and Read Processes

2.3.1 Write Process

During the write process, the data bits are converted into a rectangular current waveform called a write current as shown in Figure 2.3. This write current is applied to the windings of the write head to produce a magnetic write field in the medium near the head gap. The write field must be larger than the medium coactivity to magnetize the medium along the field direction. By switching the direction of the write field (or the write current), magnetization transitions can be written in the medium.

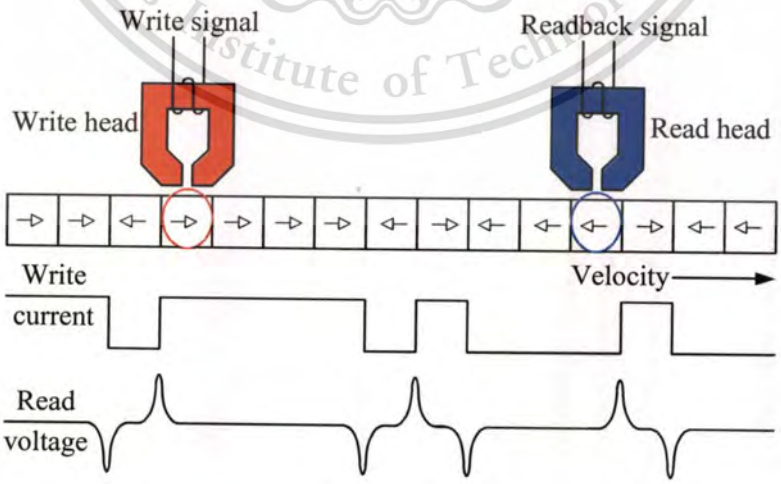

Figure 2.3 Illustration of the principle of magnetic recording.

Commercial digital recording systems normally employ binary saturation recording, i.e., the magnetization saturated on the medium in only one direction or the opposite. This is because if more than two data levels were recorded, nonlinearities would cause a major problem and signal-to-disturbance ratios would diminish considerably.

2.3.2 Read Process

During the read process, the read head senses the change in the flux via the transitions of the magnetization pattern, resulting in an induced voltage pulse in the coil because of the Faraday's law. For an isolated transition, the read head produces a read voltage pulse, $g(t)$, or its inverse, $-g(t)$, depending on the direction of the transition as seen in Figure 2.3. The pulse $g(t)$ is commonly known as the transition response, which has finite amplitude and a finite half-amplitude pulse width. The transition response for longitudinal recording, also known as the Lorentzian pulse, is given by [16]

$$g(t) = \frac{1}{1+\left(\frac{2t}{\mathrm{PW}_{50}}\right)^2}, \tag{2.1}$$

where PW_{50} determines the width of $g(t)$ at half of its peak value. For perpendicular recording, we are interested in a transition response form

$$g(t) = \mathrm{erf}\left(\frac{2t\sqrt{\ln 2}}{\mathrm{PW}_{50}}\right), \tag{2.2}$$

where $\mathrm{erf}(\cdot)$ is an error function defined by $\mathrm{erf}(x) = \frac{2}{\sqrt{\pi}}\int_0^x e^{-t^2}\,dt$ [32], and PW_{50} determines the width of the derivative of $g(t)$ at half its maximum. In the context of magnetic recording, the ratio $\mathrm{ND} = \mathrm{PW}_{50}/T$ (where T is the bit duration) represents a normalized recording density [16], which defines how many data bits can be packed within the resolution unit PW_{50}. Figure 2.4 shows the pulse width at 50% of the maximum amplitude at ND = 3 and normalized to the bit period T.

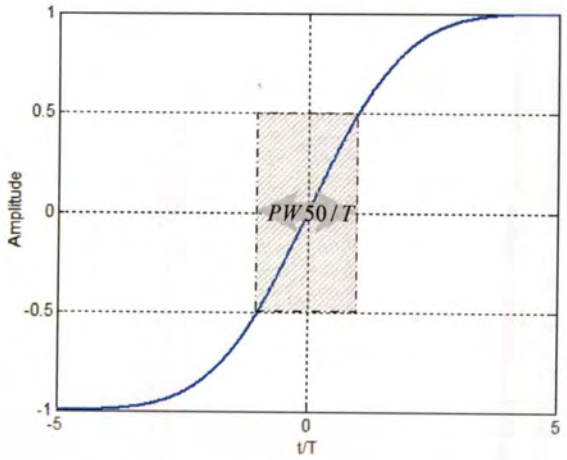

Figure 2.4 Normalized recording density is defined as ND = PW_{50}/T at ND = 3.5.

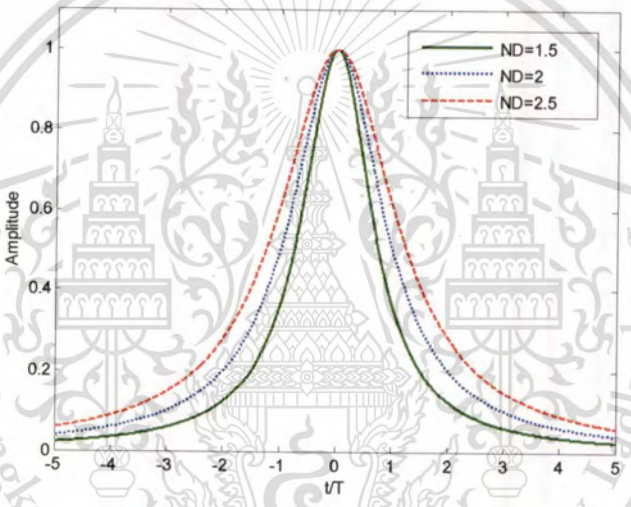

(a)

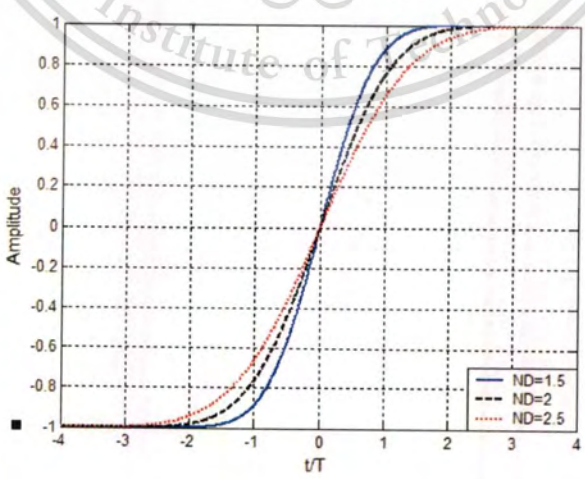

(b)

Figure 2.5 Transition responses for (a) Longitudinal and (b) Perpendicular recording.

The transition responses of longitudinal and perpendicular recording channels are plotted in Figure 2.5 (a) and (b), respectively, for different NDs. Clearly, the transition response spans many symbol intervals as ND increases. This implies that the effect of inter-symbol interference (ISI) becomes more severe as ND increases.

Additionally, the response of the head to an isolated bit is commonly known as the dibit response [16], which is expressed as

$$m(t) = g(t) - g(t-T), \tag{2.3}$$

as shown in Figure 2.6 for longitudinal recording and perpendicular recording, respectively.

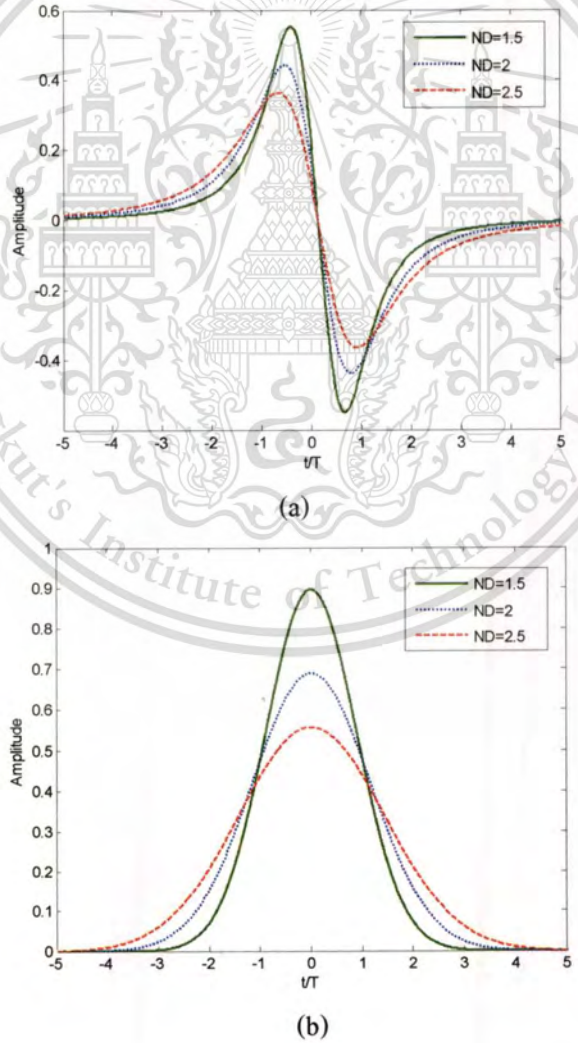

Figure 2.6 Dibit responses for (a) Longitudinal and (b) Perpendicular recording.

It is easy to show that the frequency response of $m(t)$ for longitudinal recording is given by

$$M(\Omega) = \exp(-\pi|\Omega|\mathrm{ND})\{1-\exp(-j2\pi\Omega)\}, \tag{2.4}$$

whereas for perpendicular recording,

$$M(\Omega) = \frac{T}{j\pi\Omega}\exp\left(-\frac{\pi^2\Omega^2 ND^2}{ln(16)}\right)\{1-\exp(-j2\pi\Omega)\}, \tag{2.5}$$

where $\Omega = fT$ is a normalized frequency variable, f is a frequency variable in Hertz and $j = \sqrt{-1}$ is an imaginary number.

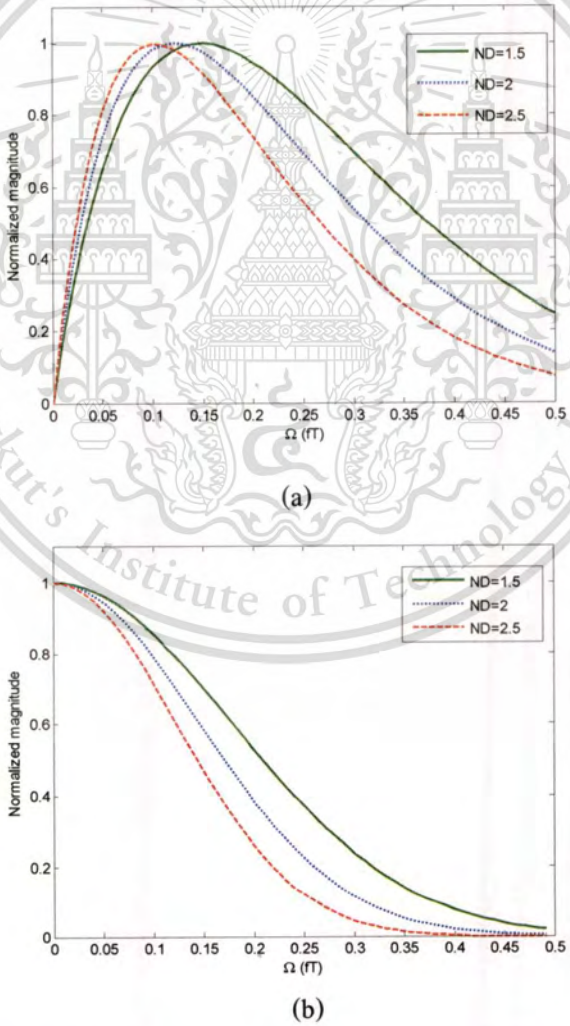

(a)

(b)

Figure 2.7 Frequency responses of the dibit responses for (a) Longitudinal and (b) Perpendicular recording.

Figure 2.7 shows the normalized frequency responses of the dibit responses for different ND's. Apparently, the signal energy becomes more concentrated at low frequencies as ND increases for both channels. Furthermore, a longitudinal recording channel exhibits a spectral null at d.c., while a perpendicular recording channel contains a d.c. component.

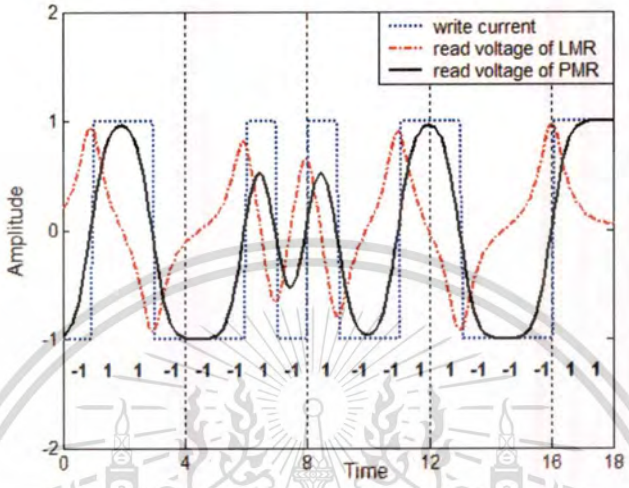

Figure 2.8 Read back waveform of the perpendicular recording system and the longitudinal recording system at ND = 1.

In Fig. 2.8 the signals from a perpendicular recording system look dramatically different than those from a conventional longitudinal system. Every frequency component gets shifted by 90 degrees in phase (corresponding to the 90 degree rotation of magnetization from longitudinal to perpendicular). This totally alters the appearance of the waveforms. The signal processing in the Read/Write electronics must be modified to accommodate these waveforms. In addition to the phase-shift, there is also a lot more signal energy at low-frequencies, but is also careful to avoid the signal disturbances and noise that sometimes can occur in these low-frequency regions [11].

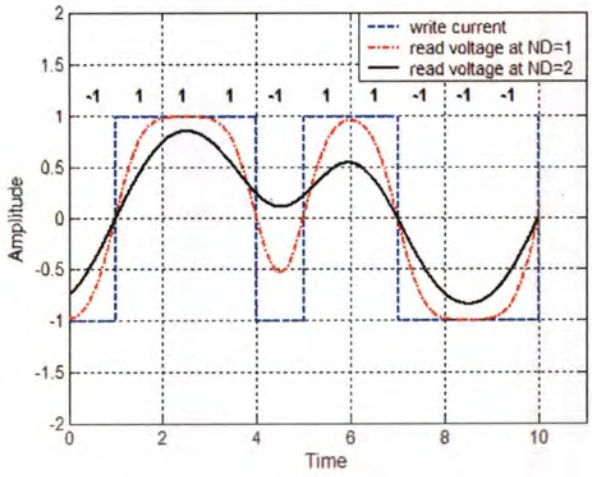

Figure 2.9 Write current and read-back waveform of the perpendicular recording system at ND = 1 and 2.

Figure 2.9 shows the Write/Read back waveform of the perpendicular recording system for different ND's. Apparently, the signal energy of read back signal is decreased as ND increases.

2.4 Signal processing for PMR channels

The transition from LMR to PMR entails changes not only in the head and media technologies, but also in the signal processing technology. Current HDDs employ partial response (PR) targets for shaping the read back signal. Unlike LMR, PMR has a nonzero DC response. This suggests that the optimal PR targets of PMR and LMR are different [17].

The basic ideas of partial response applied to digital recording channels reside in inter symbol interference ISI combat by accepting and controlling it. In an attempt to increase recording densities, adjacent read channel responses to transitions in recording media tend to interact with each other and so the ideal single transition shape is degraded randomly, leading to difficulties in considering it as an appropriate transition symbol at detector stages. The partial channel response resides in linear superposition of well -known individual symbol shapes. So the interference between adjacent transitions can be anticipated and taken into consideration in detector strategies. Two important modifications are presupposed for the classical channel:

equalization of the response channel to a standard shape and the Viterbi maximum likelihood detector. Equalization favors the ISI control by placing the sampling moments in such a position on response shape that shall guarantee controlled interference. The Viterbi detector analyses the received signal shape, based on an appropriate succession of samples which can hint at a most valuable decision. Partial response channels coupled with appropriate detectors enable an increased density in digital magnetic recording [18].

A polynomial operator D characterizes the partial response channel, which applies to an NRZ random binary sequence of recording media, through polarization and conversion into a ternary sequence forwarded to the detector input. The classical channel shows a 1-D polynomial characteristic to express differential action of the media-head interaction, with a single sample in the center of the received symbol.

The generally accepted PR target for longitudinal recording is of the form $H(D) = (1-D)(1+D)^n$, whereas the PR target for perpendicular recording is $H(D) = (1+D)^n$, where n is an integer. Obviously, the term $(1-D)$ is not needed for perpendicular recording because the perpendicular recording channel contains a d.c. component. Thus, we can divide the PR targets into 2 types

1. PR Target with DC component

The characteristic is the sum of coefficient "[…]" $\neq 0$ two sub types are

1.1 DC-full: the coefficients are positive only and balanced (from left to right)

1.2 DC attenuation: the coefficients can be positive or negative (DC unbalanced), with first coefficient is 2 and the sum of coefficient is not zero [19].

2. PR Target without DC component

The characteristic is the sum of coefficient "[…]" = 0 two sub types are

2.1 DC-free: the coefficients can be positive or negative and balanced (from left to right)

2.2 DC attenuation: the coefficients can be positive or negative and unbalance (from left to right) but sum of the coefficients is zero.

Table 2.1 shows the classification of PR systems by Y. Okamoto [19], the PR system of class 1, 2 and 3 has DC-responses, while those of class 4 and 5 have no DC-responses. As it is clear from the sum of the respective coefficients, PR1 and PR2 system had been applied to the PMR.

Table 2.1 Fundamental PR target.

Target type	$n = 1$	$n = 2$	$n = 3$	$n = 4$
DC – full $(1+D)^n$	PR1 [1 1]	PR2 [1 2 1]	EPR2 [1 3 3 1]	EEPR2 [1 4 6 4 1]
DC – attenuation $(2-D)(1+D)^n$	---	PR3 [2 1 -1]	EPR3 [2 3 0 -1]	EEPR3 [2 5 3 -1 -1]
DC – free (DC-balance) $(1-D)(1+D)^n$	---	PR4 [1 0 -1]	EPR4 [1 1 -1 -1]	EEPR4 [1 2 0 -2 -1
DC – free (DC-unbalance) $(1-D)^m(1+D)^n$	where n and m is positive value			

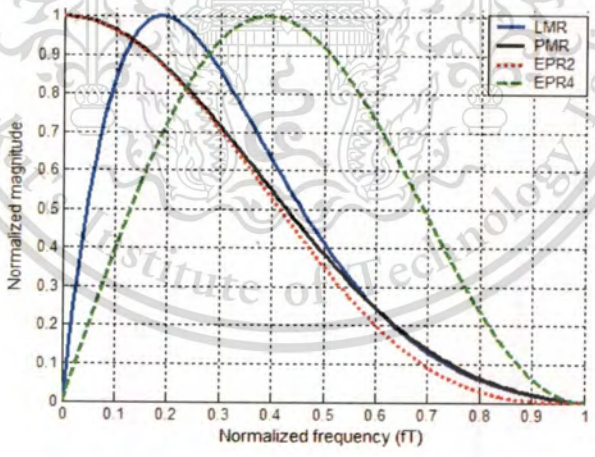

Figure 2.10 Channel frequency response and PR target at ND = 1.5.

Figure 2.10 compares the channel frequency responses and PR target suited for longitudinal and perpendicular magnetic recording at ND = 1.5. We can see that, the class II PR target (EPR2 = [1 3 3 1]) has frequency response close to that of the perpendicular signal with the

strong energy at low-frequency. On the other hand, the class IV PR target (EPR4 = [1 1 -1 -1]) has the frequency response close to that of the longitudinal signal.

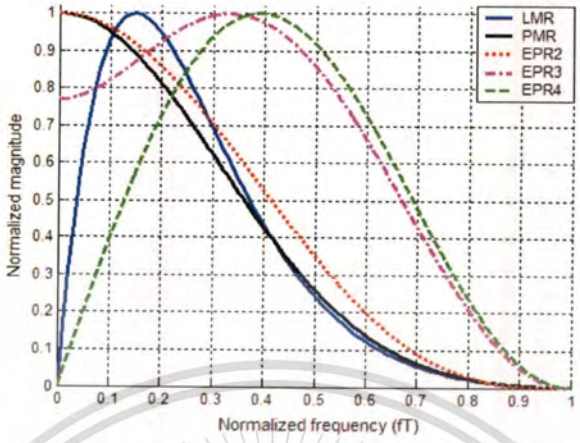

Figure 2.11 Channel frequency response and PR target at ND = 2.0.

Figure 2.11 shows the channel frequency responses for longitudinal and perpendicular magnetic recording and various PR targets at ND = 2.0. We can see that the class II PR target has d.c. full frequency response and the class IV PR target has d.c. free frequency response, both of which match the read-back signal of longitudinal and perpendicular magnetic recording. The class III PR target has frequency response attenuation at low-frequency, suitable for low-frequency noise dominant in the system.

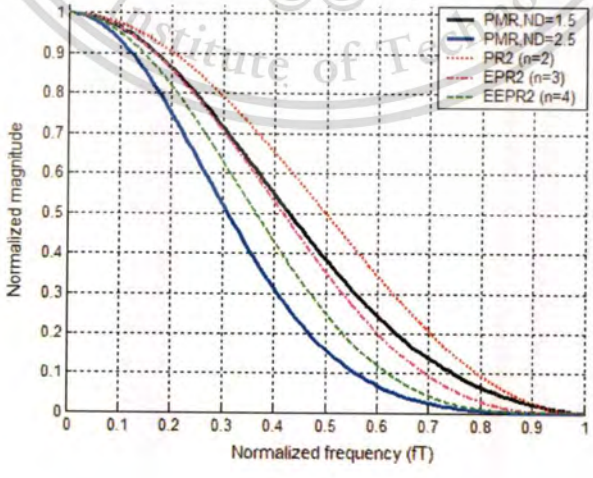

Figure 2.12 Channel frequency response of PR target for PMR at ND = 1.5 and 2.5.

Figure 2.12 compares the frequency responses of different order n based on class II PR target. It is clear that as ND increases, a larger value of n is required because the effect of ISI becomes more severe at high NDs. Hence, at high NDs, a long target allowing more controlled ISI will provide a better match to the channel response than a short target.

2.5 Noises in Magnetic Recording System

In order to achieve reliable high-density magnetic recording, the architectures of read channels are designed to well suppress the noise and distortions found in the read-back signal. The noise in perpendicular recording with any kind of noise/distortion cause effects at low frequencies, including the thermal asperity (TA), GMR nonlinearity and BLW effects that cause degradation in the system performance.

2.5.1 Thermal Asperity (TA)

For the perpendicular magnetic recording (PMR), an important source of distortions is thermal asperity (TA). The TA is a defect that thermally induces a resistance transient in the MR stripe of the read head. Among the several types of TAs, we consider the most commonly occurring contact positive grown TAs that develops after the disk is manufactured. When the read head comes into contact with a heated asperity on the disk surface, the resulting thermal transient causes a change in the resistance of the MR head element, which appears as an additive voltage transient in the read back signal. A simplified model for TA effects is necessary in order to quantify the efficiency of TA estimation and cancellation techniques and to aid in modeling on the fly methods to handle TA events. Figure 2.13 illustrates such a model described by Stupp et al. [20]. This model fits captured spin stand data and drive data very well. It shows the linear heating of the MR element, the peak temperature, and the exponential decay that characterizes a TA event. According to the model, the decay immediately after the TA event is approximated by an exponential function, but later the decay slows down. However, the high pass filter in the preamplifier helps masking this slow decay. Thus, we can completely specify the effect of TA with this model together with four parameters [4], [21]. These are:

1. Start-time: This is set where the TA effect start.

2. Max-amplitude: Whenever there is TA, the value of the signal baseline changes from zero to the value specified in this parameter times the zeros to peak signal voltage.

3. Rise-time: This specifies the rise time required for its base line to rise from zero to its maximum value (specified at Max-amplitude).

4. Decay-constant: The TA effect is assumed to decay exponentially, and this parameter specifies the decay constant of the exponential function.

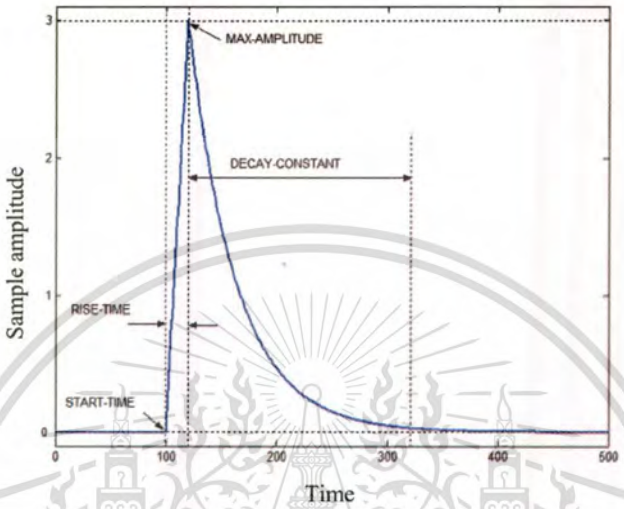

Figure 2.13 Simplified models which describe the TA event.

The TA signal $u(t)$ can be modeled and expressed as

$$u(t) = \begin{cases} A_0 \left(\dfrac{t}{T_r} \right), & 0 \le t \le T_r \\ A_0 \exp\left(-\dfrac{t - T_r}{T_d} \right), & T_r < t \le T_f \end{cases} \qquad (2.6)$$

where $A_0 = \beta \sum_K |h_k|$ is the peak TA amplitude, $\beta \ge 0$ is the peak-factor, h_k is the coefficients of PR target, T_r is the rise time, T_d is the decay constant (i.e., time constant), and T_f is the TA duration. A decay time equal to four times the decay constant is sufficient since it will reduce the magnitude of the TA signal to only 1.8% of its peak amplitude. Thus, we choose the TA duration as $T_f = T_r + 4T_d$. Typically, a TA signal experiences a sharp and short rise (60-150 ns) followed by a longer decay (25-50 μs). The capacitance in the preamp circuit, which follows the MR head, shortens the TA signal decay time at the preamp output to approximately 1-5 μs) 1-5

μs . The TA signal amplitude is usually about 3 to 5 times the peak of the magnetic read-back signal. If the TA signal exceeds certain a limit, the resulting sum of the two signals will exceed (saturate) the upper limit of preamplifier, filter, or ADC [7].

The estimation and cancellation block represent the proposed method to reduce the effects of TA, which is followed by the Viterbi detector and ECC decoder through the interleaved parity-check code.

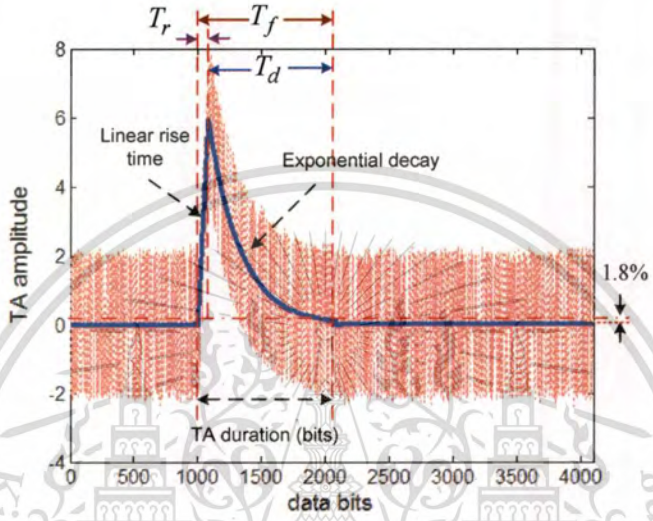

Figure 2.14 The simplified model and read-back signal with TA from TA model.

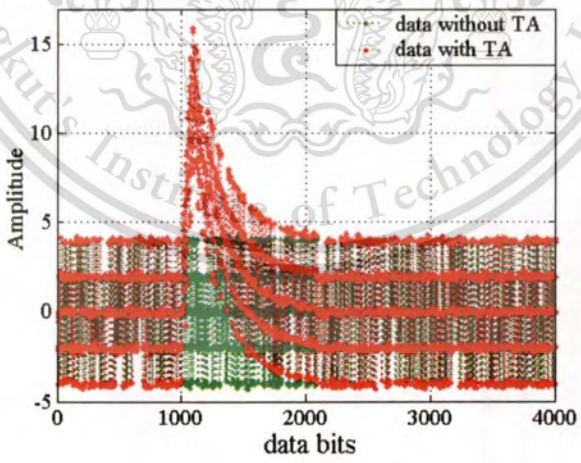

Figure 2.15 The typical read-back signal without TA and with TA of PR2 target from read-back system model.

2.5.2 Giant Magneto Resistive (GMR) reader nonlinear response

Giant Magneto Resistive (GMR) heads have been widely used in digital magnetic recording systems due to their high signal-to-noise ratio (SNR) and high resolution. However, GMR head has a nonlinear response to the applied field the behavior of GMR heads is nonlinearity slope asymmetry between the positive response and negative response. The peak position of the differential waveform is decided by the maximum slope position of the convolution of the medium recording transition and the GMR readout function, depending on GMR transfer curve.

The GMR nonlinearity $v(t)$, can be modeled as the transfer curve of GMR $[V(h)]$ approximating a hyperbolic-tangent curve [22] with

$$V(h) = \begin{cases} \dfrac{\tan[a(h-dh)]}{a} + dh & (h > dh) \\ \dfrac{\tan[b(h-dh)]}{b} + dh & (h < dh) \end{cases} \tag{2.7}$$

The normalized field h is defined as the applied field divided by the maximum applied field. A positive saturated parameter $V(1)$ and a negative saturated parameter $V(-1)$ approach linear $V(+1) = V(-1) = 1$. The asymmetry is caused when a and b is not equal to 1. The shift parameter dh indicates the field shift value of maximum transfer curve slope position. The asymmetry was defined as percentage of $\left|\frac{a-b}{a+b}\right|$, and where a is positive peak and b is negative peak. The GMR saturation were also estimated by calculation, with the GMR saturated transfer curve approximated by a hyperbolic-tangent curve and a calculated saturation parameter defined as a ratio of the amplitude of the curve to the amplitude approximated line. Fig. 2.16 shows the calculated plot of GMR asymmetry positive peak and the readout isolated waveform amplitude as shown in Fig. 2.17.

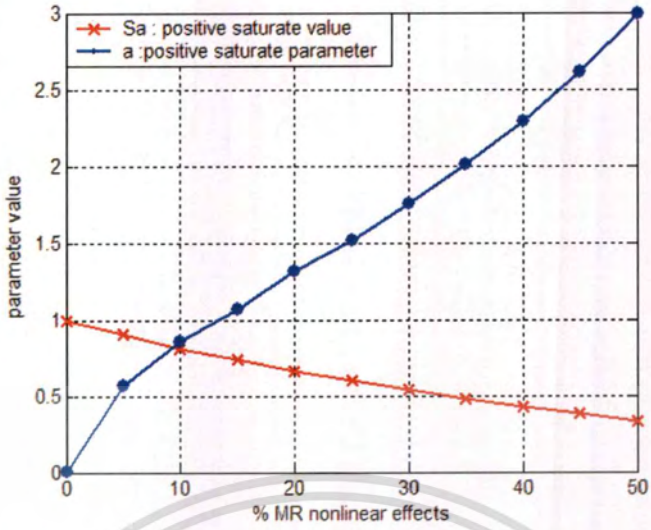

Figure 2.16 The percentage of GMR asymmetry with a parameter on the positive response.

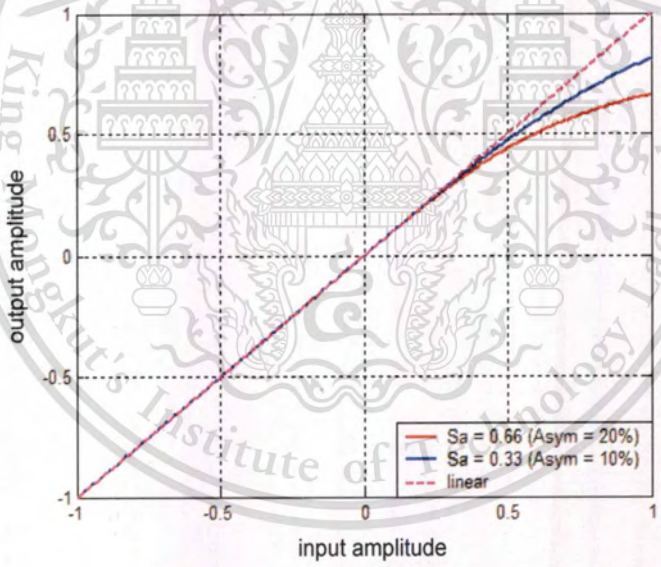

Figure 2.17 The correlation between the different percentages of GMR asymmetry and readout isolated waveform amplitude.

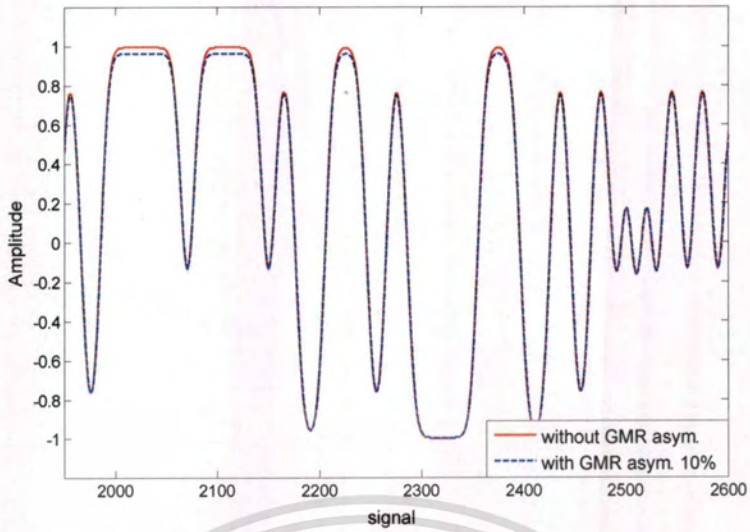

Figure 2.18 The read-back signal with and without GMR asymmetry effect.

Figure 2.19 compares the read-back signal amplitude with and without GMR asymmetry. We can see that the amplitudes of read-back signal are reduced following the GMR asymmetry effect.

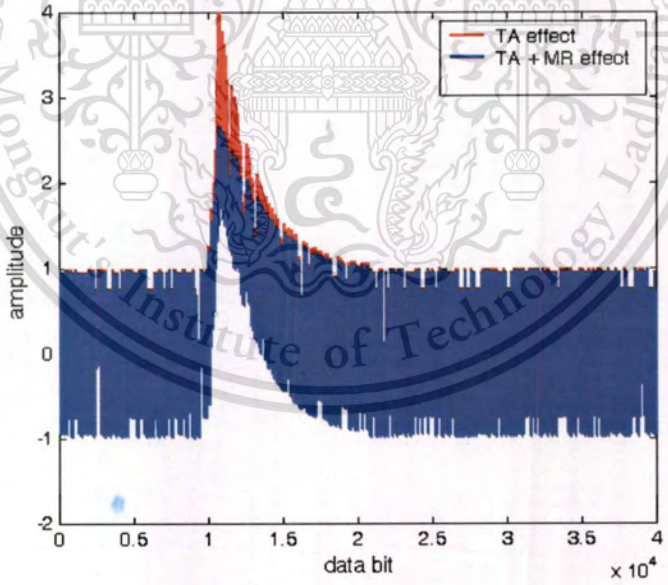

Figure 2.19 The equalized signal with and without GMR asymmetry dominant with TA effect.

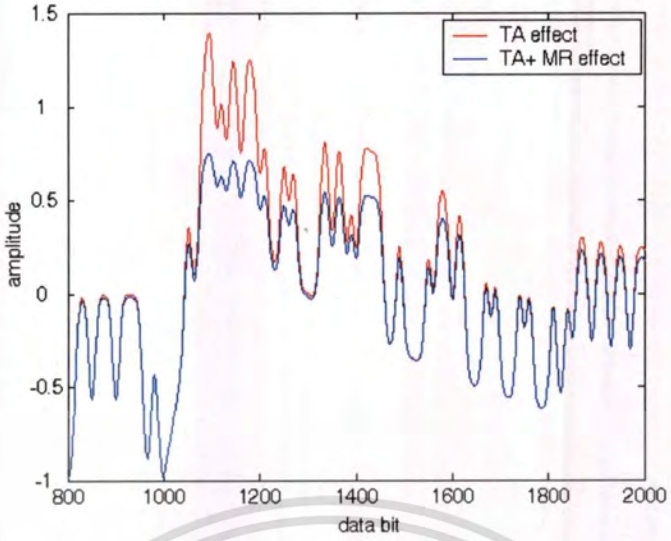

Figure 2.20 The equalized signal with and without GMR asymmetry dominant based on TA effect.

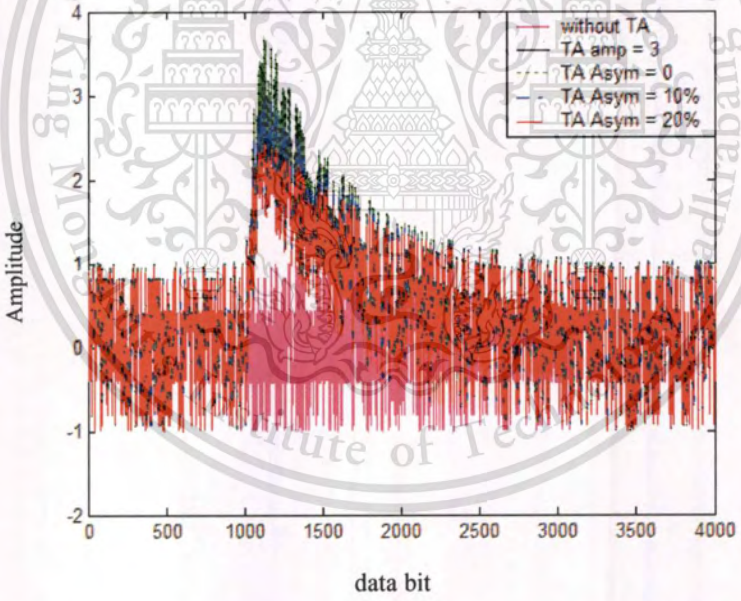

Figure 2.21 The severity level of GMR asymmetry base on TA effect.

2.5.3 Baseline Wander (BLW) effect

The preamplifiers used in current perpendicular read channels are ac coupled with the recording channel itself and cannot pass dc. The preamplifier acts as a high-pass filter which causes the baseline of the read-back signal to wander slowly. This variation of the baseline introduces a low-frequency distortion called the baseline wander (BLW) effect [22].

On the other hand, as noted earlier, BLW occurs only in a perpendicular channel. An idealized perpendicular pulse response contains energy at zero frequency, or DC. However, due to finite permeability in either the soft under layer or the reader shields and due to nonzero spacing between soft under layer and recording layer, the perpendicular channel, at the read head output, will have a notch at DC as shown in Fig. 2.22 (a) [23]. As illustrated in Figure, the differentiation between longitudinal and perpendicular responses is due to the low frequency contents of the two pulse responses. More specifically, the abrupt amplitude variation of the perpendicular channel around the DC notch results in a long narrow tail of the pulse response in time domain as shown in Fig. 2.22(b).

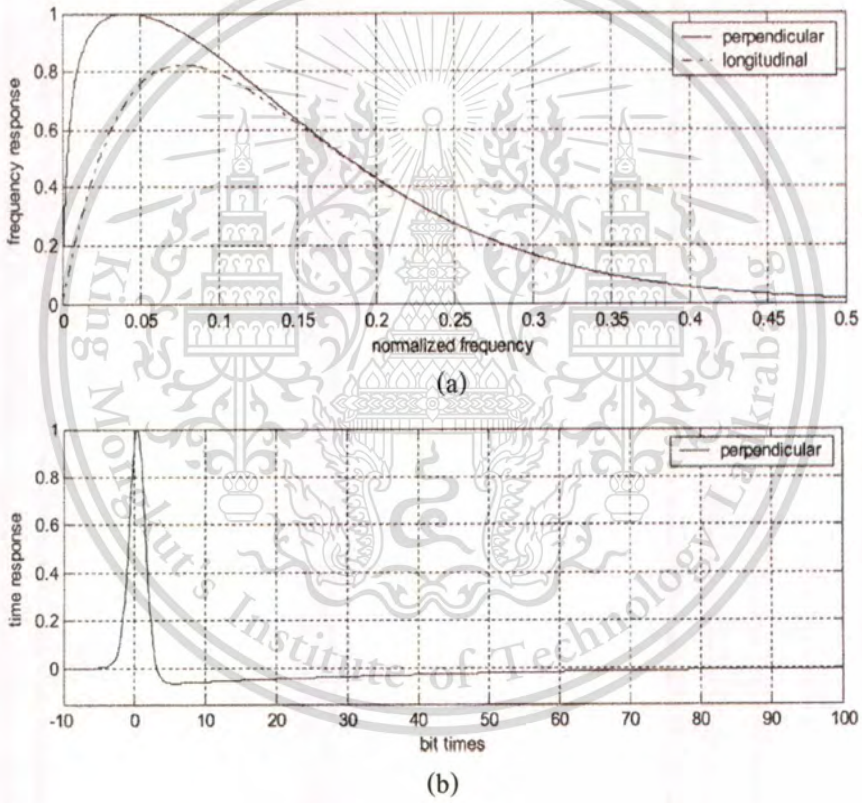

Figure 2.22 Qualitative diagrams of (a) pulse frequency response for both a perpendicular and longitudinal channel and (b) pulse response of a perpendicular channel in time domain.

The BLW effect is generated by the high-pass pole of the preamplifier [23], [24], [25]. It can be modeled by a steep high-pass filter (HPF) in the channel as

$$H(s) = \frac{a_1 s}{s + \alpha_0} \tag{2.8}$$

where a_1 and α_0 are the parameters which determine the high-frequency gain and cutoff frequency of $H(s)$.

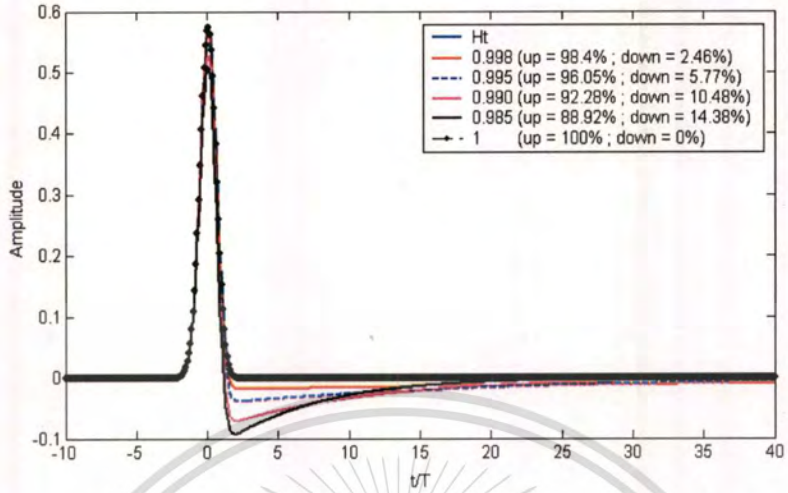

Figure 2.23 The dibit pulse response in the time domain results in a long tail due to BLW effect from preamplifier.

Figure 2.23 shows the severity of the baseline wander is dependent on the HPF cut-off frequency, which is a BLW increase as the HPF cut-off frequency increases. We assume the transfer function of the HPF is $\frac{\alpha(1-Z^{-1})}{1-\alpha Z^{-1}}$ with α a number very close to 1 (e.g., 0.995).

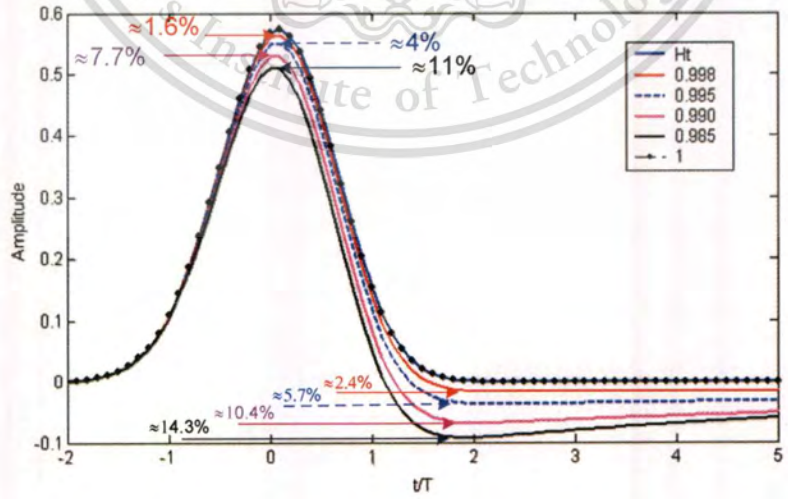

Figure 2.24 The dibit pulse response at different percentages and without BLW effects.

In Fig. 2.24, we can see the percentage of amplitude reduced as the HPF cut-off frequency increases and can calculate to compare with the dibit pulse without BLW effects.

2.6 Summary

In this chapter, we describe the backgrounds of digital magnetic recording systems and basic communication channel model for magnetic storage as well as principle process of writing and reading process in the hard disk drives. The transition responses, dibit responses, and frequency responses for both the longitudinal and the perpendicular magnetic recordings are shown. In addition, we also explain the dominant noises which occur in a magnetic recording system.

CHAPTER 3

DETECTION METHODS

3.1 Introduction

In communications, maximum likelihood sequence detectors (MLSD) [26] are often used to perform signal detection in ISI channels. A salient feature of sequence detection is that its complexity grows exponentially as the ISI length increases. To reduce the cost of implementing MLSD, it is thus a common practice to first process the read-back signal by an equalizer, which shapes the overall channel response to some desired target function (referred to as Partial-Response) that is much shorter than the natural channel response, before forwarding the signal to the sequence detector. Since the noise incurred in the channel is also filtered by the equalizer, a direct consequence of employing equalization is that the equalized signal becomes corrupted by correlated noise. Since traditional sequence detectors are optimized for white Gaussian noise, it is thus necessary to whiten the noise to achieve optimal performance. The term "partial response" comes from the fact that the sample of the equalized signal at time kT (T is a signaling interval). The number of adjacent bits that determine the sample at kT is referred to as channel memory. The channel memory and the details of the partial response selection are made based on an attempt to have the partial response be as close a match to the channel as possible. The main idea in partial response equalization is to equalize the channel to a known and short target that is match to the channel spectrum so that noise enhancement is minimal. The partial-response signaling with maximum likelihood (PRML) sequence estimation is proposed for use in magnetic recording by Kobayashi [27]. Today's all read channel are based on the PRML. Also significant improvements in all the subsystems have been made during long time ago.

Noise prediction emerges as an efficient technique to implement noise whitening. Briefly, by exploiting the correlation between noise samples, the noise predictive technique uses past noise samples to estimate the current one. Subtracting the predicted/estimated value from the current noise sample results in a "prediction-error" signal with lower noise variance and diminished or negligible correlation (with sufficient noise-prediction taps). Hence, noise prediction is able to accomplish noise whitening and noise reduction. When noise prediction is integrated into the sequence detector, the so-called noise-predictive maximum-likelihood (NPML)

detection arises [28], [29]. The present chapter is devoted to a comprehensive theoretical and practical treatment of detection techniques.

3.2 The Viterbi Decoder

Viterbi decoding was developed by Andrew J. Viterbi in 1967, a founder of Qualcomm Corporation. The Viterbi algorithm is a well-known maximum-likelihood algorithm for decoding of convolution codes. A convolution encoder is a linear system. A binary convolution encoder can be represented as a shift register. The outputs of the encoder are modulo 2 sums of the values in the certain register's cells. A combination of registers cells that forms one of the output streams is defined by a polynomial [30], [31]. For example, Fig. 3.1 shows the convolution encoder of PR2 channel with polynomial $H(D) = (1 + 2D + D^2)$. The symbol D represents a memory element, its input signal being taken over into the memory at the transition from step k to step $k + 1$ (D: delay) [32].

The Viterbi algorithm was extended to the detection of signals transmitted over linear ISI. The basic idea behind Viterbi detection is to consider the received sequence as a finite-state machine (FSM). Each state corresponds to some value of the encoder's register. Given the input bit value, from a certain state the encoder can move to two other states. These state transitions constitute a diagram which is called a trellis diagram. Can see as Figure 3.2 and 3.3 shown an example the finite state machine and trellis diagram of PR2 channel. A dash line corresponds to input, a_k is -1 and a solid line corresponds to input 1. The detector assigns a metric each branch of the trellis, proportional to the error signal between the received value and the ideal signal resulting from that transition. The maximum-likelihood (ML) sequence is the one which results in the minimum accumulated error throughout the trellis.

The Viterbi algorithm is applicable when the following properties hold:

- The signal is generated by a finite-state machine.
- The noise component in each sample is independent
- A maximum-likelihood criterion is used, maximizing the sequence likelihood.

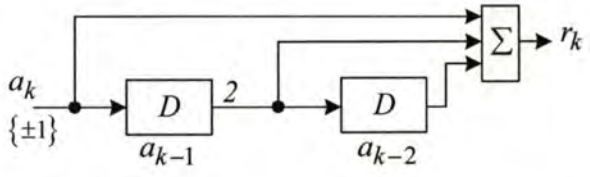

Figure 3.1 The PR2 channel model, $H(D) = (1 + 2D + D^2)$.

Table 3.1 The state table for PR2 channel.

Current state, (k)	a_k	a_{k-1}	a_{k-2}	r_k	Next state, (k+1)
S_0	-1	-1	-1	-4	S_0
S_0	1	-1	-1	-2	S_1
S_1	-1	1	-1	0	S_2
S_1	1	1	-1	2	S_3
S_2	-1	-1	1	-2	S_0
S_2	1	-1	1	0	S_1
S_3	-1	1	1	2	S_2
S_3	1	1	1	4	S_3

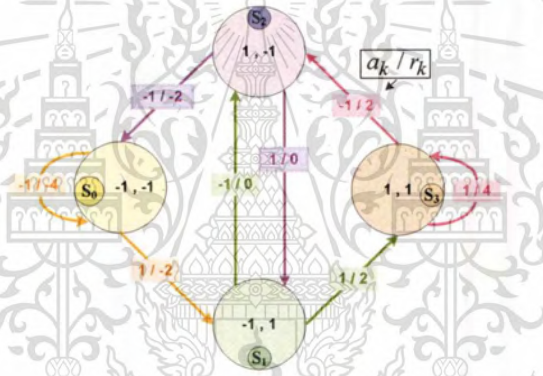

Figure 3.2 Finite State Machine (FSM) of PR2 channel.

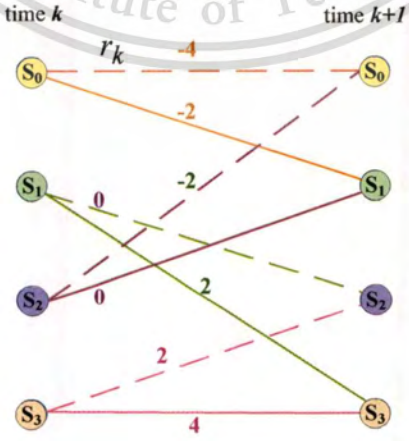

Figure 3.3 Trellis diagram of PR2 channel.

3.2.1 Trellis Diagram

The number of states for the detector is governed by the channel's trellis structure. A trellis is an illustration of a finite-state machine's (FSM) state diagram, but it explicitly shows the passage of time. The states are determined by the memory elements of the FSM, with each unique combination of the bits in the memory elements creating a new possible state. Each branch in the trellis denotes a possible movement from state at time k-1 to state at time k. The detector uses these possible state transitions to determine the most probable input bits to the FSM. The number of states Trellis is $2^{\nu} = 2^{K-1}$, where K is length of PR channel and the number of branch merging into one stage is equal to the number of possible information symbol (is 2 for the binary symbol). A certain number of computations are associated with each state in the trellis. So, as the number of states increase, so does the overall complexity. With each new memory element in the binary FSM, the trellis size doubles, which leads to a complexity that is exponential in relation to the FSM's memory length. From figure 3.1, example of the PR2 [1 2D 1D^2] channel has memory ν = 2 and channel length K =3 . Thus, the number of state trellis = 2^2 = 4 state and the number of branch in the trellis = 2^3 = 8 branches.

Note that each state transition on the diagram corresponds to a pair of output bits. There are only two allowed transitions for every state, so there are two allowed pairs of output bits, and the two other pairs are forbidden. If an error occurs, it is very likely that the receiver will get a set of forbidden pairs, which don't constitute a path on the trellis diagram. So, the task of the decoder is to find a path on the trellis diagram which is the closest match to the received sequence [33], [34].

Let's define a free distance (d_{free}) as a minimal Hamming distance between two different allowed binary sequences (a Hamming distance is defined as a number of differing bits). A free distance is an important property of the convolution code. It influences a number of closely located errors the decoder is able to correct. From figure 3.3, the *free distance* can be compute as

$$d_{free} = |(-4)-(-2)| + |(0)-(2)| + |(-2)-(0)| + |(2)-(4)| = 8 \qquad (3.1)$$

3.2.2 Implementation

A Viterbi decoder for basic code usually consists of the following major blocks:

1. Branch Metric Unit (BMU)
2. Path Metric Unit (PMU)
3. Survivor Memory Unit (SMU)

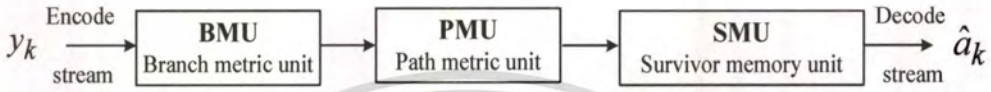

Figure 3.4 Viterbi decoder data flow.

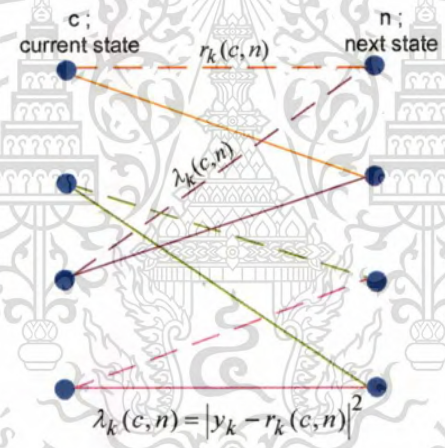

Figure 3.5 Trellis diagram to explain calculation parameter.

1. Branch Metric Unit (BMU)

This part is Branch metric calculation for each value in received compute along the part through trellis, which is norm distances between every possible symbol in the code alphabet, and the received symbol. For a hard decision decoder, a branch metric is a Hamming distance between the received pair (y_k) of bits and the possible "ideal" pair (r_k), as shown in Fig. 3.5.

$$\lambda_k(c,n) = |y_k - r_k(c,n)|^2 \tag{3.2}$$

Where $\lambda_k(c,n)$ is branch metric cost from current state to next state.

y_k is received symbol

r_k is noise channel from PR target defined as

$$r_{k=}\mathcal{F}^{-1}[A(D)H(D)] \tag{3.3}$$

Here $\mathcal{F}^{-1}[\cdot]$ is the inverse discrete Fourier transform, $A(D) = \sum_k a_k D^k$ and $H_{eff}(D)$ is the transfer polynomial of effective partial response targets.

2. Path Metric Unit (PMU)

Path metrics are calculated using a procedure called ACS (Add-Compare-Select). The ACS operation compares the metric distance between the received symbol y_k and any symbols in the code alphabet whose paths merge at a node in the corresponding trellis, $r_k(c,n)$. This procedure is repeated for every encoder state. We calculate the path metric for the path leading to state γ_k by adding the path metric of the previous state γ_{k-1} and corresponding branch metrics, $\lambda_k(c,n)$.

1. *Add* – for a given state, we know two states on the previous step which can move to this state, and the output bit pairs that correspond to these transitions. To calculate new path metrics, we add the previous path metrics with the corresponding branch metrics.

$$\gamma_k = \{\gamma_{k-1} + \lambda_k(c,n)\} \tag{3.4}$$

2. *Compare,select* – we now have two paths, ending in a given state. One of them (with the greater metric) is dropped.

$$\gamma_k = \arg\min\{\gamma_{k-1} + \lambda_k(c,n)\} \tag{3.5}$$

As there are 2^v encoder states, we have 2^v survivor paths at any given time.

3. Survivor Memory Unit (SMU)

In order to finally retrieve this path and corresponding sequence of information symbols a_k , either the sequence of information symbols or the sequences of ACSU decisions corresponding to each of N survivor paths for all state and all step k have to be stored in the survivor memory unit.

Example Consider the trellis diagram of PR4 channel and the receive signal y_k is [1.5 -1 2.2 0.2 -0.2 -2 0.2], we calculating the branch metric and path metric to deciding on the path through the trellis diagram.

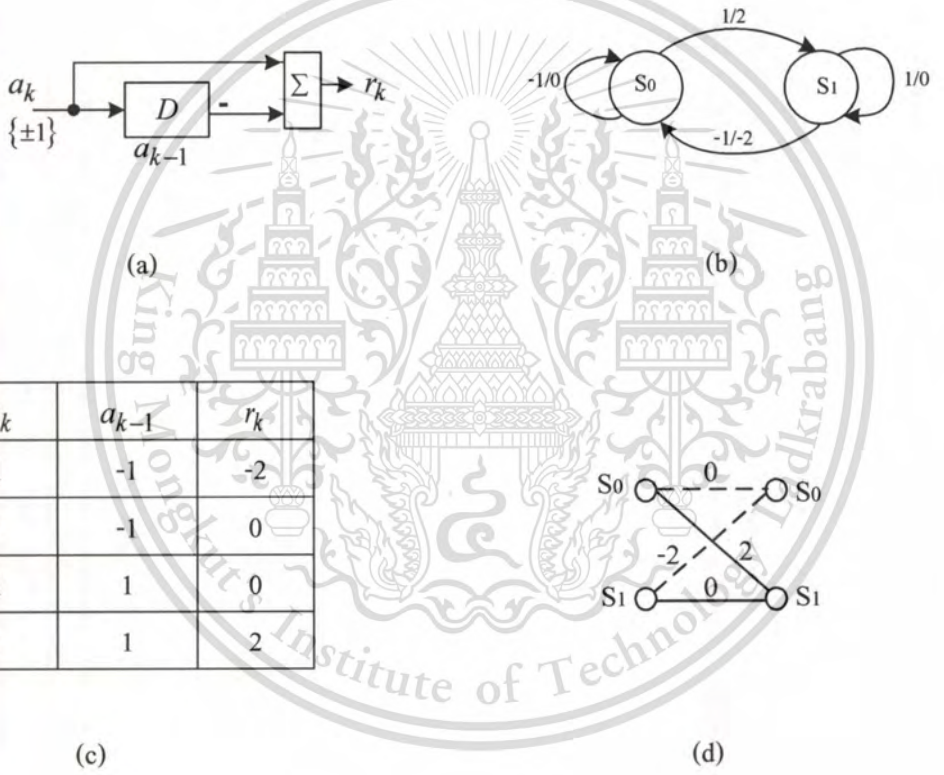

a_k	a_{k-1}	r_k
-1	-1	-2
1	-1	0
-1	1	0
1	1	2

(c)

Figure 3.6 (a) The PR4 channel model, $H(D) = (1 - D)$ = [1 0 -1], (b) The FSM, (c) The state table and (d) The trellis diagram.

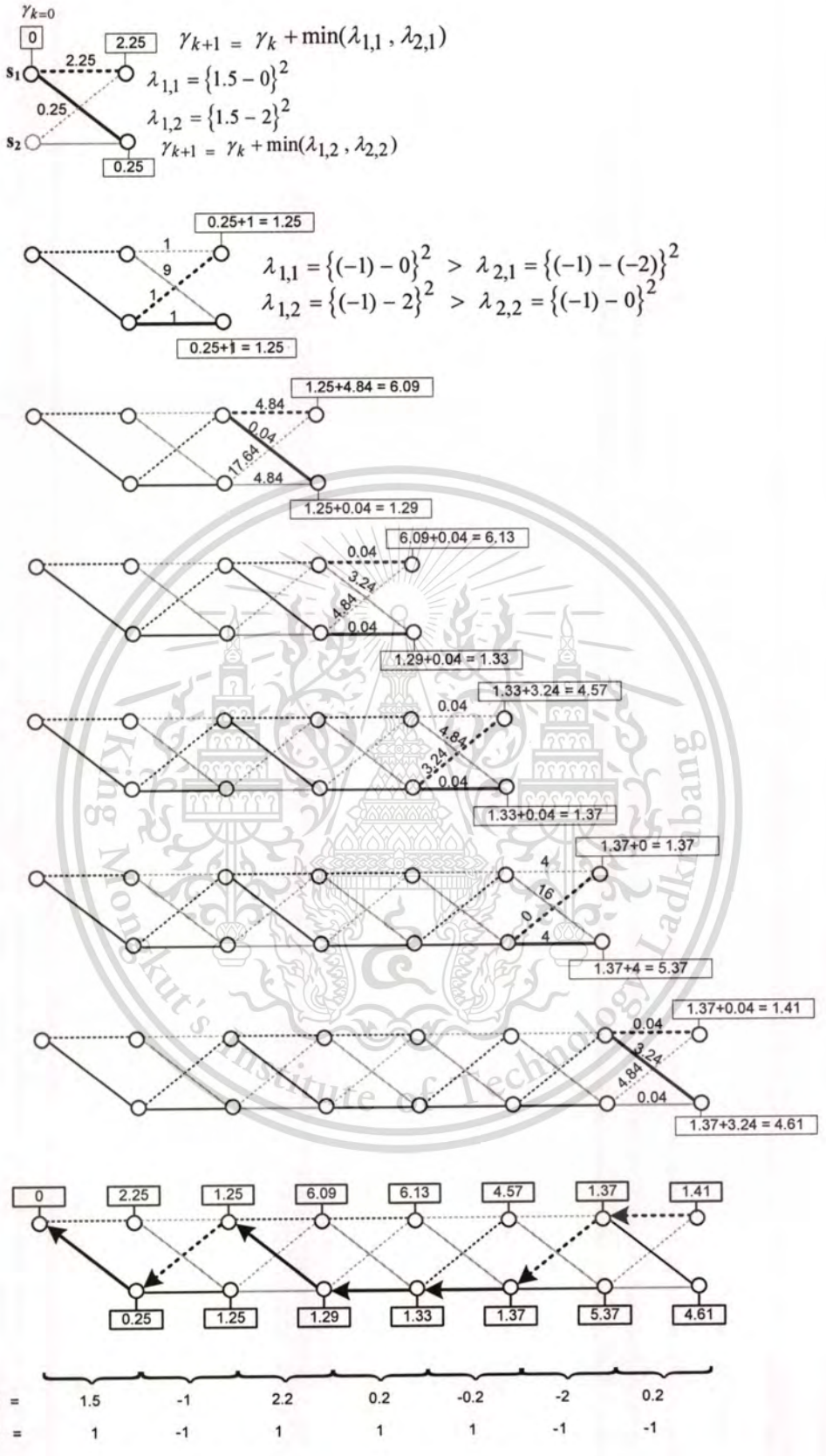

Figure 3.7 The examples of the branch metric and path metric to decide on the path through the trellis diagram of the PR4 channel.

3.3 Noises Predictive Maximum-Likelihood (NPML) Detector

At higher normalized linear densities, generalized partial-response polynomials with real coefficients reduce noise enhancement at the output of the equalizer. The power of the colored noise component can be reduced by noise prediction, which the detection process is composed of two components. The first component is a noise-predictive filter that estimates the noise correlation of the equalized signal. The second component is the Viterbi detector based on trellis of the PR targets with adjusted trellis to the output of the noise predictor [35], [36], [37].

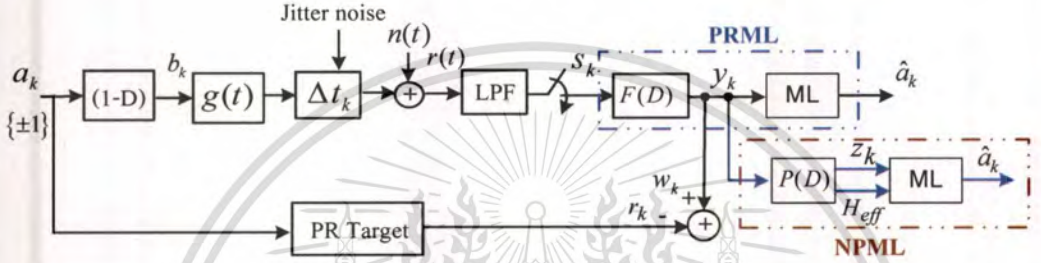

Figure 3.8 The magnetic recording channel model with NPML system.

The binary random sequence $a_k \in \{\pm 1\}$ is channel input, where k represents the discrete-time index, $k = 1 \sim K$ (K is the total number of transmitted bits). The input data sequence with a bit period T is then filtered by an ideal differentiator $(1 - D)$ to form a transition sequence $b_k \in \{-2, 0, 2\}$, where $b_k = \{\pm 2\}$ corresponds to a positive and negative transition, and $b_k = \{0\}$ corresponds to the absence of a transition. The sequence b_k passing through the channel is convolved with the transition response $g(t)$. The noise in PMR can be model as a mixture of additive white Gaussian noise (AWGN) with two-sided power spectral density $N_0 / 2$ and media noise, assume to be transition jitter dominated. We apply a jitter noise modeled as a random shift in the transition position, which has a Gaussian distribution function with zero mean specified as a percentage of T and $|\Delta t_k| \le T / 2$. We can define the SNR at the reading point as [4].

$$\text{SNR} = 10 \log_{10} \frac{E_i}{N_o} \text{ [dB]}, \tag{3.6}$$

where E_i is the energy of the impulse response of the recording channel. Here, the isolate transition response is normalized so that the energy of the impulse response becomes unity.

Hence the read-back signal $r(t)$ can be expressed as

$$r(t) = \sum_{k=-\infty}^{\infty} b_k g(t - kT + \Delta tk) + n(t), \tag{3.7}$$

where $n(t)$ is additive white Gaussian noise (AWGN), and Δt_k is transition jitter noise

The read-back signal $r(t)$ is filtered by a Butterworth low-pass filter with cutoff frequency at $1/2T$, which is sampled at a symbol rate. Its function is to eliminate out-off-band noise and then sampled at the symbol rate, assuming the perfect timing. The received sequence S_k is equalized by 21-tap finite impulse response (FIR) filter calculated to minimize the mean-square error (MMSE) of the equalizer output and target response such that y_k resembles d_k. Let y_k be output data sequence of the PR equalizer at instant k. The finite impulse response (FIR) filter has the polynomial of the PR targets in the form of

$$F(D) = (1 + f_1 D + f_2 D^2 + f_N D^N), \tag{3.8}$$

where the f_i $(i = 1,2,...,N)$ is the coefficients of the filter. The equalized output is

$$y_k = a_k + \sum_{i=1}^{n} f_i a_{k-i} + w_k, \tag{3.9}$$

where w_k is the colored noise sequences at the output of equalizer. The NPML system uses a predictor with N-coefficients. Given the transfer polynomial of the FIR noise predictor filter is $P(D) = (p_1 D + p_2 D^2 + ... + p_N D^N)$ or, equivalently, $E(D) = [1 - P(D)]$ denotes the transfer polynomial of the predictor error filter, then the whitened noise component e_k from the predictor can be computed by

$$e_k = w_k - \hat{w}_k, \tag{3.10}$$

where the noise predicted sample $\hat{w}_k$ can be defined as

$$\hat{w}_k = \sum_{i=1}^{N} w_{k-i}\, p_i\,, \tag{3.11}$$

then

$$e_k = w_k - \sum_{i=1}^{N} w_{k-i}\, p_i \tag{3.12}$$

The length N coefficients of a noise prediction filter are determined by solving the system of well-known normal equation given by [38]

$$r_{ww}(i) = \sum_{j=1}^{N} p_i R_{ww}(i-j) \tag{3.13}$$

where R_{ww} is the autocorrelation function, which can be written in the matrix form as

$$\underbrace{\begin{bmatrix} r_{ww}(1) \\ r_{ww}(2) \\ \vdots \\ r_{ww}(N) \end{bmatrix}}_{\mathbf{r}} = \underbrace{\begin{bmatrix} R_{ww}(0) & R_{ww}(1) & \cdots & R_{ww}(N-1) \\ R_{ww}(1) & R_{ww}(0) & \cdots & R_{ww}(N-2) \\ \vdots & \vdots & \ddots & \vdots \\ R_{ww}(N-1) & R_{ww}(1) & \cdots & R_{ww}(0) \end{bmatrix}}_{\mathbf{R}} \underbrace{\begin{bmatrix} p_1 \\ p_2 \\ \vdots \\ p_N \end{bmatrix}}_{\mathbf{p}}, \tag{3.14}$$

where **R** represents the square matrix, p_i is determined by

$$\mathbf{p} = \mathbf{R}^{-1}\mathbf{r}\,, \tag{3.15}$$

where $\mathbf{p} = p_1\ p_1 \cdots p_N$ and $\mathbf{r} = [r_{ww}(1)\, r_{ww}(2) \cdots r_{ww}(N)]^T$.

The NPML detection results from the embedding the noise prediction/whitening process into the branch metric computation of the viterbi detector. The output of noise predictor error filter Z_k to viterbi detector can be computed by

$$z_k = y_k + \sum_{i-1}^{n} p_i y_{k-1} \tag{3.16}$$

or in D domain is

$$Z_k = (y_k)[1 - P(D)] \tag{3.17}$$

and

$$H_{eff}(D) = H(D)[1 - P(D)] \tag{3.18}$$

where $H_{eff}(D) = (1 - g_1 D - g_2 D^2 - ... - g_{N+v} D^{N+v})$ represents the transfer polynomial of effective targets which corresponds to noise predictor error filter, where the g_i $(i = 1, 2, ..., N+v)$ is the N-tap coefficients of the effective targets, v is the memory of PR targets and $H(D)$ is partial response targets, then the viterbi detector uses a state trellis with the number of state 2^{v+N}. The branch metric of the NPML detector for effective targets samples corresponding to a transition from state p to state q takes the form

$$\lambda_k(p,q) = \left| Z_k - \hat{O}_k(p,q) \right|^2, \tag{3.19}$$

where $\lambda_k(p,q)$ represents the branch metric cost from state p to state q, and $\hat{O}_k$ is noiseless channel output from effective targets ($H_{eff}(D)$) defined as

$$\hat{O}_k = \mathcal{F}^{-1}\left[A(D) H_{eff}(D) \right], \tag{3.20}$$

where $\mathcal{F}^{-1}[\cdot]$ is the inverse discrete Fourier transform, $A(D) = \sum_k a_k D^k$ and $H_{eff}(D)$ is the transfer polynomial of effective partial response targets. We can compared the number of state trellis between PRML and NPML detector as

PRML state trellis = 2^v

NPML state trellis = 2^{v+N}

where v is memory of PR target and N is memory of noise predictive filter.

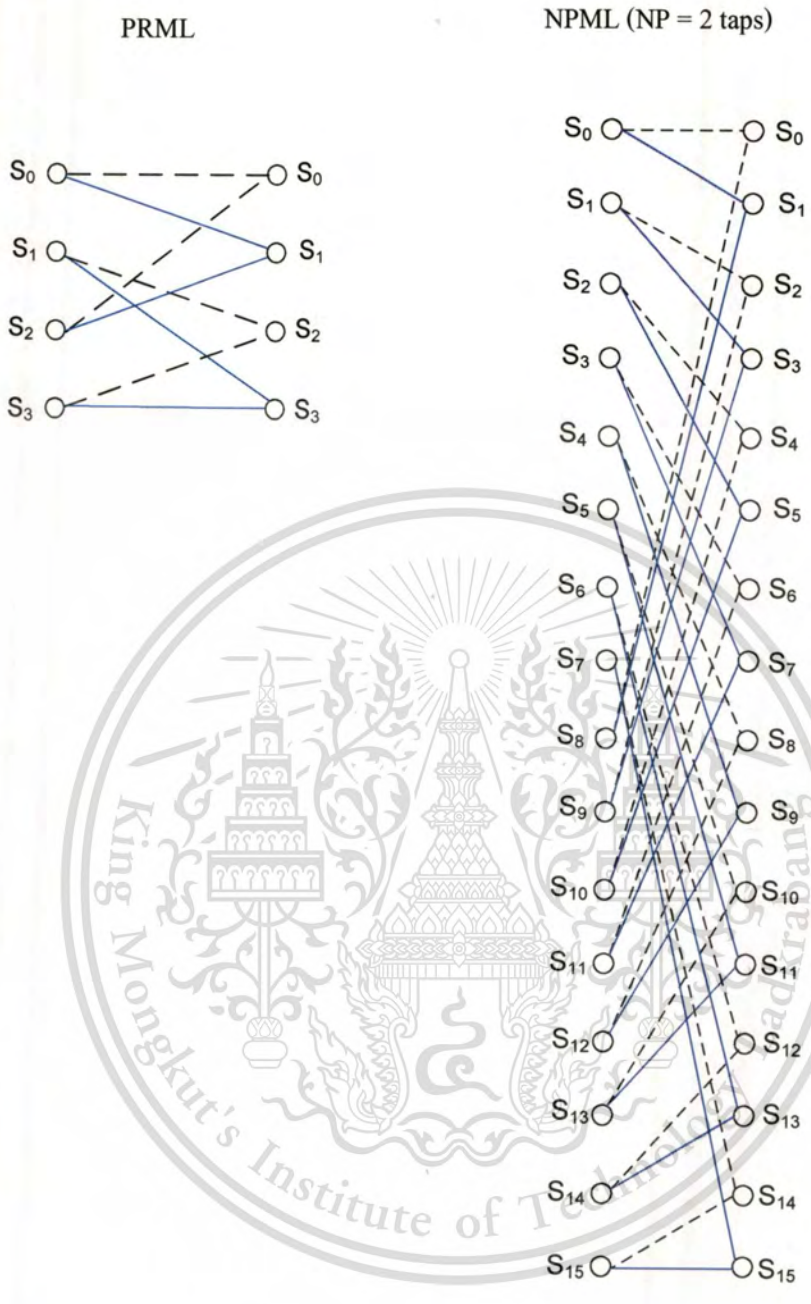

Figure 3.9 Comparison the number of state trellis of PR2 target, [1 2 1] between PRML detector and NPML detector at noise predictor = 2 tap.

3.4 Type of errors

There are mainly two types of errors that occur in magnetic recording system, that are single-bit errors and bursts of errors. Normally, single bit errors occur caused a short-duration noise event, which results in an extra pulse or a missing pulse as shown is in Figure 3.10 (a). Burst of errors occur when a bit's group is detected erroneously an example of a burst of three errors in Figure 3.10 (b). The defect of magnetic medium such as a scratch of a defective spot spanning over many bit periods might be the cause of burst of errors. However, burst of errors may also occur at the output of the ML detector in a PRML channel. The ML detector decision contains a group of channel bit. Any event in the ML detector will result in detecting a wrong sequence of bits [15].

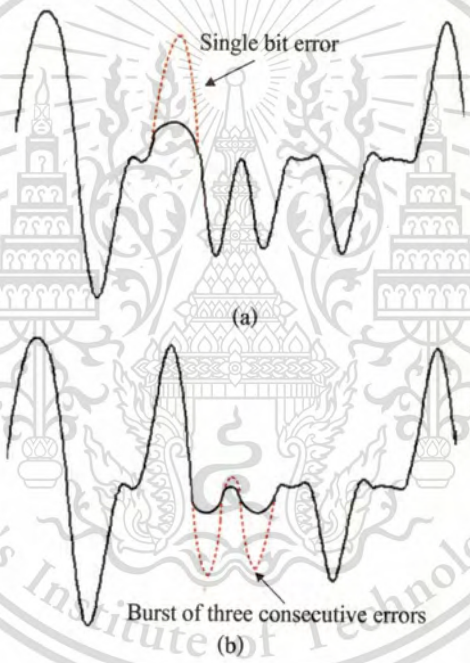

Figure 3.10 Illustration of a single bit error and a burst of errors.

3.5 Error Event Analysis for Perpendicular Magnetic Recording

The concept of error event is essential for performance analysis of partial response channels. An error event ε corresponds to a distinct separation between the correct path and the estimated path in the trellis of the associated Viterbi algorithm [26]. The relative likelihood of the error events in white noise is determined by its Euclidean distance. A smaller distance corresponds to a more probable error event. When the noise is not white, the Euclidean metric is

no longer an accurate measure of distance. The concept of the effective distance of an error event has been introduced to better gage the error event probability under such conditions. A list of the Euclidean distance for the error events associated with the most common partial response polynomials was presented in [26]. Effective distances for PRML systems corrupted by only white noise colored by the equalizer have been calculated in [27], [28]. Some error event analysis assuming the presence of transition noise has been performed [26]. The most significant error events in longitudinal recording contain an odd number of erroneous bits (e.g., $\pm[2]$, $\pm[2,-2,2]$, $\pm[2,-2,2,-2,2]$, as observed in [38]-[40]). In perpendicular recording, however, the critical error events take different forms, as the inter-symbol interference (ISI) characteristics are substantially different from the longitudinal recording. At moderately high densities for example, perpendicular recording is most prone to the error events of the types $\pm[2,-2]$, $\pm[2,-2,0,2,-2]$ and $\pm[2,-2,0,2,-2,0,2,-2]$.

Consider a partial response (PR) target $h(D) = h[0] + h[1]D + \cdots + h[v]D^v$, where D is the delay operator and v is the memory of the PR channel. Let $A(D) = \sum_k a_k D^k$ be an input sequence to the PR channel and $a_k \in \{\pm 1\}$. The output of the PR channel $r_k = \mathcal{F}^{-1}[A(D)H(D)]$ is the output sequence of the PR channel in the absence of noise. In the presence of noise n(k), the output sequence will be $y_k = r_k + n_k$. With that output sequence, the Viterbi algorithm produces a maximum-likelihood estimate $\hat{a}_k$, where $\hat{a}_k \in \{\pm 1\}$. An input error sequence is defined as

$$\varepsilon_x(D) = (a_{k1} - \hat{a}_{k1}) + (a_{k2} - \hat{a}_{k2})D + (a_{k3} - \hat{a}_{k3})D^2 + \cdots + (a_{kn-v-1} - \hat{a}_{kn-v-1})D^{n-v}$$

An error event can be represented by the associated input error sequence since they are in one-to-one correspondence. We can denote the input error sequence $\varepsilon_a(D)$ associated with an error event ε as, where $\varepsilon_x = \sum_{k=1}^{l(\varepsilon)} \varepsilon a_k D^k$ and $l(\varepsilon)$ is the length of input error sequence or simply the length of the error event [38]. The input error sequences are often denoted using {- , 0 , +} instead of using {-2, 0,+2}. The number of errors in the associated input error event ε is defined as the Hamming weight, $w_H(\varepsilon)$ of the event (equal to the number of nonzero coefficients in $\varepsilon_a(D)$). For example, an error event can be indicated as '+0+-' and for the error event we have $l(\varepsilon) = 4$ and $w_H(\varepsilon) = 3$. It is clear that the first coefficient of an input error sequence is nonzero since the correct path a_k and the estimated path $\hat{a}_k$ must separate from each other at that position in order to create an error event. If we have v consecutive zeros in input error sequence, the correct path a_k and the estimated path $\hat{a}_k$ converge into the same state,

which means the end of an error event. Thus, an input error sequence $\varepsilon_x(D)$ cannot contain v consecutive zero coefficients and the last element must be nonzero. Note that the ending v zeros of input error sequence is left out for short notation. The Hamming weight of an input error sequence cannot be greater than the length of the input error sequence. In addition, since the maximum run length of zeros in input error sequence is the memory of PR channel (v) -1, we have a lower bound of the Hamming weight of an input error sequence. Therefore we have

$$\left\lceil \frac{l(\varepsilon)-1}{v} \right\rceil + 1 \leq wH(\varepsilon) \leq l(\varepsilon) \ , \tag{3.21}$$

where $\lceil . \rceil$ is mean ceiling and v is memory of PR target. An output error sequence of PR target is defined as

$$\varepsilon_x(D) = \varepsilon_a(D) * H(D) = \varepsilon x(D) = \sum_{k=1}^{l(\varepsilon)} \varepsilon a_k D^k \tag{3.22}$$

The squared distance $d^2(\varepsilon)$ or $d^2\{\varepsilon_x(D)\}$ of an error event ε is defined as

$$d^2\{\varepsilon_x(D)\} = \|\varepsilon_x(D)\|^2 = \sum_{k=1}^{l(\varepsilon)+v} \varepsilon a_k{}^2 \tag{3.23}$$

The SNR of an error event at the input to the detector is defined as

$$SNR\{\varepsilon_x(D)\} = \frac{d^2\{\varepsilon_x(D)\}}{\sigma_w} \tag{3.24}$$

With white noise, the noise variance is the same in all directions so the relative probability of the error is specified by their square distance or Euclidean distance. When the noise is colored, the variance depends upon the direction of the error event. Hence the squared effective distance $d_{eff}^2(\varepsilon)$ of an error event ε is defined as

$$d_{eff}{}^2\{\varepsilon_x(D)\} = \sigma_w{}^2 \frac{(\varepsilon^T \varepsilon)^2}{\varepsilon^T R_{ww} \varepsilon} \tag{3.25}$$

The effective SNR of an error event at the input to the detector is defined as

$$SNR_{eff}\{\varepsilon_x(D)\} = \frac{{d_{eff}}^2\{\varepsilon_x(D)\}}{{\sigma_w}^2} \tag{3.26}$$

where ${\sigma_w}^2$ is the noise variance at the output of the equalizer, ε is the column vector of $\varepsilon_x(D)$, ε^T is the transpose vector of ε and R_{ww} is the autocorrelation function of the noise.

Error Performance

We can calculate an approximate bit error rate (BER) or the symbol probability of error $\Pr(e)$, can be computed by weighting each error event ε by the Hamming weight $w_H(\varepsilon)$ is

$$BER \approx K_2 Q\left(\frac{1}{2}\sqrt{SNR_{eff}}\right) \tag{3.27}$$

$$Pr(e) \approx K_2\, Q\left(\frac{d_{eff\,min}}{2\sigma_w}\right), \tag{3.28}$$

and

$$K_2 = \sum_{\varepsilon \in d_{min}} \left[wH(\varepsilon) \prod_{i=0}^{n-v} \frac{m - |\varepsilon_{xi}|}{m} \right] \tag{3.29}$$

where K_2 is a constant independent of the noise variance at the output of the equalizer,

ε_{xi} : is the number of nonzero coefficients in output error sequence $\varepsilon_x(D)$,

m : is level in data sequence a_k (in this work is 2),

n : is length of output error sequence $\varepsilon_x(D)$ and

$Q(\bullet)$: is the probability of error function can define as

$$Q(x) = \sqrt{(2\pi)} \int_x^{\infty} dy\, e^{-(y^2/2)} \tag{3.30}$$

3.6 Detector performance

In this section, we present BER simulation results for two target type for PMR system, and investigate the BER performance in PRML detector and NPML detector, as seen in Fig. 3.7. In the simulations, the received sequence S_k is equalized by 21-tap finite impulse response (FIR) filter calculated to minimize the mean-square error (MMSE) of the equalizer output and target response such that y_k resembles d_k. We process each sector consisting of 4096 information bits and let the parameter of normalized recording density (ND) = 2.5, media jitter noise (J2) various 10% 30% and 50%. The noise predictive filter (NP Tap) has 4 taps. The average BER from the results are plotted versus the SNR (dB). The dc-attenuation targets polynomials are (2 3 0 -1) and (5 6 0 -1), while the dc-full targets are (1 6 7 2) and (4 6 4 2). We compare the performance of PRML and NPML detector at different target types.

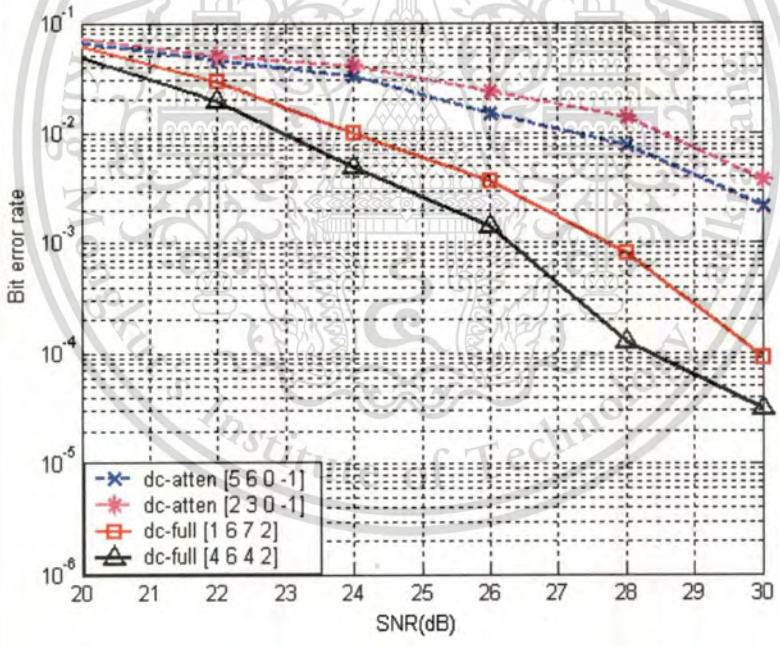

Figure 3.11 The PRML performance between dc-attenuation targets (5 6 0 -1), (2 3 0 -1) and dc-full targets (1 6 7 2), (4 6 4 2).

In Fig. 3.11, the BER performance of PRML detector at different target types between dc-attenuation targets (5 6 0 -1), (2 3 0 -1) and dc-full targets (1 6 7 2), (4 6 4 2) with 10% jitter noise is shown. We can see that the dc-full targets achieve than dc-attenuation targets.

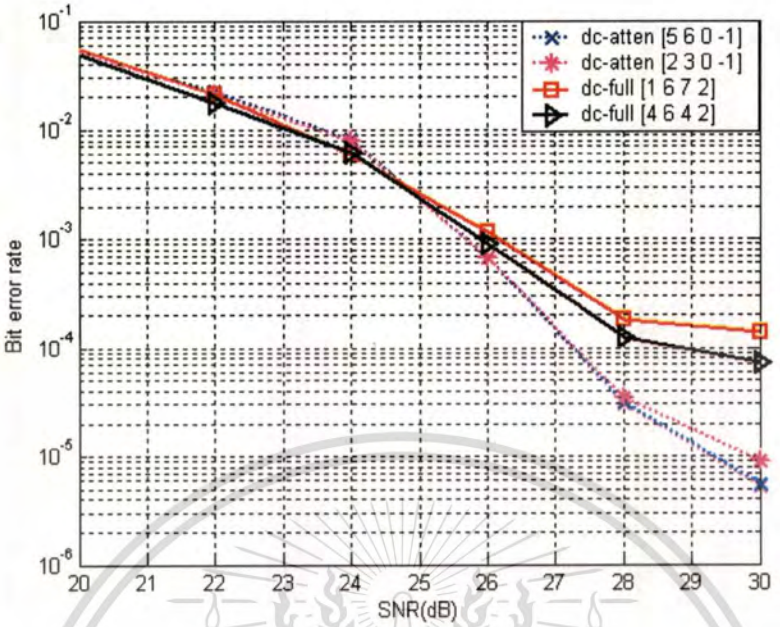

Figure 3.12 The NPML performance between dc-attenuation targets (5 6 0 -1), (2 3 0 -1) and dc-full targets (1 6 7 2), (4 6 4 2).

In Fig. 3.12, the BER performance of NPML detector at different targets types between dc-attenuation targets (5 6 0 -1), (2 3 0 -1) and dc-full targets (1 6 7 2), (4 6 4 2) versus the system performance is shown. We can see at higher SNR, the dc-attenuation targets achieve better performance than dc-full targets. For the example, at BER $\approx 1\times10^{-4}$, the dc-attenuation targets (5 6 0 -1) have gain more than dc-full targets (4 6 4 2) about 1.8 dB at the jitter noise is 10% and noise predictor is 4 tap.

In Fig. 3.13, the BER performance of PRML and NPML detector with dc-full targets (1 6 7 2) at percentages jitter noise various 10%, 30%, 50% and NP_Tap = 4 tap. We can see at BER $\approx 8\times10^{-4}$, the NPML have gain more than PRML about 1.8 and 1.4 dB at the jitter noise is 10% and 50% sequentially.

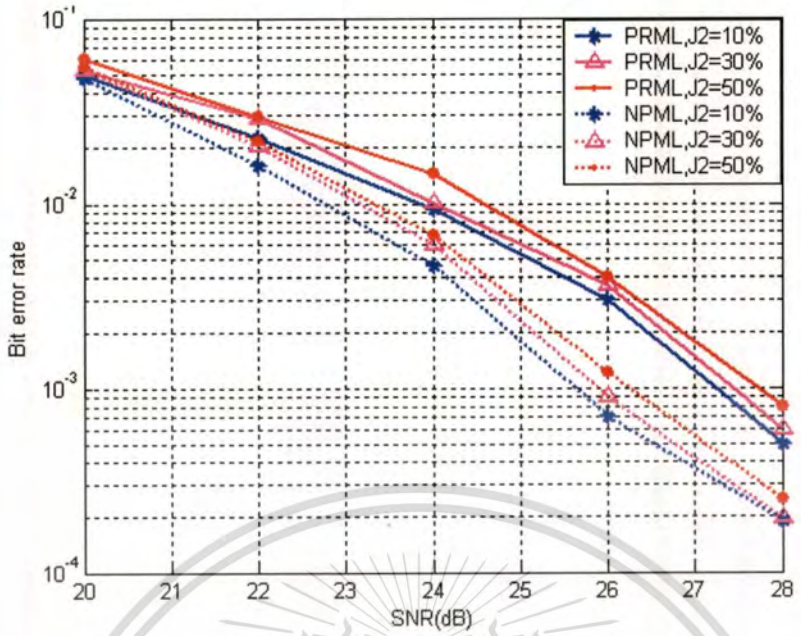

Figure 3.13 The PRML and NPML performance of percentages jitter noise various with dc-full targets (1 6 7 2).

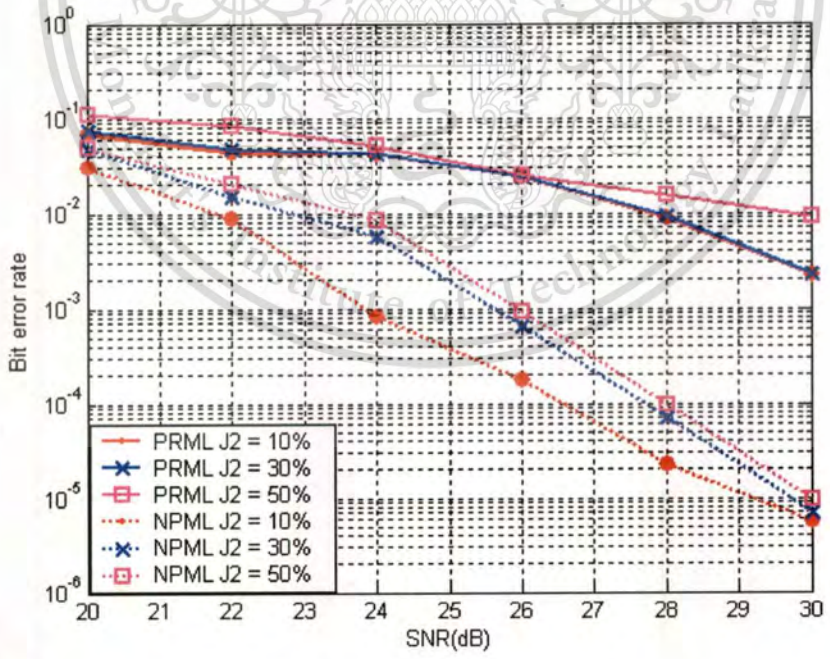

Figure 3.14 The PRML and NPML performance of percentages jitter noise various with dc-attenuation targets (5 6 0 -1).

In Fig. 3.14, the BER performances of PRML and NPML detector with dc-attenuation targets (5 6 0 -1) with transition jitter noise of 10%, 30% and 50% are shown. We found that the NPML detector achieves better performance than PRML detector.

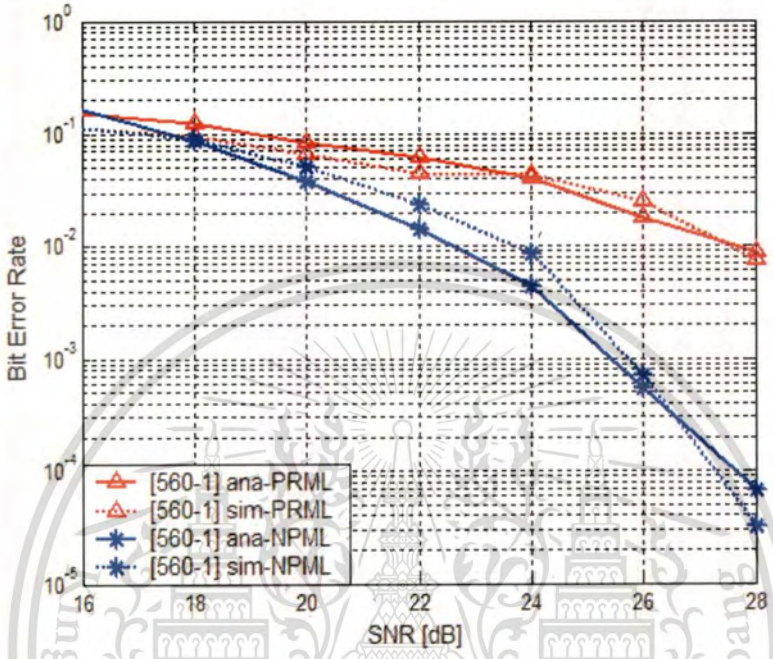

Figure 3.15 BER from error event analysis and simulation, error pattern is [2 -2], ND=2.5, NP=4 tap, J2=10%.

In Fig. 3.15, we compare the BER of PRML and NPML system based on MEPR3 [5 6 0 -1] target. The analytical curves were obtained by the error event probability calculation. Mat lab simulation result was obtained by counting 500 bit errors for each point at ND = 2.5, noise predictor 4 taps and Transition shift (Jitter noise) = 10%.

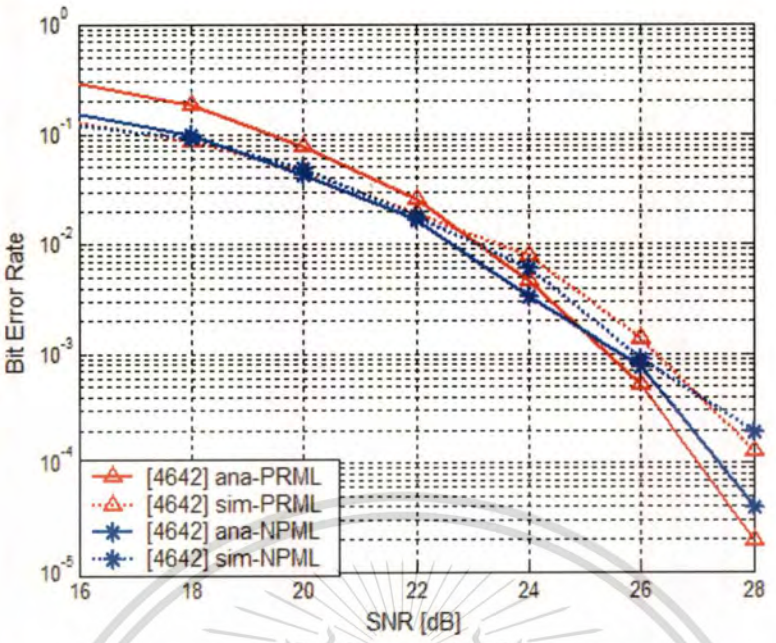

Figure 3.16 BER from error event analysis and simulation, error pattern is [2 -2], ND = 2.5, NP=4 tap, J2=10%.

In Fig. 3.16, we compare the BER of PRML and NPML system based on MEPR2 [4 6 4 2] target. The analytical curves were obtained by the error event probability calculation. The simulation mat lab result was obtained by counting 500 bit errors for each point at ND = 2.5, noise predictor 4 taps and Transition shift (Jitter noise) = 10%. We can see that the BER of simulation and analysis result is very close to each other in moderate SNR.

3.7 Summary

We investigate using PRML and NPML detector for partial response targets types appropriate for high density perpendicular magnetic recording (PMR) channel with the environment of electronics noise and jitter noise. From the simulation results, the bit error rate (BER) performance of NPML system with dc-attenuation targets is better than that of PRML system, while the dc-full targets is more suited to PRML system at low jitter noise. However, with media-noise-dominant model, the NPML detector achieves higher improvement gain over PRML detector at high SNR.

In addition, we explain and compare the performance of PRML and NPML from error event analysis and simulation. We can see that the BER of simulation and analysis are closely, while the analytical method can be calculated without the need for time-consuming simulation.

CHAPTER 4

THERMAL ASPERITY

This chapter deals with the thermal asperity (TA) effects and the previous works in detection and cancellation of the thermal asperity effects in the perpendicular magnetic recording system. After that, we propose a new method to estimate and reduce its effects through the state trellis of the partial response (PR) targets.

4.1 Thermal Asperity in Perpendicular Magnetic Recording

The magnetic storage industry has been increasing the storage capacity of hard disk drive through technology advancement such as perpendicular magnetic recording system and magneto-resistive (MR) heads. The MR head includes an MR element made out of a material with greater sensitivity and changes electrical resistance in response to the strength of the magnetic field [1]. The MR head normally glides over the spinning magnetic disk. When the MR head hits an asperity on the disk surface or hovers closely to the media, the MR element heats up rapidly then decays relatively slowly and is typically known as thermal asperity (TA). The effect of this transient phenomenon is a change in the baseline of the read-back signal coming from the MR head. This transient change contains a substantial low-frequency component, which causes loss of read-back data. The severity of the loss depends on the robustness of the data detection system and the rate at which TA event occurs [9].

Therefore, the recording head signal of perpendicular recording systems typically experiences the increased rate of TA events as well as the longer duration of each event. With the increased likelihood of errors, it is possible that the error correcting code (ECC) that is used in the recording system may not be able to generate the user data.

In previous works, perpendicular magnetic recording with a dc-full component was considered the best choice for a PMR system in the absence of disturbances other than an additive white Gaussian noise (AWGN) [2]. With a media-noise dominant channel as in PMR, however, it is reported that the bit error rate (BER) can be further improved when a partial response (PR) target with a dc component is used. It is well-known that a dc-attenuation (or dc

component) PR targets is suitable for the transition jitter-noise dominant channels when an NPML detector is employed [36].

A common method to reduce the effect of TA is to implement a high-pass filter (HPF) in the system and adjust its cut-off frequency according to [3], [4]. Dorfman and Wolf proposed a method for TA suppression with the technique using the $(1-D)$ filter before processing the sample in a Viterbi detector, where D is the delay operator which represents a delay of a bit interval T. Two Viterbi detectors are run in parallel, one for an extended partial response class-4 (EPR4) channel and the other for a partial response class-5 (PR5) channel equipped with the filter when TA occurs. However, this improvement in the TA operations reduces the overall performance of the system. Similarly, for the PMR system, Ueno proposed a method to reduce error deterioration due to TA by switching from the PR targets with DC component to the PR targets without DC component [6]. Both methods use two channels running in parallel to avoid the impact when TA occurs. This approach requires an increased detector complexity to account for the different equalization targets. Alternatively, the TA signal can be estimated and used for the cancellation. In [8], Mathew and Tjhia proposed a simple TA estimation method using window averages, consequently, the TA cancellation of the read-back signal can be done by a straightforward subtraction. Here, we will focus on the proposed method in [8], or Matthew's method, to compare its performance with the proposed TA estimation method using the trellis.

4.2 Mathew's Thermal Asperity Estimation and Cancellation Method

Mathew proposed method of TA detection is also based on the fact that a TA will cause a shift in the baseline of the read back signal. The average value of the normal read-back signal is zero while that of the TA-affected read-back signal is not. Hence, the first criterion for detecting the occurrence of a TA is that the average value of the read-back signal must exceed a particular threshold value. The average value, $q(n)$, of the read-back signal, is given by

$$q(n) = \frac{1}{L} \sum_{i=n-\beta}^{n+\beta} c(i)\,, \tag{4.1}$$

where $\beta = \left(\frac{L-1}{2}\right)$ and L (an odd integer) is the length of the window for calculating the average value of the read-back signal. Based on this criterion, a TA is detected when $q(n) \geq m_1$ where $m_1 > 0$ is a condition. The method of detecting a TA based on this criterion is called "Method 1." This method can be further improved to ensure accurate TA detection. It is observed that the

occurrence of a TA causes not only a shift the baseline of the read-back signal but also an increase in the individual samples of the read-back signal itself. Therefore, an additional criterion that can be used to detect a TA is that the values of the read-back signal samples themselves must exceed a particular threshold value for a few consecutive samples. This helps to reduce a false detection. In other words, $c(n) \geq m_2$ for a few consecutive samples where $m_2 > 0$ is a condition. Combining these two criteria, a TA is detected when $q(n) \geq m_1$ and $c(n) \geq m_2$ for a few consecutive samples, this is called "Method 2."

After the TA is detected, the next step will be to eliminate or reduce its effect by subtracting a reconstructed TA signal from the TA-affected read-back signal. The TA signal can be reconstructed from the read-back signal using the average value, $q(n)$, of the read-back signal at averaging window length. Once a TA is detected, the TA compensation operation is activated. The TA detector is disabled during TA compensation, i.e., for a duration of T_f. The read-back signal after compensating for the TA distortion is given by

$$d(n) = \begin{cases} c(n) - q(n) & ;\text{if TA present} \\ c(n) & ;\text{other wise} \end{cases} \tag{4.2}$$

where the TA compensation $q(n)$ is computed as in (3-1). The TA-compensated signal $d(n)$ is fed to the equalizer and the equalizer output is sent to a Viterbi detector for data detection.

4.3 Proposed Thermal Asperity Estimation and Cancellation System

For the longitudinal magnetic recording (LMR) read channel, PR target has been chosen so as to match the high-frequency response of the read-back signal, and the term $(1-D)$ gives the polynomial of a dc-free response that matches the low-frequency response of the dc-free LMR signal. If it is used in a perpendicular magnetic recording (PMR) system, the strong low-frequency energy of the PMR signal must be filtered out [4]. Thus, we propose an estimation and cancellation method of TA based on a dc-full response targets through the trellis. A calculation method is to estimate the TA signal from the equalized signal and eliminate the TA effects before feeding it to the Viterbi detector.

The schematic diagram illustrating a model of the new method to estimate and effectively reduce thermal asperity in the PMR channels with a state trellis is shown in Fig. 4.1.

Figure 4.1 Proposed methods for thermal asperity estimation and cancellation.

Fig. 4.1 shows the block diagram of the new method to estimate and effectively reduce thermal asperity in the PMR channels. This consists of two blocks. In the first block, the trellis is used to obtain the estimate of TA noise, *TA_est*, and the other is the moving average to smooth the TA noise estimate. Then, we subtract the results from the equalized signal. The block will be explained in details in the following subsections.

4.3.1 Trellis estimate TA noise

We can divide the tasks into two parts.

(a) TA detection

The TA detection here is used to determine the start and stop positions in the PR equalized signal sequence. The estimated TA is then canceled before the Viterbi detector. The TA is found from comparing the amplitude of the PR equalized signal with the threshold. Here, the threshold Γ (Gamma) is set as $\Gamma = \lambda_{max} + \delta$, where λ_{max} is the maximum value of the noiseless channel output from PR targets and δ is an incremental value obtained from the simulation to ensure the accurate start-stop position of the TA. The TA affected start position is determined when the PR equalized sample y_k is higher than the threshold value, Γ and the TA affected stop position occurs when the PR equalized sample y_k is lower than 1.8 % of maximum TA amplitude and at least $2^v \times 2$ samples, where v is the memory of PR targets.

(b) TA Estimation

Once the TA start and stop positions are known, the TA estimator will provide the noise and TA estimates. The estimation is processed through the trellis of the PR target for all samples. For the TA affected samples, the TA part is estimated, otherwise, only the noise part is estimated. These two cases are described as follows.

Case I. The samples without TA

When the equalized sample y_k is less than the threshold value for detecting TA, we can find the noise estimate through the state trellis of the PR target. Given that the selected path at time $k-1$ ends at state s_i, the best path on the trellis at time k is selected based on the minimum distance, $\hat{\lambda}_k$, between y_k and λ_k is given by

$$\hat{\lambda}_k = \min_{j\in\{-1,1\}} |y_k - \lambda_k(j)| \tag{4.3}$$

where $\lambda_k(j)$ is a noiseless PR channel output from state s_i with input $j \in \{-1, 1\}$. Note that the best path is selected from the minimum distance chosen only; there is no metric accumulation like in the Viterbi algorithm.

Case II. The samples with TA

For the samples with TA, we compute the minimum distance to select the best path from

$$\hat{\lambda}_k = \min_{j\in\{-1,1\}} |\tilde{y}_k - \lambda_k| \,, \tag{4.4}$$

where $\tilde{y}_k$ is computed from

$$\tilde{y}_k = y_k - |TA_{est,k-1}| \tag{4.5}$$

For both case I and II, once the best path is selected, the corresponding noiseless PR channel output $\hat{\lambda}_k$ on the branch is used to estimate the TA (or noise) level at time k by subtracting from the equalized signal, i.e.,

$$TA_{est,k} = y_k - \hat{\lambda}_k \,. \tag{4.6}$$

Note that for the samples without TA, we have the noise estimates rather than the TA estimates.

4.3.2 Moving average and cancellation block

After the TA (noise) estimations are completed, we obtain the moving average of the TA (noise) estimates and then subtract the result from the equalized signal y_k. Based on (4.7), the moving-averaged TA (noise) estimates $MATA_{est,k}$ can be formed

$$MATA_{est,k} = \frac{1}{n}\sum_{i=k-\phi}^{k+\phi} TA_{est,i} \quad . \tag{4.7}$$

and the adjusted PR equalized signal y_k is

$$\acute{y_k} = y_k - MATA_{est,k} \quad . \tag{4.8}$$

where $\phi = (n-1)/2$ and n (an odd integer) is the window length. This signal is then used as input to the Viterbi detector.

In Fig.4.2, an example the finite state machine and trellis diagram of a PR2 target to explain the TA detection. We can define the threshold Γ (Gamma) is 6, where the maximum value of the noiseless channel output from PR targets (λ_{max}) is 4 and an incremental value (δ) is 2. That is the TA start when the PR equalized signal y_k is large than 6 and TA stop is when the PR equalized signal y_k is lower than 1.8% of maximum TA amplitude to the amount more than $2^v + 1 = 8$ consecutive sample are shown in Fig. 4.3 and Fig.4.4.

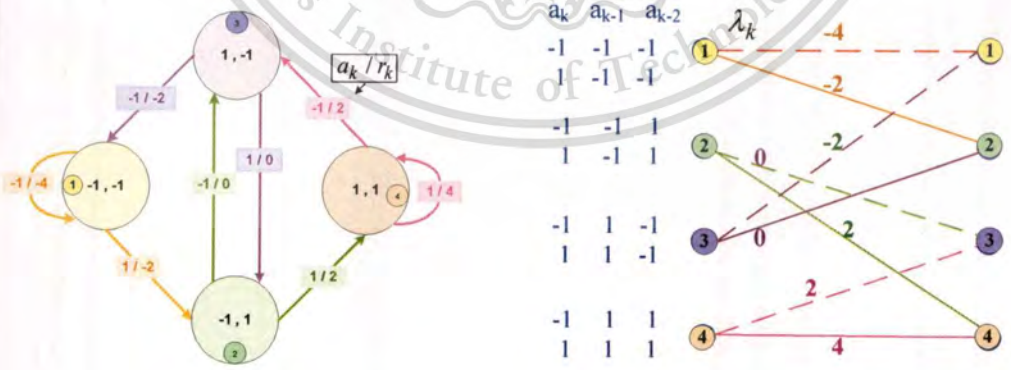

a_k is the input bit

r_k is noiseless channel output from PR target

Figure 4.2 Example of finite state machine and trellis diagram of a PR2 target.

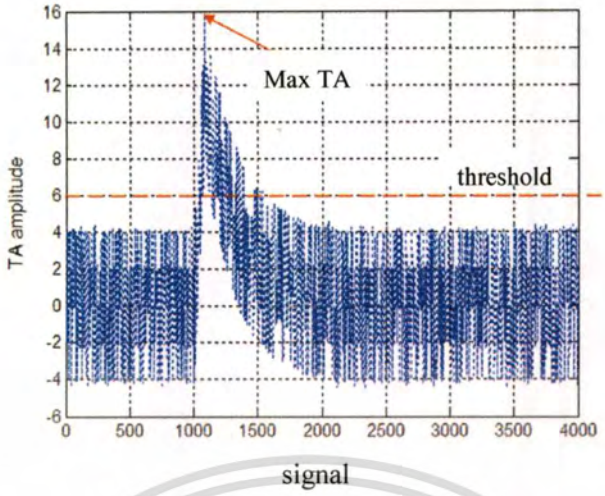

Figure 4.3 The Equalized signal with TA and threshold mark for TA detection of PR2 target at ND = 1.5, SNR = 25 dB, $A_o = 3$, $T_d = 250$ bits and $T_f = 1080$ bits.

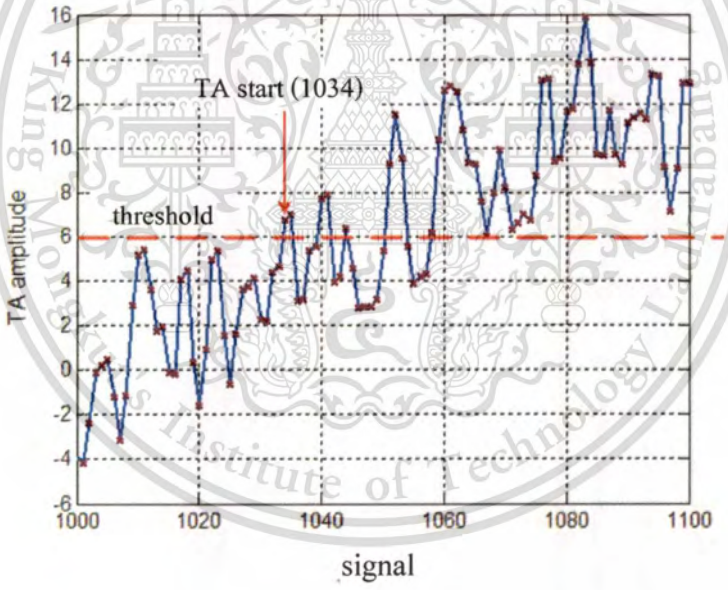

Figure 4.4 The Equalized signal with TA zoom area on TA start from TA detector.

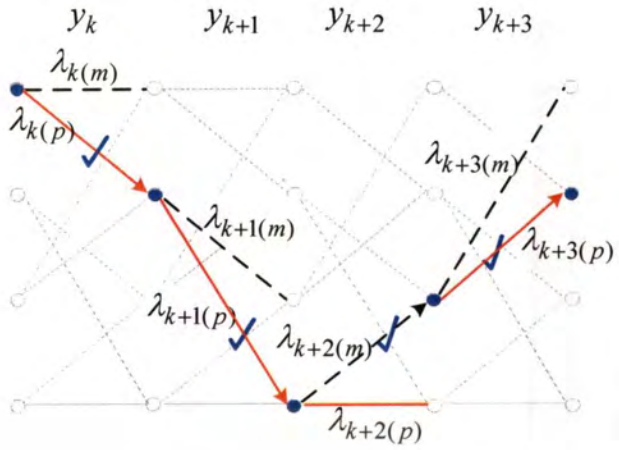

Figure 4.5 Shows an example of the path selection at time k to $k+3$.

From Fig. 4.6 example, to calculation method to select the best path to estimate noise based on a PR2 target through the trellis and noise estimate at each time. The $\lambda_{k(m)}$ is noiseless channel output from PR target at input bit {-1}, $\lambda_{k(p)}$ is noiseless channel output from PR target at input bit {1} and y_k is equalized signal at time k. The arrow lines denote the selected branch (path). At each time instant, only two branches are considered, that is

$|y_k - \lambda_{k(m)}| > |y_k - \lambda_{k(p)}|$; $\lambda_{k(p)}$ is the best path to select (λ_{k_select}).

$|y_{k+1} - \lambda_{k+1(m)}| > |y_{k+1} - \lambda_{k+1(p)}|$; $\lambda_{k+1(p)}$ is the best path to select (λ_{k+1_select}).

$|y_{k+2} - \lambda_{k+2(m)}| < |y_{k+2} - \lambda_{k+2(p)}|$; $\lambda_{k+2(m)}$ is the best path to select (λ_{k+2_select}).

$|y_{k+3} - \lambda_{k+3(m)}| > |y_{k+3} - \lambda_{k+3(p)}|$; $\lambda_{k+3(p)}$ is the best path to select (λ_{k+3_select}).

$TA\_est_k = y_k - \lambda_k(p)$.

$TA\_est_{k+1} = y_k - \lambda_{k+1}(p)$.

$TA\_est_{k+2} = y_k - \lambda_{k+2}(m)$.

$TA\_est_{k+3} = y_{k+3} - \lambda_k(p)$.

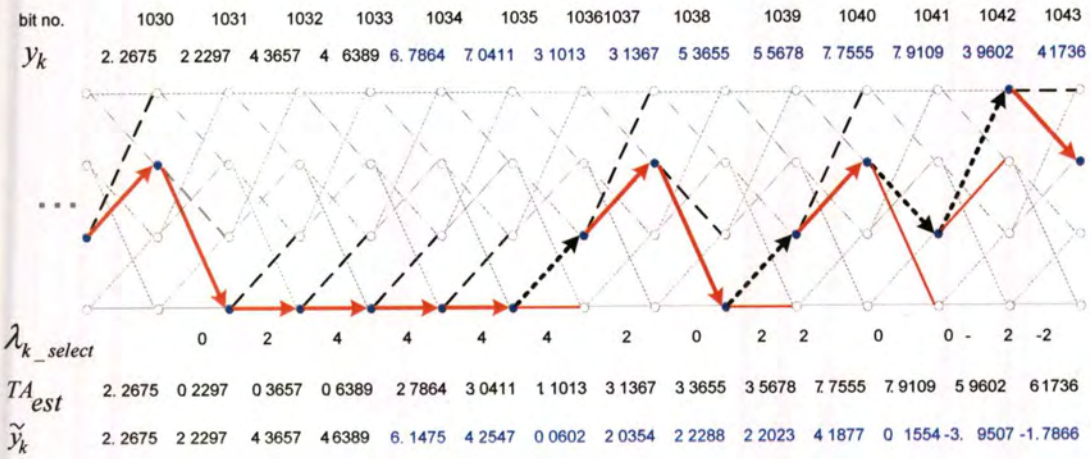

Figure 4.6 Examples for calculate noise estimate from the state trellis.

4.4 Summary

In this chapter, we describe the previous works to reduce the TA effect. In this research, we focus on Mathew's method to estimate and reduce the impact of TA. A new method proposed to estimate and reduce the TA effects through the state trellis of the DC-full partial response (PR) targets. In addition, we have shown examples for calculate the noise estimate from state trellis and the output signal from the proposed method.

CHAPTER 5

SYSTEM SIMULATION AND RESULTS

In this Chapter, we evaluate the BER performance of PRML system with the proposed thermal asperity canceller and compared to that without a canceller. We compare the performance of the proposed method TA estimation and cancellation with the Mathew method. In addition, the GMR nonlinearity and BLW are also included in this work. However, this work mainly focuses on how to estimate and reduce the impact of TA, so that the GMR nonlinearity and BLW affects are not compensated. Finally, we have shown the simulation result and conclusion.

5.1 System model

Figure 5.1 The magnetic recording channel model used in the simulation.

A block diagram of the read-back system for PMR that will be used for the simulation is shown in Fig. 5.1. The binary random sequence $a_k \in \{\pm 1\}$ is channel input, where k represents the discrete-time index, and $k = 1 \sim K$ (k is the total number of transmitted bits). The input data sequence with a bit period T is then filtered by an ideal differentiator to form a transition sequence $b_k \in \{-1, 0, 1\}$, and where $b_k \in \{\pm 1\}$ corresponds to a positive and negative transition, and $b_k \in \{0\}$ corresponds to the absence of a transition. The sequence b_k passing through the channel is convolved with the transition response $g(t)$. The transition response for perpendicular recording can be expressed as [43].

$$g(t) = erf\left(\frac{2t\sqrt{ln2}}{PW50}\right) \tag{5.1}$$

where $erf(\cdot)$ is an error function defined by $erf(x) = \frac{2}{\pi}\int_0^x e^{-Z^2}\,dZ$, and PW_{50} determines the pulse width of the derivative of $g(t)$. The normalized recording density is defined by $ND = \frac{PW_{50}}{T}$ which defines how many data bits can be packed within the resolution unit PW_{50}, and the digit response is defined as $h(t) = g(t) = g(t-T)$. The noise in PMR can be modeled as a mixture of the presence of TA, giant magneto-resistive (GMR) reader nonlinearity and AWGN with a two-sided power spectral density $\frac{N_0}{2}$. The signal to noise ratio (SNR) definition given as

$$SNR = 10\log_{10}\frac{E_i}{N_0} \quad [dB], \tag{5.2}$$

where E_i is the energy of the impulse response of the recording channel. Here, the isolated transition response is normalized so that the energy of the impulse response becomes unity.

The read-back signal $r_c(t)$ can be expressed as

$$r_c(t) = \sum_{k=-\infty}^{\infty} b_k\, g(t-kT) + u(t) + n(t) \tag{5.3}$$

where $n(t)$ is an AWGN, $u(t)$ is the thermal asperity effects. We obtain the read-back signal $r(t)$ after preamp by filtering the signal $r_c(t)$ by a first-order high-pass filter. After obtaining $r(t)$, it is filtered by a Butterworth low-pass filter and then sampled at the symbol rate assuming the perfect timing. The sampled sequence S_k is equalized so that the output sequence y_k resembles the desired sequence d_k. The error w_k between the equalizer output and the desired target output is assumed to be minimized. The estimation and cancellation block represents the proposed method to reduce the effects of TA, which is followed by the Viterbi detector as the maximum-likelihood (ML) detector.

5.2 Simulation Results and Discussion

We present the simulation results for the proposed method in the PMR channels with the thermal asperity and investigate the BER performance of the PRML system. In the simulation, we consider the dc-full targets at ND = 1.5 to compare the performance improvement based on each sector with 4096 information bits.

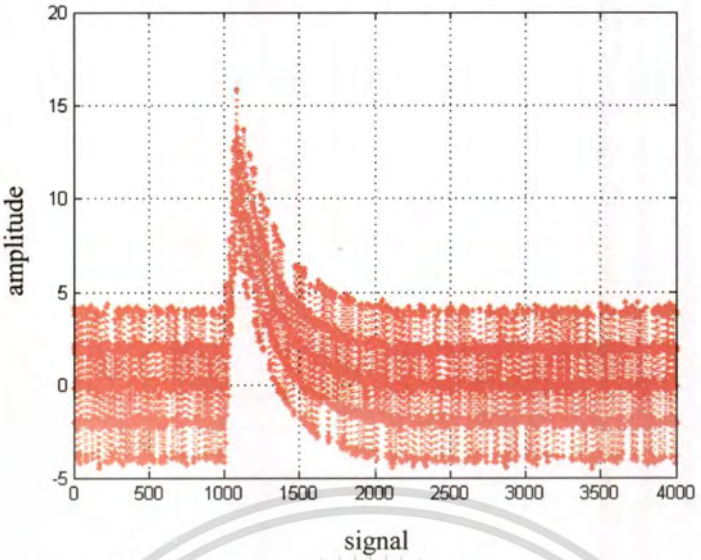

Figure 5.2 The equalized signal with TA of PR2 target at ND = 1.5, SNR = 22 dB, β = 3 and T_f = 1080 bits.

Fig. 5.2 shows the simulation result of the read-back signal based on PR2 target at SNR = 22 dB, ND = 1.5, β = 3. Since T_f = 80 bits and T_d = 250 bits are also given, the TA effect range T_f becomes 1080 bits.

The obtained signals at each point in the proposed method are shown in Fig. 5.3.

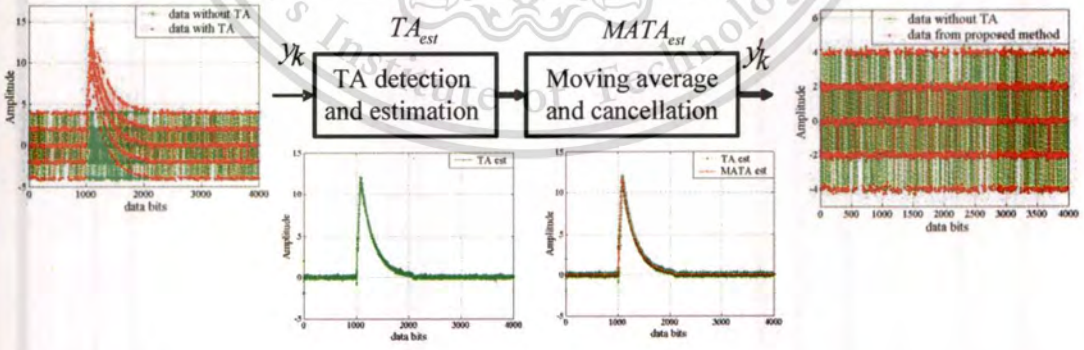

Figure 5.3 The signal from each proposed method block of PR2 target at ND = 1.5, SNR = 22 dB, β = 3 and T_f = 1080 bits.

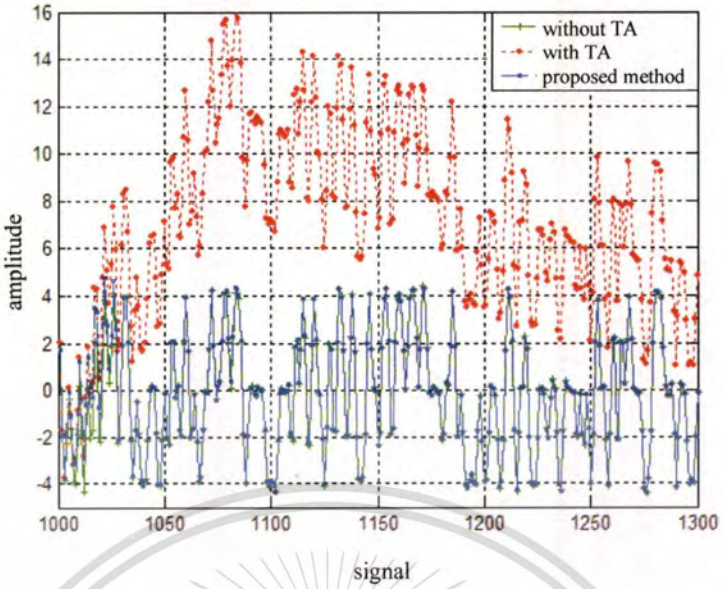

Figure 5.4 The comparison between the equalized signal with TA, without TA and the signal from the proposed method.

Fig 5.4 shows the equalized signal with and without TA of PR2 target at ND = 1.5, SNR = 22 dB, $\beta = 3$ and $T_f = 1080$ bits. This figure compares the signal from the TA estimate and cancellation TA from this proposed method (blue line), we can see that the signal from the proposed method can follow the signal without TA closely.

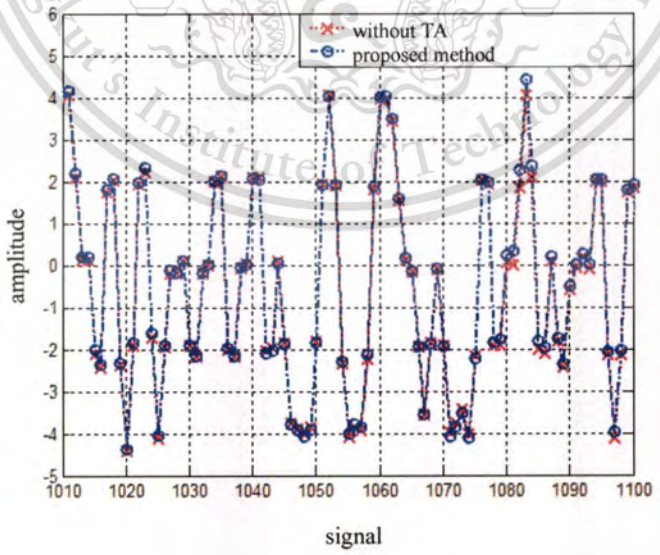

Figure 5.5 The equalized signal without TA and the signal from proposed canceller with TA for PR2 target at ND = 1.5, SNR = 22 dB, $\beta = 3$ and $T_f = 1080$ bits.

In Fig. 5.5, we compare the equalized signal without TA with the output signal of the proposed TA canceller for the equalized signal effected by TA for the PR2 target at SNR = 22 dB and β = 3. We can see that the signal from the canceller accurately follows the signal without TA. This means that we can expect the considerable improvement in the BER performance.

5.2.1 Results on the channels with TA only

In this section, we need to shows the system performance improvement for the proposed method in the PMR channels with TA effects only. The results show the system improvement in the BER compared between the proposed method, Mathew method and the system without TA canceller.

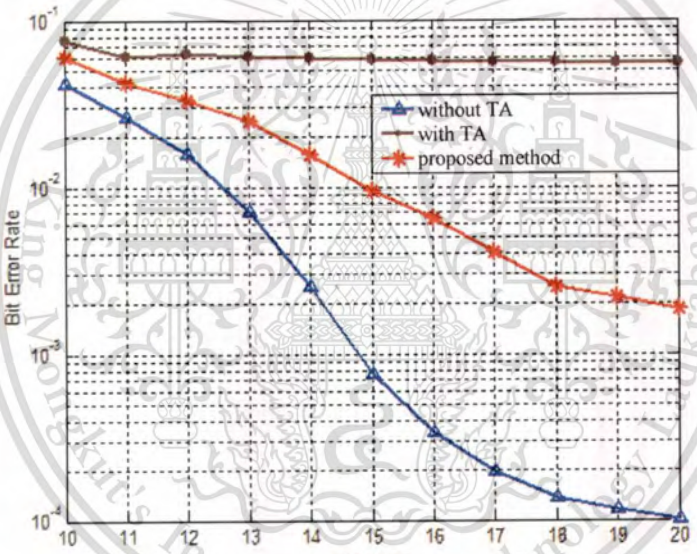

Figure 5.6 The BER performance of the PR2ML systems at ND = 1.5, β = 3 and T_f = 1080 bits.

Fig. 5.6 shows the BER performance of the PR2ML system for the equalized signal with TA, the output signal from proposed canceller and the equalized signal without TA, where ND = 1.5, β = 3 and T_f = 1080 bits. We can see that the proposed method provides more than an order of magnitude improvement in BER at SNR = 20 dB compared with the conventional one when TA occurs. However, it is still inferior to the case of the equalized signal without TA.

The degradation is caused by the noise estimation error in the early TA detection as can be seen in Fig. 5.7.

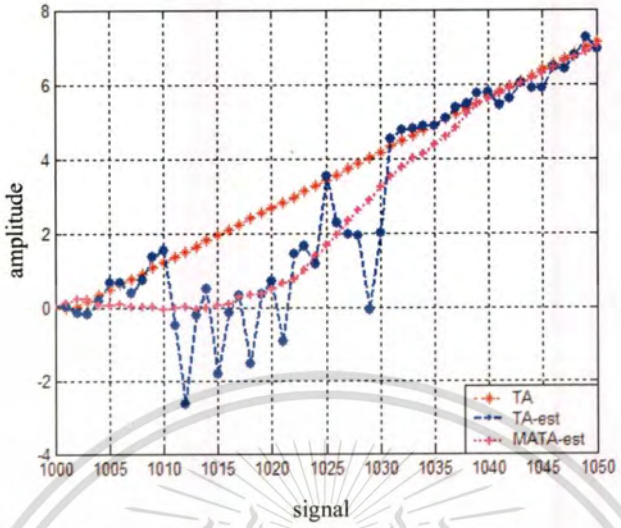

Figure 5.7 The noise estimation error in early TA detection of the PR2ML system at SNR = 22 dB, ND = 1.5, β = 3 and T_f = 1080 bits.

Fig. 5.7 shows the noise estimation error in the early TA detection where ND = 1.5, β = 3 and T_f = 1080 bits. We can see that the TA_{est} and $MATA_{est}$ deviate from the real TA at the start of TA and the estimation block cannot detect well. It takes about 20 bits before TA is accurately estimated. The estimation error results in the difference of BER.

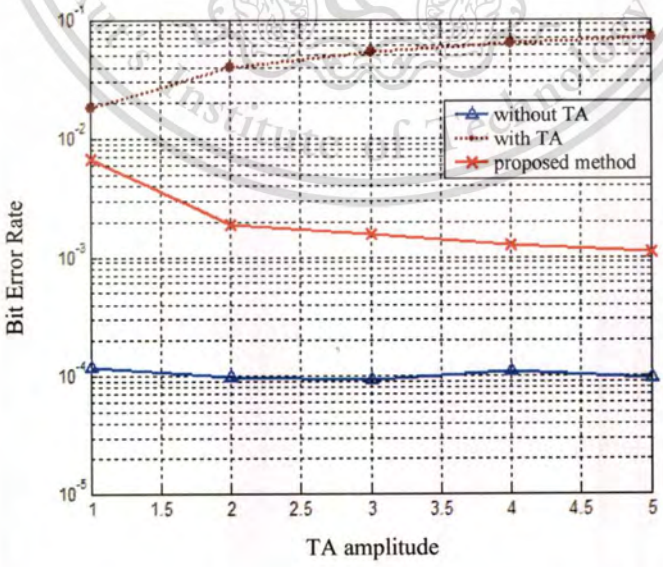

Figure 5.8 The BER of the PR2ML system versus TA amplitude at SNR = 22 dB, ND = 1.5 and T_f = 1080 bits.

Fig. 5.8 shows the relationship between the BER and TA amplitude for PR2ML system, where ND = 1.5, SNR = 22 dB and T_f = 1080 bits. We can see that the proposed method has higher accuracy in TA estimation compared to the method without TA canceller as the TA amplitude increases.

As this thesis compares the system performance improvement between the proposed method and Mathew's method. Thus, we will show the equalized signal with and without TA compared with the signal from the method proposed by Mathew's of PR2 target at ND = 1.5, SNR = 22 dB, β= 3 and T_f = 1080 bits as seen in Figure 5.9.

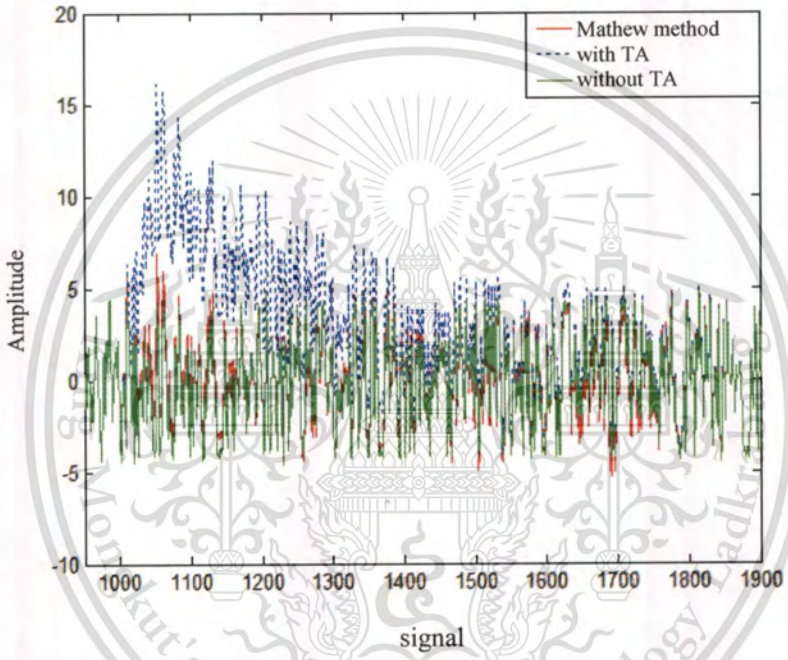

Figure 5.9 The equalized signals zoom in on the TA effect after pass through the proposed method by Mathew's and without TA effect.

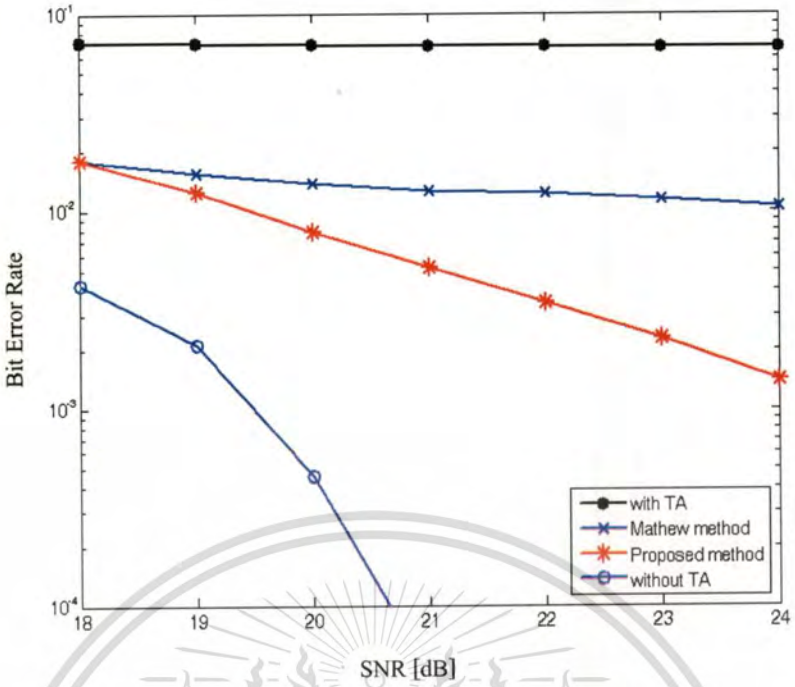

Figure 5.10 BER performance of the PR2ML systems with TA effects at ND = 1.5, $\beta = 3$ and $T_f =$ 1080 bits.

In Fig. 5.10, we compare the system performance improvement between the proposed method and the method proposed by Mathew [8] for the PR2ML system with ND = 1.5, $\beta = 3$ and T_f = 1080 bits. Mathew *et al.* proposed a method to detect the TA by comparing the read back amplitude and the window averaged read back signal with two separate thresholds. Afterward, the TA is canceled by subtracting the average TA from the read back signal. At SNR = 24 dB, we can observe that the proposed method provides more than an order of magnitude improvement in BER compared with the Mathew method. Nonetheless, it is still inferior to the case of the equalized signal without TA.

The performance gap between the system without TA effects and the proposed method can be explained from the fact that the proposed method still cannot predict the TA well during the rise time. Hence, the estimation error is resulted during this period. The severity of TA can be categorized into the following three levels [4], i.e.,

1. Severe: around 1000 bits per sector,
2. Medium: around 800 bits per sector, and
3. Minimum: around 500 bits per sector.

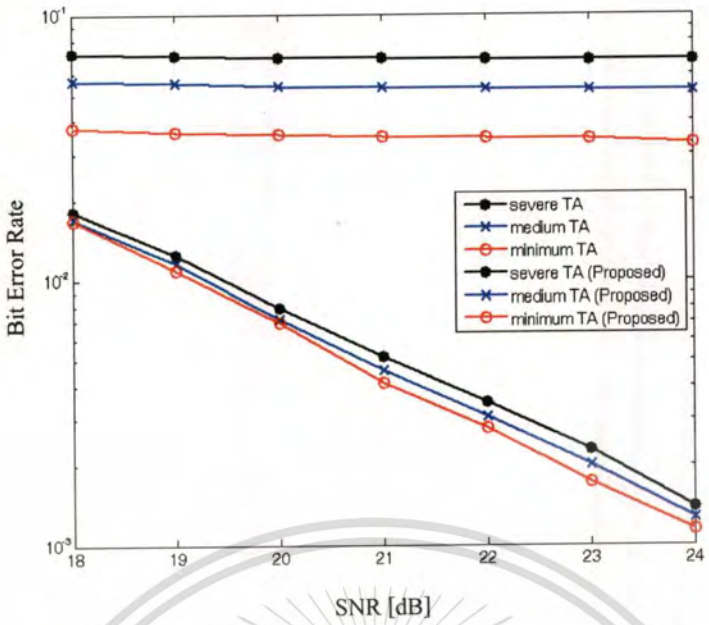

Figure 5.11 BER performance of the PR2ML system for different severity level of TA at ND = 1.5 and $\beta = 3$.

In Fig. 5.11, the BER comparison between the PR2ML system with and without TA cancellation for different severity levels of TA, where ND = 1.5 and $\beta = 3$ are shown. Without TA cancellation, the BER performance degrades due to the increased bit ranges of TA. The proposed method provides a better resilience since the BER degradation is not as evident.

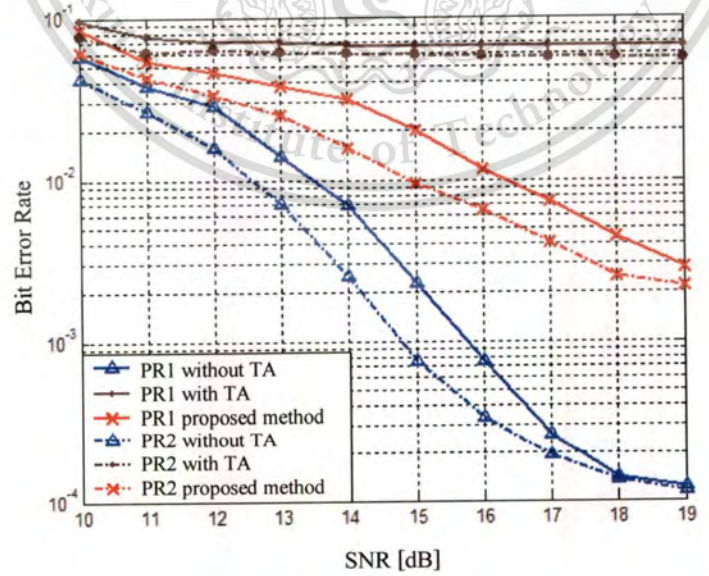

Figure 5.12 BER performances for the PR1ML and PR2ML channels with and without TA at ND = 1.5, $\beta = 3$ and $T_f = 1080$ bits.

Fig. 5.12 shows the BER performances of the PR1ML and PR2ML channels with and without the TA effect, where ND = 1.5, β = 3 and T_f = 1080 bits. We can see that the proposed method for both PR targets provides more than an order of magnitude improvement in BER at an SNR of greater than 17 dB compared with the conventional one. The PR2ML system achieves a gain of about 1.2 dB over PR1ML system at BER $\approx 3\times10^{-3}$.

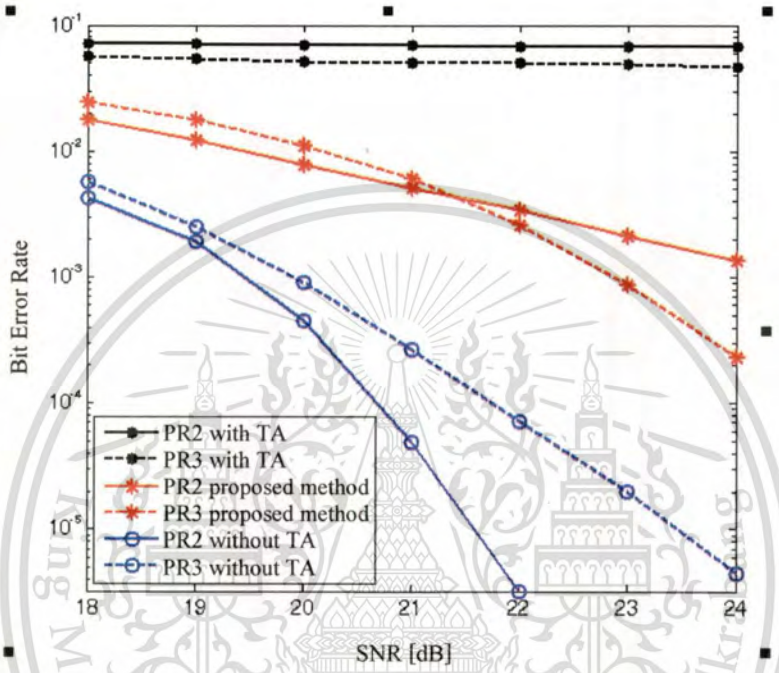

Figure 5.13 BER performances for the PR2ML and PR3ML channels with and without TA at ND = 1.5, SNR = 22 dB, β = 3 and T_f = 1080 bits.

In Fig. 5.13, we compare the BER performances between the PR2ML and PR3ML system, where ND = 1.5, β = 3 and T_f = 1080 bits. We can see that the proposed method for both PR targets provides more than an order of magnitude improvement in BER when TA occurs. Specifically, the PR3 target provides more than two orders of magnitude improvements compared with the system without TA canceller and achieves the gain over PR2ML system of about 1.4 dB at BER $\approx 1.4 \times 10^{-3}$ when only TA is present. This is contrary to the previous findings in [1] that the PR2 target with DC full response is the best target for PMR system with AWGN only. When the GMR nonlinearity and the BLW effect are included, the read back signal is changed in appearance.

5.2.2 Results on the channels with TA, GMR nonlinearity and BLW

In this sub section, we present the simulation results for the proposed method included the MR nonlinearity and BLW effects and it's not compensated. We consider the BER performance compare with the Mathew method respectively. Finally, we have shown the statistic of burst error between the proposed method and the system without TA canceller.

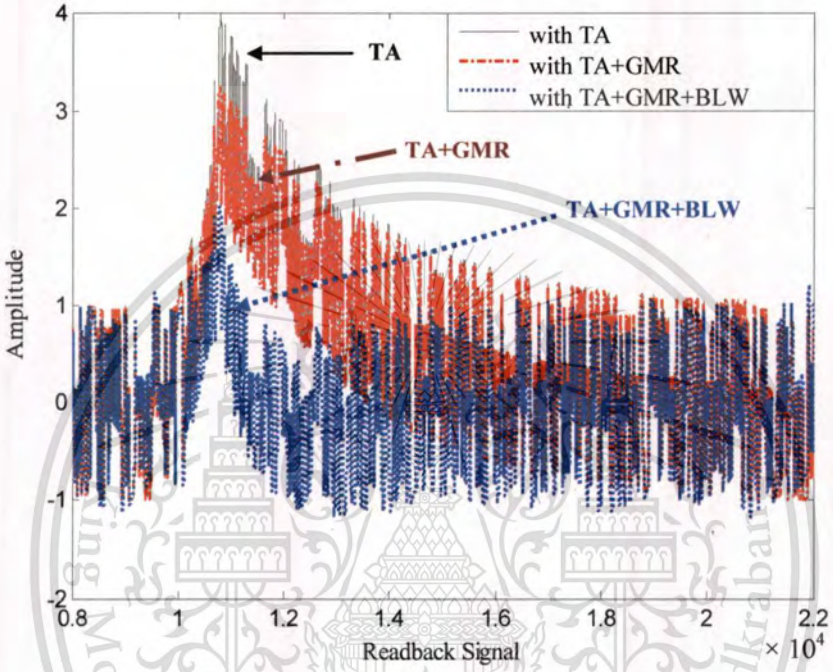

Figure 5.14 The Equalized signal with TA, GMR asymmetry 10% and BLW effects of PR2 target at ND = 1.5, SNR = 22 dB, $\beta = 3$ and $T_f = 1080$ bits.

Fig. 5.14 compares the amplitude of the equalized signal with TA, 10% GMR nonlinearity and the BLW effect as decaying of the dc-level approximate 1.5 % based on [6], respectively. In the simulation, we consider the PR2 target at SNR = 22 dB, ND = 1.5 and β = 3. For T_f = 80 bits and Td = 250 bits, the TA effect range T_f becomes 1080 bits. For the signal with TA only, the high peak with decay time is observed. With GMR asymmetry effects, the same peak is somewhat reduced. When the BLW effect is included, however, it is evident that the TA peak and decay time are reduced [3].

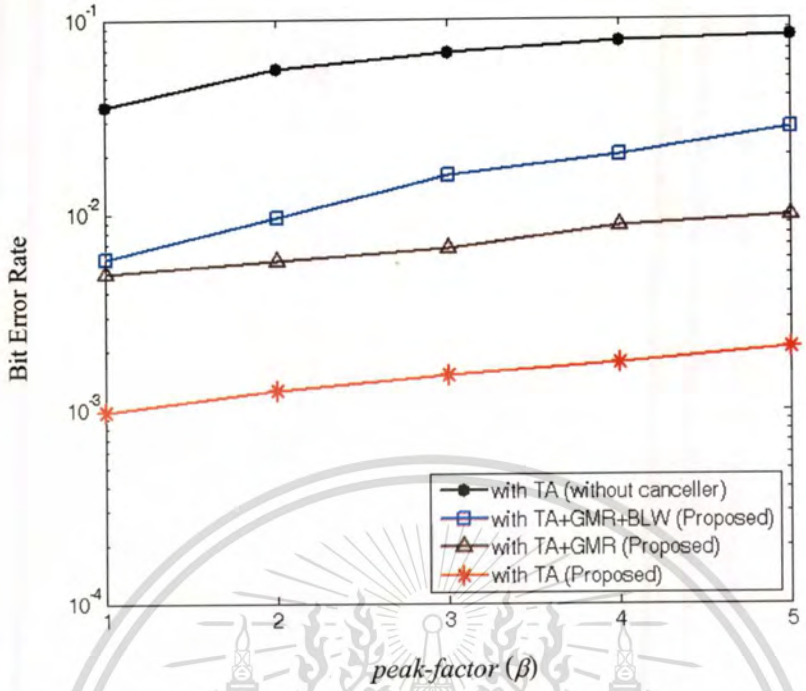

Figure 5.15 BER of the PR2ML system versus TA amplitude at SNR = 24 dB, ND = 1.5, T_f= 1080 bits, GMR Asym. = 10% and BLW effects ≈ 1.5 %.

Fig. 5.15 shows the relationship between the BER and TA amplitudes for PR2ML system, where ND = 1.5, SNR = 24 dB, T_f = 1080 bits, GMR asymmetry 10% and BLW effect ≈ 1.5 %. We can see that the system performance is reduced when the TA amplitude increases and the accuracy in TA estimation and detection is decreased when the GMR nonlinearity and BLW effect is included. However, the proposed method still shows the BER improvement compared with the system without TA cancellation and the previous work.

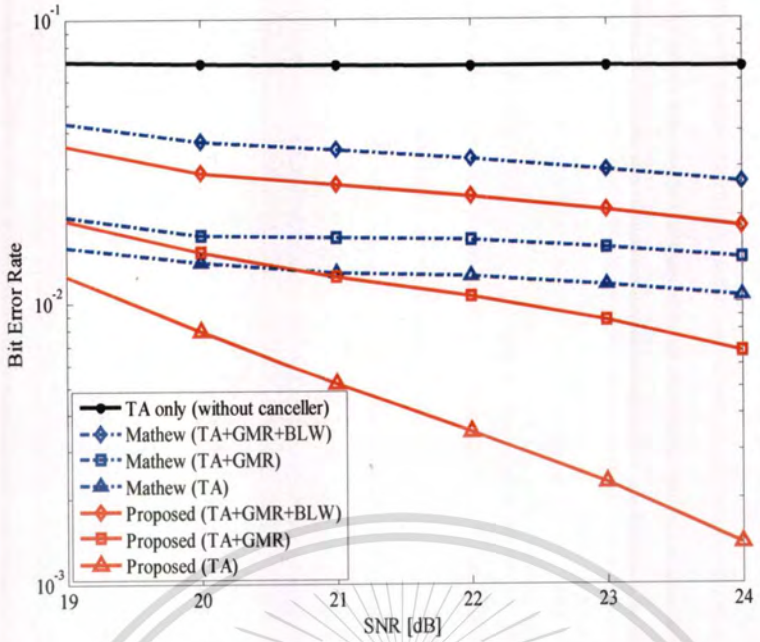

Figure 5.16 BER performances of the PR2ML systems with TA amp. = 3, GMR nonlinearity 10% and BLW effects ≈ 1.5 % at ND = 1.5, $\beta = 3$ and $T_f = 1080$ bits.

In Fig. 5.16, we present the performances of the proposed method in the PR2ML systems with the following three cases: (1) TA + GMR nonlinearity + BLW, (2) TA + GMR nonlinearity and (3) only TA effect. The GMR nonlinearity is 10% and BLW effects ≈ 1.5 %. With only TA, at SNR = 24 dB, the proposed method provides nearly an order of BER improvement over with Mathew method [8] and more than an order of BER reduction when compared with a the system without a TA canceller. Under the presence of GMR nonlinearity and BLW effect, the proposed method outperforms Mathew method slightly. The results indicate the severe performance degradation of both of these effects.

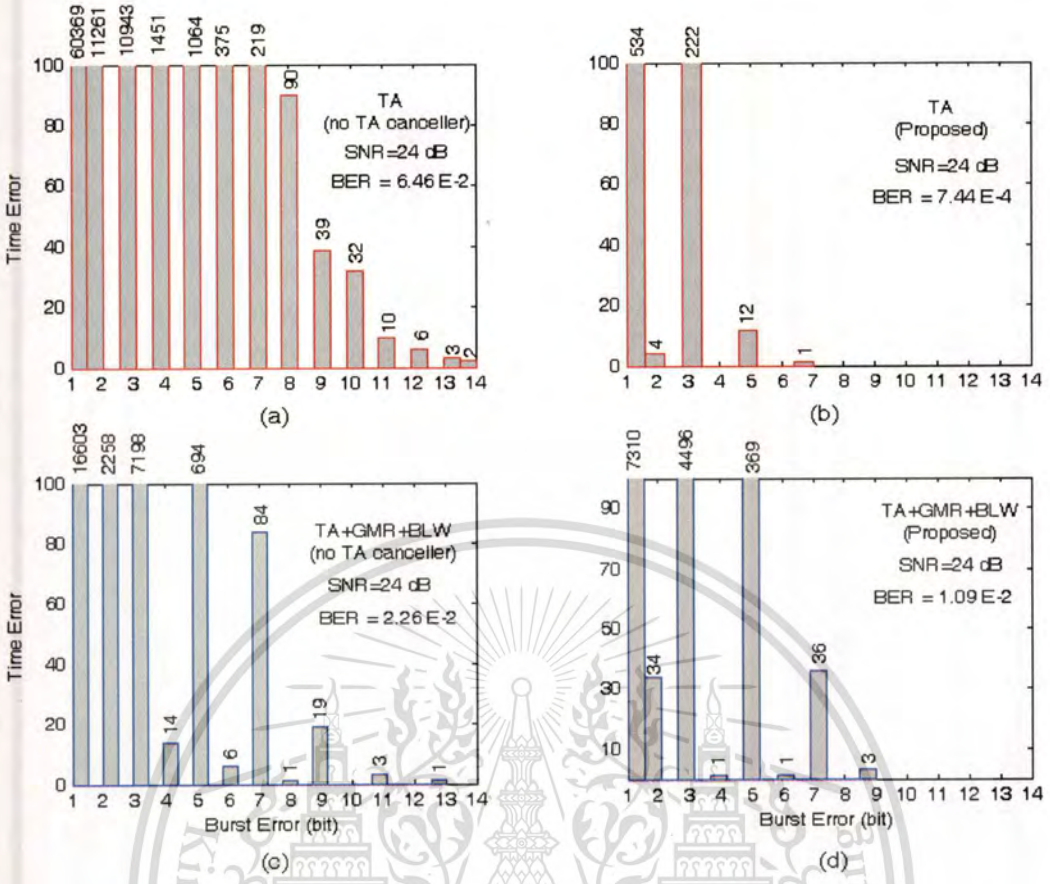

Figure 5.17 The statistics of burst errors between the proposed method and the system without TA canceller in the PR2ML channel.

In Fig. 5.17, we compare the statistics of burst errors between the proposed method and the system without TA canceller in the PR2ML channel at SNR = 24 dB. The GMR nonlinearity 10% and the BLW affect $\approx$ 1.5 %. From Fig. 5.17(a) and (b), when only TA is present, the proposed method drastically reduces the BER level as well as the number of burst errors at all lengths. Specifically, the burst length of over 7 bits is all eliminated. Under the presence of GMR nonlinearity and BLW effect as shown in Fig. 5.17(c) and (d), the burst error statistics are also improved by about 50% using the proposed method. All the burst errors of length over 9 bits disappear. We can see that the proposed method provides fewer and shorter burst errors compared with the system without TA canceller in both cases.

5.3 Summary

We proposed the new method to estimate and cancel of TA effect from an equalized signal by using the state trellis of the partial response (PR) target with dc-full component in perpendicular magnetic recording. We also studied the bit error rate (BER) performance of PRML system with a proposed thermal asperity canceller and compared to that without a canceller and the Mathew method.. We can see that the proposed method provides more than and nearly an order of magnitude improvement in BER compared with the system without TA canceller and the Mathew method. The system performance is reduced when the TA amplitude increases and the accuracy in TA estimation and detection is decreased when the GMR nonlinearity and BLW effect are included. The statistics of burst errors statistics are also improved by about 50% using the proposed method. Specifically, the burst length of over 7 bits is all eliminated.

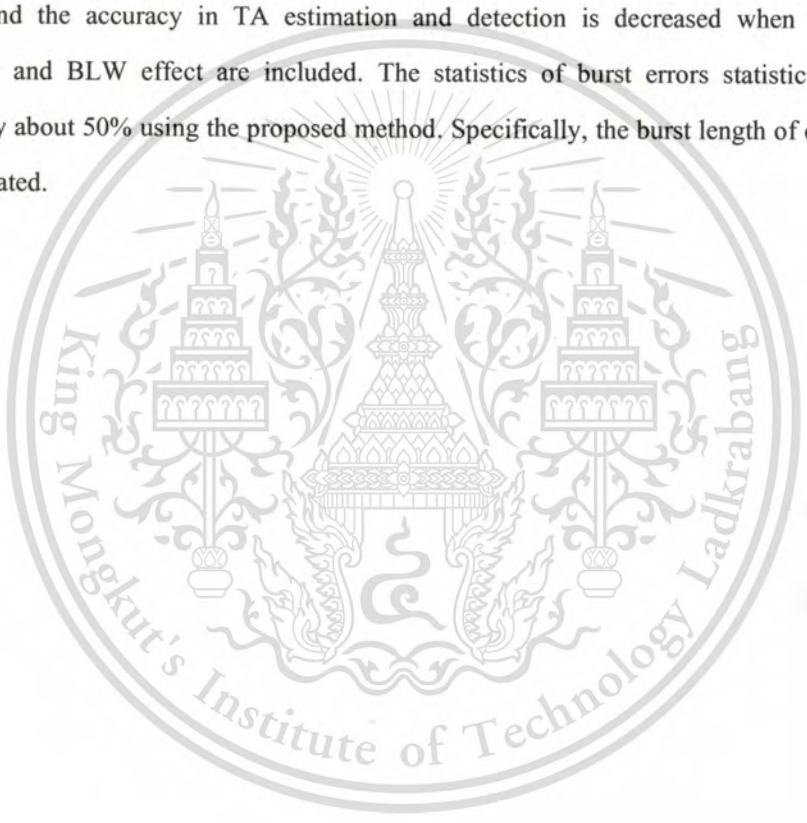

CHAPTER 6

CONCLUSIONS

6.1 Summary

For perpendicular magnetic recording (PMR), an important source of distortions is thermal asperity (TA). This phenomenon occurs when the slider comes into contact with or it is very close to the media. The thus induced heat causes a sharp increase and decay in the signal amplitude, which if not detected and corrected appropriately, will undoubtedly degrade the system performance. In this thesis is we propose a new method to estimate the TA and reduce its effects through the state trellis of the partial response (PR) target with dc-full component. The partial response (PR) target with dc-full component was considered to be the best choice for a PMR system in the absence of disturbances other than an additive white Gaussian noise (AWGN). Thus, we will apply the relative of the noiseless channel values on the state trellis to estimate the TA and reduce its effects of PRML system in PMR channel. In addition, the GMR nonlinearity and BLW effect are included. We compare the performance of PRML system in PMR channel with Mathew's method and the proposed method to estimate and reduce the impact of TA. The results show that the proposed method can improve the BER performance of the PRML system in the PMR channel with TA by more than an order of magnitude improvement in the BER performance. When compared with the Mathew's method, the proposed method provides nearly an order improvement in BER at SNR = 24 dB with TA effect. In addition, we show the system performance degrades with GMR nonlinearity and BLW effect included in the system, respectively. Nonetheless, the proposed method provides improvement in the BER compared with the system without a thermal asperity canceller.

6.2 Future Works

In this work, we proposed a new method to estimate and effectively reduce the effect of TA in the PMR channel with the state trellis. From the result, the proposed method provides more than an order of magnitude improvement in the BER performance when compare with the system without TA canceller. However, it is still inferior to the case of the equalized signal without TA.

The degradation is caused by the estimation block which cannot detect the TA start and stop well. As a result, the noise estimation error in the early TA detection which invalid estimation brings error and results from the different of BER performance. In future work, we will develop the estimation block which can detect the TA start and stop position with higher accuracy. Furthermore, the GMR nonlinearity and BLW often appear at the front end; therefore, they need to be included in this system. The idea is to estimate and reduce the impact of the GMR nonlinearity and BLW effect by using the proposed technique.

REFERENCES

[1] R. D. Hempstead "Thermally Induced Pulses in Magneto-resistive Heads." **IBM J. Res. Develop.**, Vol. 18, 1974. pp. 547-550.

[2] M. Madden, M. Oberg, Z. Wu and R. He "Read Channel for Perpendicular Magnetic Recording." **IEEE Trans. on Magnetics,** Vol. 40, No. 1, Jan. 2004. pp. 241-246.

[3] M. Fatih Erden, and E. M. Kurtas "Thermal Asperity Detection and Cancellation in Perpendicular Magnetic Recording Systems." **IEEE Trans. on Magnetics**, Vol. 40, No. 3, May 2004. pp. 1732-1737.

[4] B. Vasic, E. M. Kurstas 2005. **Coding and signal processing for magnetic recording System**. New York: CRC Press.

[5] V. Dorfman and J. K. Wolf "A method for reducing the effects of thermal asperities." **IEEE J. Selected Areas Commun.,** Vol. 19, No. 4, April 2001. pp. 662-667.

[6] H. Ueno "Method for Reproducing Magnetic Recording and Method for Read Retry." **U.S. Patent 0221476A1**, Oct. 2006.

[7] P. Kovintavewat and S. Koonkarnkhai "A New Thermal Asperity Detection and Correction Algorithm for Perpendicular Recording Channels." **in Proc. of DST-CON 2009**, Thailand Science Park Convention Center, Bangkok, Thailand, May 13 – 15, 2009. pp. DST-117.

[8] G. Mathew and I. Tjhia "Thermal Asperity Suppression in Perpendicular Recording Channels." **IEEE Trans. on Magnetics**, Vol. 41, No. 10, Oct. 2005. pp. 2878-2880.

[9] A. Takeo, T. Taguchi, Y. Sakai and Y. Tanaka "Characterization of GMR Nonlinear Response and the Impact on BER in Perpendicular Magnetic Recording." **IEEE Trans. on Magnetics**, Vol.40, No. 4, July 2004. pp. 2582-2584.

[10] A. Patapoutian "Baseline Wander Compensation for the Perpendicular Magnetic Recording Channel." **IEEE Trans. on Magnetics**, Vol. 40, No. 1, Jan. 2004. pp. 235-240.

[11] R. Wood, Y. Hsu and M. Schultz "**Perpendicular Magnetic Recording Technology**." www. hitachigst.com.

[12] S. B. Wicker 1995. **Error control systems for digital communication and storage**. Upper Saddle River, New Jersey: Prenticed Hall International.

[13] P. H. Siegel "Recording Codes for digital Magnetic Storage." **IEEE Trans. on Magnetics,** Vol. MAG-21, Sep. 1985. pp. 1344-1349.

[14] K. A. S. Immink "Run length-Limited Sequences." **Proceeding of the IEEE,** Vol. 78, Nov. 1990. pp. 1745–1759.

[15] C. WARISARN. 2011 "A Novel Infinite-impulse Response Equalizer Design and Iterative Timing Recovery for Magnetic Recording Channels." Ph.D. Thesis of Faculty of Engineering, King Mongkut's Institute of Technology Ladkrabang, Thailand.

[16] J. W. M. Bergman 1996. **Digital baseband transmission and recording**. Boston, Massachusetts: Kluwer academic publishers.

[17] I. Kaitsu, R. Inamura, J. Toda and T. Morita "Ultra High Density Perpendicular Magnetic Recording Technologies." **FUJITSU Sci. Tech. J.,** Vol. 42, Jan. 2006. pp.122-130.

[18] S. Stancescu and V. Soare (no date). "Partial Response and Viterbi Detection Channel Simulator for Digital Magnetic Recording." **Department of Applied Electronics and Information Technology, Faculty of Electronics and Telecommunications, Politehnica University of Bucharest**, ROMANIA.

[19] Y. Okamoto, H. Osawa, H. Saito, H. Muraoka and Y. Nakamura "Performance of PRML systems in perpendicular magnetic recording channel with jitter-like noise." **Journal of Magnetism and Magnetic Materials 235**, 2001. pp. 259–264.

[20] S. Stupp, A. Baldwinson, P. McEwen, M. Crawford and T. Rogers "Thermal Asperity Trends." **IEEE Trans. on Magnetics,** Vol. 35, No. 2, Mar. 1999. pp. 752-757.

[21] M. Fatih Erden, and E. M. Kurtas "Thermal Asperity Detection and Cancellation in Perpendicular Magnetic Recording Systems." **IEEE Trans. on Magnetics,** Vol. 40, No. 3, May 2004. pp. 1732-1737.

[22] A. Takeo, T. Taguchi, Y. Sakai and Y. Tanaka "Characterization of GMR Nonlinear Response and the Impact on BER in Perpendicular Magnetic Recording." **IEEE Trans. on Magnetics,** Vol. 40, No. 4, July 2004. pp. 2582-2584.

[23] J. Xie, B.V.K. Vijaya Kumar and X. Hu "Base Line Wander Compensation by Per-Survivor-Processing." **IEEE Trans. on Magnetics**, Vol. 42, No. 10, October 2006. pp. 2609-2611.

[24] M. Fatih Erden and E. M. Kurtas "Baseline Wander Compensation for Perpendicular Recording." **IEEE Trans. on Magnetics**, Vol. 40, No. 4, July 2004. pp. 3114-3116.

[25] X. Hu and B. V. K Vijaya Kumar "Evaluation of Low-Density Parity-Check Codes on Perpendicular Magnetic Recording Model." **IEEE Trans. on Magnetics**, Vol. 43, No.2, Feb. 2007. pp. 727-732.

[26] G. D. Forney "Maximum-likelihood sequence estimation of digital sequences in the presence of intersymbol interference." **IEEE Trans. Inf. Theory**, Vol. 18, No. 3, May 1972. pp. 363–378.

[27] H. Kobayashi and D. Tang "Application of Partial-response Channel Coding to Magnetic Recording Systems." **IBM Journal of Research and Development**, July 1970. pp. 368-375.

[28] E. M. Kurtas, J. Park, X. Yang and A. Kavcic (no date). **Detection Methods for Data-dependent Noise in Storage Channels.** Seagate Technology, 1251 Waterfront Place, Pittsburgh, PA 15222, USA and Harvard University, 33 Oxford Street Cambridge, MA 02138, USA.

[29] C. Derrick Wei. 1996. **An Analog Magnetic Storage Read Channel based on a Decision Feedback Equalizer.** Integrated Circuits & Systems Laboratory Electrical Engineering Department University of California Los Angeles, CA 90095-1594.

[30] H. Dawid, O. J. Joeressen and H. Meyr (no date). **Chapter 17 Viterbi Decoders High Performance Algorithms and Architectures.**

[31] S. Stiglmayr and A. Fahrner "Signal Processing and Detection Aspects of Digital Magnetic Storage Systems,'' **in Proc. IEEE Winter school on Coding and Information Theory**, 2005.

[32] P. Kovintavewat. 2007. **Signal Processing for Digital Data Storage**. Vol. 2: Receiver Design, NECTEC and HDDI publishers.

[33] 1-CORE Technologies (no date). **Viterbi Algorithm for Decoding of Convolution Codes**. Moscow, Russia.

[34] Lecture 9. 2010. **Viterbi Decoding of Convolutional Codes**. MIT 6.02 DRAFT Lecture Notes, October 6.

[35] S. Yupin and S. Pornchai "The Performance Comparison between DC-Full and DC-Attenuation Partial-Response Targets in Perpendicular Magnetic Recording Channel." **in Proc. ITC-CSCC 2008**, Shimonoseki, Yamagushi, Japan, July 2008. pp. 933-936.

[36] J. Lee and J. Lee "A Simplified Noise-Predictive Partial Response Maximum Likelihood Detection Using M-Algorithm for Perpendicular Magnetic Recording Channels." **IEEE Trans. on Magnetics**, VOL. 41, No. 2, Feb. 2005.

[37] J. D. Coker, E. Eleftheriou, R. L. Galbraith and W. Hirt "Noise-predictive maximum likelihood detection." **IEEE Trans. on Magnetics,** Vol. 34, No. 1, Jan. 1998. pp.110-117.

[38] S. Jeonand, B.V.K. and V. Kumar "Error Event Analysis of Partial Response Targets for Perpendicular Magnetic Recording." **IEEE GLOBECOM,** 2007. pp. 272-282.

[39] J. Caroselli and J. Keil Wolf "Error Event Characterization of Partial Response Systems in Magnetic Recording System with Media Noise." **in Proc. IEEE Global Telecommunications Conference**, Vol. 5, Australia, 1998. pp. 2724–2729.

[40] S. A. Altekar, M. Berggren, B. E. Moision, P. H. Siegel, and J. K. Wolf "Error-event characterization on partial-response channels." **IEEE Trans. Inf. Theory,** Vol. 45, No. 1, Jan. 1999. pp. 241–247.

[41] W. Feng, A. Vityaev, G. Burd, and N. Nazari "On the Performance of Parity Codes in Magnetic Recording Systems." **IEEE GLOBECOM 2000**, 2000. pp. 1877–1881.

[42] J. Moon and J. Park "Detection of Prescribed Error Events: Application to Perpendicular Recording." **IEEE International Conference on Communications**, 2005. pp. 2057-2062.

[43] P. Kovintavewat, I. Ozgunes, E. M. Kurtas, J. R. Barry and S. W. McLaughlin "Generalized Partial Response Targets for Perpendicular Recording with Jitter Noise." **IEEE Trans. on Magnetics,** Vol. 38, Issues 5, Sep. 2002. pp. 2340-2342.

AUTHOR BIOGRAPHY

Author: Mrs. Yupin Suppakhun

Date of Birth: June 25, 1970

Address: 126/9 Moo 7 Banpra, Maung, Prachinburi, Thailand 25230

Education Background:

1992 B. S.I.Ed. Department of Telecommunication Engineering.
Faculty of Science in Industrial Education.
King Mongkut's Institute of TechNology Ladkrabang.

1996 M. Eng. Department of Telecommunication Engineering.
Faculty of Engineering.
King Mongkut's Institute of TechNology Ladkrabang.

Interested Research: Signal Processing for Channels with Thermal Asperity,

Partial-Response Targets in Perpendicular Magnetic Recording Channel

Related Publication:

[1] Yupin SUPPAKHUN, Pornchai SUPNITHI, Yoshihiro OKAMOTO, Yasuaki NAKAMURA, and Hisashi OSAWA "Performance Improvement System for Perpendicular Magnetic Recording with Thermal Asperity." **IEICE Trans. Elec.**, Vol. E94-C, No. 9, Sep. 2011.

[2] Yupin SUPPAKHUN, Pornchai SUPNITHI, Yoshihiro OKAMOTO, Yasuaki NAKAMURA, and Hisashi OSAWA "Performance Improvement System for Perpendicular Magnetic Recording with Thermal Asperity." **in Proc. PMRC 2010,** Sendai, Japan, Oct. 2010.

[3] Yupin SUPPAKHUN and Pornchai SUPNITHI "The Performance Comparison Between DC-Full and DC-Attenuation Partial-Response Targets in Perpendicular Magnetic Recording Channel " **in Proc. of ITC-CSCC 2008**, Shimonoseki City, Japan, Jul. 2008. pp. 929–932.

[4] Yupin SUPPAKHUN and Pornchai SUPNITHI "Effect of Cutoff Frequency of Low pass Filter on the Performance of Perpendicular Magnetic Recording Channel." **KKU Research Journal**, Vol.13, No. 4, May 2008. pp. 501–504.

[5] Yupin SUPPAKHUN and Pornchai SUPNITHI "Effect of Cutoff Frequency of Low pass Filter on the Performance of Perpendicular Magnetic Recording Channel." **in Proc. DST-CON 2008**, April 21-23, 2008.

IEICE TRANSACTIONS

on Electronics

VOL.E94-C
NO.9
SEPTEMBER 2011

A PUBLICATION OF THE ELECTRONICS SOCIETY

The Institute of Electronics, Information and Communication Engineers
Kikai-Shinko-Kaikan Bldg., 5-8, Shibakoen 3 chome, Minato-ku, TOKYO, 105-0011 JAPAN

IEICE TRANS. ELECTRON., VOL.E94–C, NO.9 SEPTEMBER 2011

PAPER

Performance Improvement System for Perpendicular Magnetic Recording with Thermal Asperity

Yupin SUPPAKHUN[†a)], *Nonmember*, **Pornchai SUPNITHI**[†], **Yoshihiro OKAMOTO**[††], **Yasuaki NAKAMURA**[††], *Members, and* **Hisashi OSAWA**[†††], *Fellow*

SUMMARY In this paper, we propose a new method to estimate and effectively reduce the effect of thermal asperity (TA) in the perpendicular magnetic recording (PMR) channels with the state trellis. The TA is estimated from the state trellis, then its average is used to modify the equalized signal entering the Viterbi detector. For the partial response (PR) targets with DC component, the proposed method with a maximum-likelihood detector can improve the bit error rate performance by more than an order of magnitude when TA occurs and degrades when the giant magneto-resistive (GMR) nonlinearity and base line wander (BLW) effects are present. Unlike the previous studies, this method allows the use of PR targets with DC component under the presence of TA.

key words: *perpendicular magnetic recording, thermal asperity estimate, GMR nonlinear, baseline wander, trellis, moving average*

1. Introduction

In order to achieve reliable high-density magnetic recording, the architectures of read channels are designed to well suppress the noise and distortions found in the read-back signal. For the perpendicular magnetic recording (PMR), an important source of distortions is thermal asperity (TA). This phenomenon occurs when the slider comes into contact with or it is very close to the media. The thus induced heat causes a sharp increase and decay in the signal amplitude, which if not detected and corrected appropriately, will undoubtedly degrade the system performance.

In previous works, a partial-response (PR) target with dc-full component was considered the best choice for a PMR system and the additive white Gaussian noise (AWGN) channel [1]. A common method to reduce the effect of TA is to implement a high-pass filter (HPF) in the system and adjust its cut-off frequency [2], [3]. In [4], Dorfman and Wolf proposed an approach for TA suppression in longitudinal magnetic recording (LMR) by using the filter before processing the samples in a Viterbi detector, where D is the delay operator which represents a delay of a bit interval T. Two Viterbi detectors are run in parallel, one for an extended partial response class-4 (EPR4) channel and the other for a partial response class-5 (PR5) channel equipped with the $(1 - D)$ filter when TA occurs. However, this improvement in TA operations reduces the overall performance of the system. Similarly, for the PMR system, Ueno proposed a method to reduce error deterioration due to TA by switching from the PR targets with DC component to the PR targets without DC component [5]. Both methods use two channels running in parallel to avoid an impact when TA occurs. This approach requires an increased detector complexity to account for the different equalization targets. Alternatively, the TA signal can be estimated and used for the cancellation. In [6], Mathew and Tjhia proposed a simple TA estimation method from window average, in which the TA cancellation in the read-back signal can be done by a straightforward subtraction. In practice, in addition to TA, GMR nonlinearity and BLW often appear at the front end [7], [8]. In all these previous works GMR nonlinearly and BLW effects are not considered in the system.

In this paper, we propose a new method to estimate the TA by modifying the state trellis of the PR target with DC component in PMR system. Unlike previous works, the GMR nonlinearity and BLW are also included in this work. However, this paper mainly focuses on how to estimate and reduce the impact of TA, so that the GMR nonlinearity and BLW effects are not compensated.

The results show that the proposed method can improve the BER performance of the PRML system in the PMR channel with TA by more than an order of magnitude improvement in the BER performance. When compared with the method in [6], the proposed method provides nearly an order improvement in BER at SNR = 24 dB with TA effect. In addition, we show the system performance degrades with GMR nonlinearity and BLW effect included in the system, respectively. Nonetheless, the proposed method provides improvement in the BER compared with the system without a thermal asperity canceler.

In the next section, we describe the system model of the perpendicular recording. In Sect. 3, the TA estimation through the trellis and cancellation are explained. The simulation results and discussions are in Sect. 4. Finally, the conclusions are made in Sect. 5.

Manuscript received June 18, 2010.
Manuscript revised April 27, 2011.

[†]The authors are with the Faculty of Engineering, King Mongkut's Institute of Technology Ladkrabang, Bangkok, 10520, Thailand.

[††]The authors are with the Graduate School of Science and Engineering, Ehime University, Matsuyama-shi, 790-8577 Japan.

[†††]The author is with the Institution for Collaborative Relations, Ehime University, Matsuyama-shi, 790-8577 Japan.

a) E-mail: s9060001@kmitl.ac.th

DOI: 10.1587/transele.E94.C.1472

2. Read-Back System Model

2.1 Read-Back System

A block diagram of the read-back system for PMR is shown in Fig. 1. The binary random sequence $a_k \in \{\pm 1\}$ is channel input, where k represents the discrete-time index, and $k = 1 \sim K$ (K is the total number of transmitted bits). The input data sequence with a bit period T is then filtered by an ideal differentiator $(1 - D)/2$ to form a transition sequence $b_k \in \{-1, 0, 1\}$, and where $b_k = \{\pm 1\}$ corresponds to a positive and negative transition, and $b_k = \{0\}$ corresponds to the absence of a transition. The sequence b_k passing through the channel is convolved with the transition response $g(t)$. The transition response for perpendicular recording can be expressed as [9] and [10].

$$g(t) = erf\left(\frac{2t\sqrt{\ln 2}}{PW50}\right), \tag{1}$$

where $erf(\cdot)$ is an error function defined by $erf(x) = \frac{2}{\sqrt{\pi}}\int_0^x e^{-z^2}dz$, and $PW50$ determines the pulse width of the derivative of $g(t)$. The normalized recording density is defined by $ND = PW50/T$ which defines how many data bits can be packed within the resolution unit $PW50$, and the digit response is defined as $h(t) = g(t) - g(t - T)$. The noise in PMR can be modeled as a mixture of the presence of TA, giant magneto-resistive (GMR) reader nonlinearity and AWGN with a two-sided power spectral density $N_0/2$. We can define the SNR at the reading point as

$$\text{SNR} = 10\log_{10}\frac{E_i}{N_o} \quad [\text{dB}], \tag{2}$$

where E_i is the energy of the impulse response of the recording channel. Here, the isolate transition response is normalized so that the energy of the impulse response becomes unity.

The read-back signal $r_c(t)$ in Fig. 1 can be expressed as

$$r_c(t) = \sum_{k=-\infty}^{\infty} b_k g(t - kT) + u(t) + v(t) + n(t), \tag{3}$$

where $n(t)$ is an AWGN, $u(t)$ is the GMR nonlinearity and $v(t)$ is the BLW effects. We obtain the read-back signal $r(t)$ after preamp by filtering the signal $r_c(t)$ by a first-order high-pass filter. After obtaining $r(t)$, it is filtered by a Butterworth low-pass filter and then sampled at the symbol rate assuming the perfect timing. The sampled sequence s_k is equalized so that the output sequence y_k resembles the desired sequence d_k. The error w_k between the equalizer output and the desired target output is assumed to be minimized. The estimation and cancellation block represents the proposed method to reduce the effects of TA, which is followed by the Viterbi detector as the maximum likelihood (ML) detector.

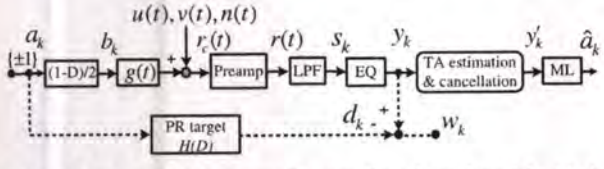

Fig. 1 The perpendicular magnetic recording channel model with thermal asperity, GMR nonlinearity and BLW effects.

2.2 Noise Model

The noise in perpendicular recording with any kind of noise/distortion cause effects at low frequencies, including the TA, GMR nonlinearity and BLW effects that cause degradation in the system performance.

We use the TA model as described in [11]. This model fits the captured spin stand data and drive data very well. It shows the linear heating of the MR element, the TA peak temperature and then exhibits an exponential decay after TA event. The TA signal $u(t)$ can be modeled and expressed as follows:

$$u(t) = \begin{cases} A_0\left(\frac{t}{T_r}\right), & 0 \le t \le T_r \\ A_0 \exp\left(-\frac{t-T_r}{T_d}\right), & T_r < t < T_f \end{cases}, \tag{4}$$

where $A_0 = \beta \sum_k |h_k|$ is the peak TA amplitude, $\beta \ge 0$ is the peak-factor, h_k is the coefficients of PR target, T_r is the rise time, T_d is the decay constant (i.e., time constant). A decay time equal to four times the decay constant is sufficient since it will reduce the magnitude of the TA signal to only 1.8% of its peak amplitude. Thus, we choose the TA duration as $T_f = T_r + 4T_d$.

The GMR nonlinearity $v(t)$, can be modeled as the transfer curve of GMR $[V(h)]$ approximating a hyperbolic-tangent curve [12] with

$$V(h) = \begin{cases} \frac{\tanh[a(h-dh)]}{a} + dh & (h > dh) \\ \frac{\tanh[b(h-dh)]}{b} + dh & (h < dh) \end{cases} \tag{5}$$

The normalized field "h" is defined as the applied field divided by the maximum applied field. A positive saturated parameter $V(1)$ and a negative saturated parameter $V(-1)$ approach linear ($V(+1) = V(-1) = 1$) as parameter "a" and "b". The asymmetry is caused when "a" is not equal to 1. The shift parameter "dh" indicates the field shift value of maximum transfer curve slope position. The asymmetry can be defined as a percentage of $|(a - b)/(a + b)|$, and where a is positive peak and b is negative peak.

The BLW effect is generated by the high-pass pole of the preamplifier [12], [13]. It can be modeled by a steep high-pass filter (HPF) in the channel as

$$H(s) = \frac{a_1 s}{s + \alpha_0}, \tag{6}$$

where a_1 and α_0 are the parameters which determine the high-frequency gain and cutoff frequency of H(s) [8]. However, this paper mainly focuses on how to estimate and reduce the impact of TA, so that the BLW and GMR nonlinearity affects are not compensated.

3. Thermal Asperity Estimation and Cancellation System

Perpendicular magnetic recording channel using a double-layer medium is basically a full response channel with a DC response [14]. The common PR target with DC component includes PR1 and PR2 targets. Here, we propose a TA estimation and cancellation method through the trellis of the PR targets. The idea is to estimate the TA signal from the PR equalized signal and then subtract the TA before feeding it to the Viterbi detector. The schematic diagram illustrating the TA estimation and cancellation in the PMR channels is shown in Fig. 2.

3.1 TA Detection and Estimation

3.1.1 TA Detection

The TA detection here is used to determine the start and stop positions in the PR equalized signal sequence. The estimated TA is then canceled before the Viterbi detector. The TA is found from comparing the amplitude of the PR equalized signal with the threshold. Here, the threshold Γ (Gamma) is set as $\Gamma = \lambda_{\max} + \delta$, where $\lambda_{\max}$ is the maximum value of the noiseless channel output from PR target and δ is an incremental value obtained from the simulation to ensure the accurate start-stop position of the TA. The TA affected start position is determined when the PR equalized signal y_k is lower than 1.8% of maximum TA amplitude and lasts at least $2^v + 1$ bits, where v is the memory of PR target.

3.1.2 TA Estimation

Once the TA start and stop positions are known, the TA estimator will provide the noise and TA estimates. The estimation is processed through the trellis of the PR target for all samples. For the TA affected samples, the TA part is estimated, otherwise, only the noise part is estimated. These two cases are described as follows.

Case I. The samples without TA

When the equalized sample y_k is less than the threshold value for detecting TA, we can find the noise estimate through the state trellis of the PR target. Given that the selected path at time $k-1$ ends at state S_i, the best path on the trellis at time k is selected based on the minimum distance, q_k, between y_k and λ_k given by

$$q_k = \min_{j\in\{-1,1\}} |y_k - \lambda_k(j)|, \tag{7}$$

where $\lambda_k(j)$ is a noiseless PR channel output from state S_i with input $j \in \{-1, 1\}$. Note that the best path is selected from the minimum distance chosen only, there is no metric accumulation like in the Viterbi algorithm.

Case II. The samples with TA

For the samples with TA, we compute the minimum distance to select the best path from

$$q_k = |\tilde{y}_k - \lambda_k|, \tag{8}$$

where $\tilde{y}_k$ is computed from

$$\tilde{y}_k = y_k - \left|TA_{est,k-1}\right| \tag{9}$$

For both case I and II, once the best path is selected, the corresponding noiseless PR channel output $\hat{\lambda}_k$ on the branch is used to estimate the TA (or noise) level at time k by subtracting from the equalized signal, i.e.,

$$TA_{est,k} = y_k - \hat{\lambda}_k \tag{10}$$

Note that, for the samples without TA, we have the noise estimates rather than the TA estimates.

Figure 3 shows an example of the path selection at time k to $k+3$. The arrow lines denote the selected branch (path). At each time instant, only two branches are considered.

3.2 Moving Average and Cancellation Block

After the TA(noise) estimations are completed, we obtain the moving average of the TA(noise) estimates and then

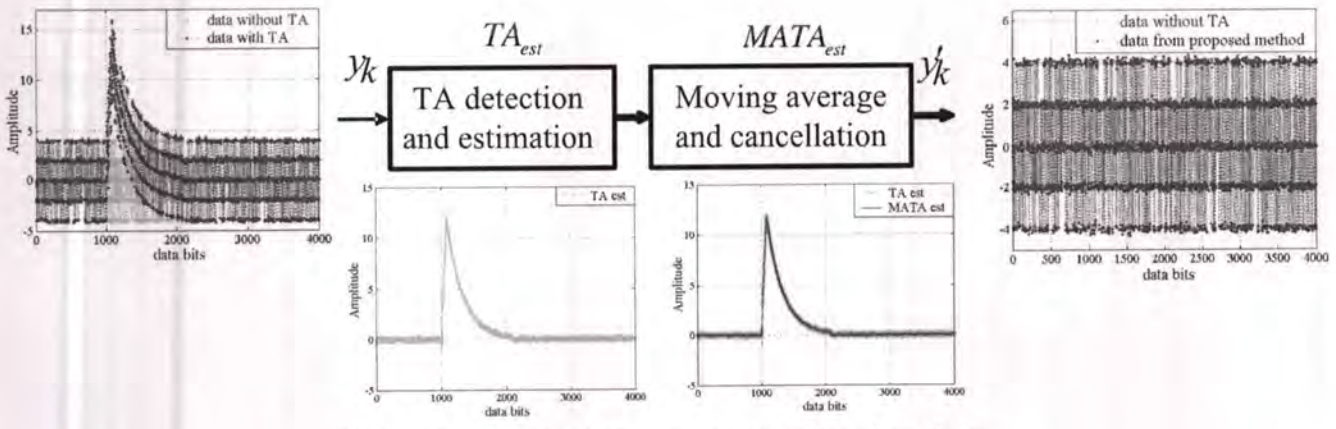

Fig. 2 Proposed method for thermal asperity estimation and cancellation.

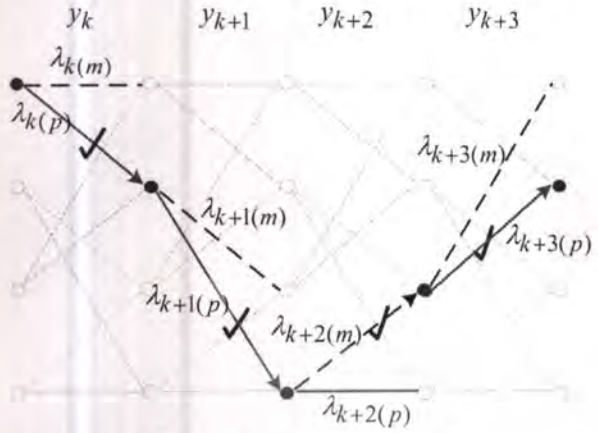

Fig. 3 An example of path selection.

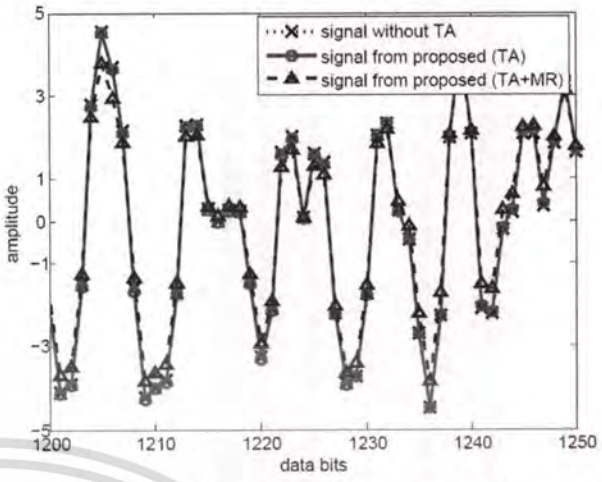

Fig. 4 The equalized signal without TA and the signal from proposed canceler with TA for PR2 target at ND = 1.5, SNR = 22 dB, A_o = 3 and T_f = 1080 bits.

subtract the result from the equalized signal y_k. Based on (10), the moving-averaged TA(noise) estimates $MATA_{est,k}$ is found from

$$MATA_{est,k} = \frac{1}{n} \sum_{i=k-\phi}^{k+\phi} TA_{est,i} \tag{11}$$

and the adjusted PR equalized signal y'_k is

$$y'_k = y_k - MATA_{est,k}, \tag{12}$$

where $\phi = (n-1)/2$ and n (an odd integer) is the window length. This signal is then used as input to the Viterbi detector.

4. Simulation Results and Discussion

In this section, we present the simulation results for the proposed method in the PMR channels with the thermal asperity. In the simulations, we consider the PR2 target at ND = 1.5 for the various TA amplitudes and affected bit ranges of TA. Each sector consists of 4096 information bits.

In Fig. 4, we compare the equalized signal without TA with the output signal of the proposed TA canceler for the equalized signal affected by TA and 10% GMR nonlinearity for the PR2 target at SNR = 22 dB and β = 3. We can see that the signal from the canceler accurately follows the signal without TA decreased accuracy from the GMR nonlinear effect.

In Fig. 5, we compare the system performance improvement between the proposed method and the method proposed by Mathew [6] for the PR2ML system with ND = 1.5, β = 3 and T_f = 1080 bits. Mathew et al. proposed to detect the TA by comparing the read back amplitude and the window averaged read back signal with two separate thresholds. Afterward, the TA is canceled by subtracting the average TA from the read back signal. At SNR = 24 dB, we can observe that the proposed method provides more than an order of magnitude improvement in BER compared with the Mathew method. Nonetheless, it is still inferior to the case of the equalized signal without TA.

The performance gap between the system without TA

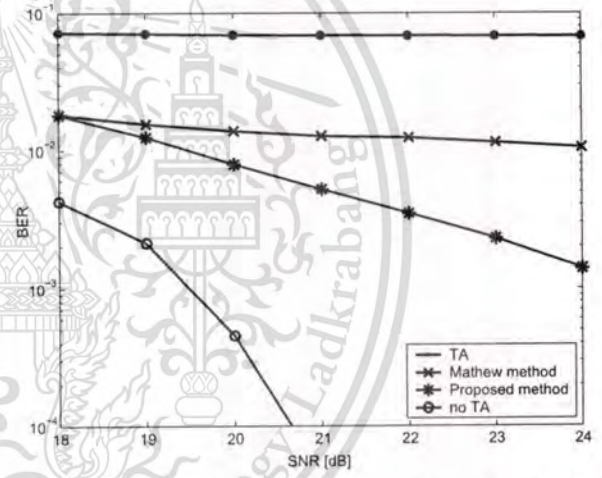

Fig. 5 BER performance of the PR2ML systems with TA effects at ND = 1.5, β = 3 and T_f = 1080 bits.

effects and the proposed method can be explained from the fact that the proposed method still cannot predict the TA well during the rise time, hence, the estimation error is resulted during this period.

The severity of TA can be categorized into the following three levels [3], i.e.,

1. severe: around 1000 bits per sector,
2. medium: around 800 bits per sector, and
3. minimum: around 500 bits per sector.

In Fig. 6, the BER comparison between the PR2ML system with and without TA cancellation for different severity levels of TA, where ND = 1.5 and β = 3 are shown. Without TA cancellation, the BER performance degrades due to the increased bit ranges of TA. The proposed method provides a better resilience since the BER degradation is not as evident.

In Fig. 7, we compare the BER performances between the PR2ML and PR3ML system, where ND = 1.5, β = 3

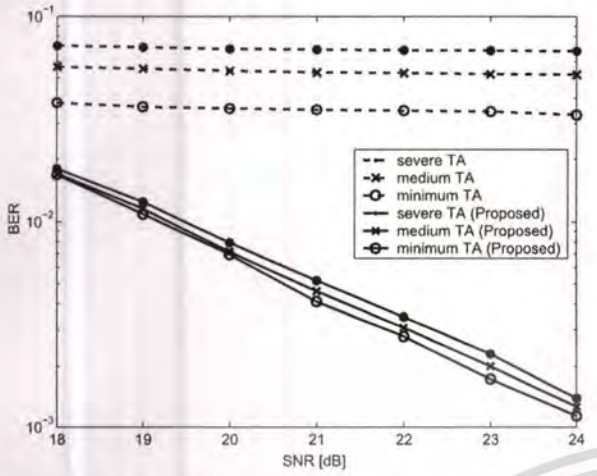

Fig. 6 BER of the PR2ML system with MR nonlinearity for different severity at $ND = 1.5$ and $\beta = 3$.

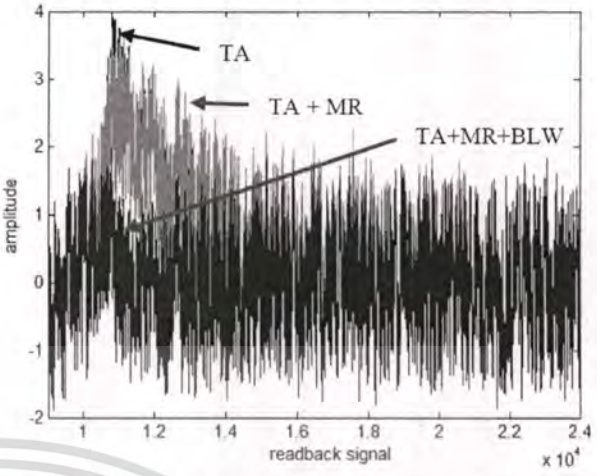

Fig. 8 The read-back signal with TA, GMR asymmetry 10% and BLW effects of PR2 target at $ND = 1.5$, SNR = 22 dB, $\beta = 3$ and $T_f = 1080$ bits.

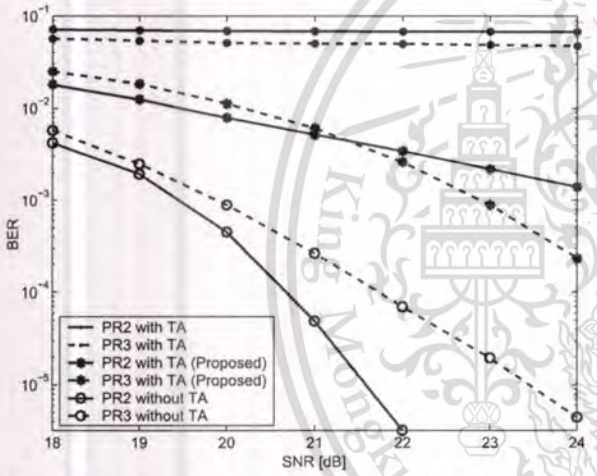

Fig. 7 BER performances for the PR2ML and PR3ML channels with and without TA at $ND = 1.5$, $\beta = 3$ and $T_f = 1080$ bits.

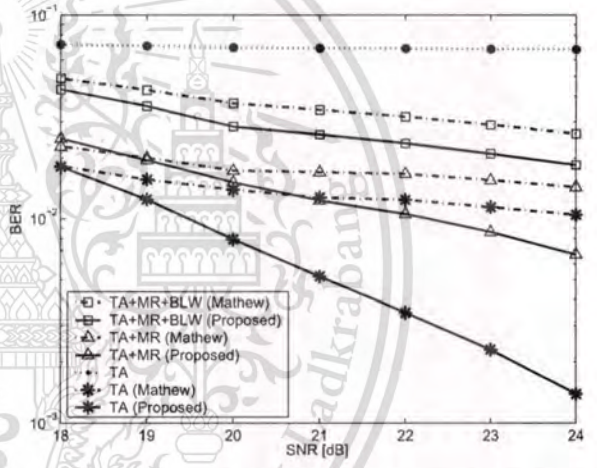

Fig. 9 BER performance of the PR2ML systems with TA amp. = 3, GMR nonlinearity 10% and BLW effects ≈ .1.5% at $ND = 1.5$, $\beta = 3$ and $T_f = 1080$ bits.

and $T_f = 1080$ bits. We can see that the proposed method for both PR targets provides more than an order of magnitude improvement in BER when TA occurs. Specifically, the PR3 target provides more than two orders of magnitude improvements compared with the system without TA canceler and achieves the gain over PR2ML system of about 1.4 dB at BER $\approx 1.4 \times 10^{-3}$ when only TA is present. This is contrary to the previous findings in [1] that the PR2 target with DC full response is the best target for PMR system with AWGN only.

When the GMR nonlinearity and the BLW effect are included, the read back signal is changed in appearance.

Figure 8 compares the amplitude of the read back signal with TA, 10% GMR nonlinearity and the BLW effect as decaying of the dc-level approximate 1.5% based on [6], respectively. In the simulation, we consider the PR2 target at SNR = 22 dB, $ND = 1.5$ and $\beta = 3$. For $T_r = 80$ bits and $T_d = 250$ bits, the TA effect range T_f becomes 1080 bits. For the signal with TA only, the high peak with decay time is observed. With GMR asymmetry effects, the same peak is somewhat reduced. When the BLW effect is included, however, it is evident that the TA peak and decay time are reduced [2].

In Fig. 9, we present the performances of the proposed method in the PR2ML systems with the following three cases: (1) TA + GMR nonlinearity + BLW, (2) TA + GMR nonlinearity and (3) only TA effect. The GMR nonlinearity is 10% and BLW effects ≈ 1.5%. With only TA, at SNR = 24 dB, the proposed method provides nearly an order of BER improvement over with Mathew method [1] and more than an order of BER reduction when compared with a the system without a TA canceller. Under the presence of GMR nonlinearity and BLW effect, the proposed method outperforms Mathew method slightly. The results indicate the severe performance degradation of both of these effects.

In Fig. 10, We compare the statistics of burst errors between the proposed method and the system without TA canceller in the PR2ML channel at SNR = 24 dB. The GMR

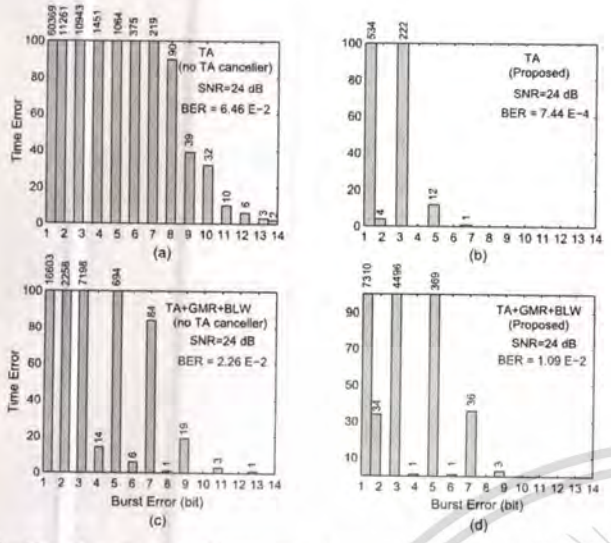

Fig. 10 The statistics of burst errors between the proposed method and the system without TA canceller in the PR2ML channel.

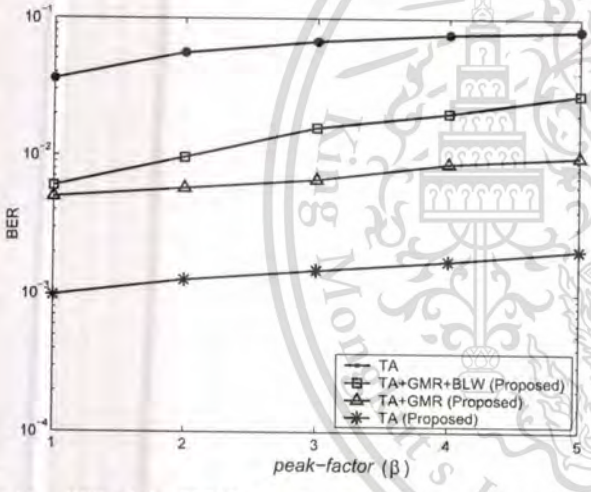

Fig. 11 BER of the PR2ML system versus TA amplitude at SNR = 24 dB, ND = 1.5, T_f = 1080 bits, GMR asym. = 10% and BLW effects ≈ 1.5%.

nonlinearity 10% and the BLW effects ≈ 1.5%. From Figs. 10(a) and (b), when only TA is present, the proposed method drastically reduces the BER level as well as the number of burst errors at all lengths. Specifically, the burst length of over 7 bits are all eliminated. Under the presence of GMR nonlinearity and BLW effect as shown in Figs. 10(c) and (d), the burst error statistics are also improved by about 50% using the proposed method. All the burst errors of length over 9 bits disappear. We can see that the proposed method provides fewer and shorter burst errors compared with the system without TA canceller in both cases.

Figure 11 shows the relationship between the BER and TA amplitudes for PR2ML system, where ND = 1.5, SNR = 24 dB, T_f = 1080 bits, GMR asymmetry 10% and BLW effect ≈ 1.5%. We can see that the system performance is reduced when the TA amplitude increases and the accuracy in TA estimation and detection is decreased when the GMR nonlinearity and BLW effect is included. However, the proposed method still shows the BER improvement compared with the system without TA cancellation and the previous work.

5. Conclusions

In this work, we proposed a new TA estimation method from an equalized signal based on the trellis of PR targets in perpendicular magnetic recording systems with thermal asperity. We compare the BER performance of the PRML system between the proposed method and previously proposed method based on window averaging. The proposed method provides more than an order of magnitude improvement in BER compared to the case without a thermal asperity canceller. Even though the performance degrades with GMR nonlinearity and BLW effect, the performance gain is evident. In addition, the proposed method is more resilient to various peak factors as compared with the system without TA cancellation.

Acknowledgments

This work is supported in part by the grant in Southeast Asia Engineering Education Development and an autonomous sub-network of the ASEAN University Network (AUN/SEED-Net), King Mongkut's Institute of Technology Ladkrabang, Bangkok, Thailand.

References

[1] M. Madden, M. Oberg, Z. Wu, and R. He, "Read channel for perpendicular magnetic recording," IEEE Trans. Magn., vol.40, no.1, pp.241–246, Jan. 2004.

[2] M.F. Erden and E.M. Kurtas, "Thermal asperity detection and cancellation in perpendicular magnetic recording systems," IEEE Trans. Magn., vol.40, no.3, pp.1732–1737, May 2004.

[3] M.F. Erden, E.M. Kurtas, and M.J. Link, "Evaluation of thermal asperity in magnetic recording," Coding and Signal Processing for Magnetic Recording Systems, ed. B. Vasic and E.M. Kurtas, pp.31-1–31-16, CRC Press LLC, 2005.

[4] V. Dorfman and J.K. Wolf, "A method for reducing the effects of thermal asperities," IEEE J. Sel. Areas Commun., vol.19, no.4, pp.662–667, April 2001.

[5] H. Ueno, "Magnetic disk apparatus, method for reproducing magnetic recording, and method for read retry," U.S. Patent 0221476A1, Oct. 2006.

[6] G. Mathew and I. Tjhia, "Thermal asperity suppression in perpendicular recording channels," IEEE Trans. Magn., vol.41, no.10, pp.2878–2880, Oct. 2005.

[7] A. Takeo, T. Taguchi, Y. Sakai, and Y. Tanaka, "Characterization of GMR nonlinear response and the impact on BER in perpendicular magnetic recording," IEEE Trans. Magn., vol.40, no.4, pp.2582–2584, July 2004.

[8] A. Patapoutian, "Baseline wander compensation for the perpendicular magnetic recording channel," IEEE Trans. Magn., vol.40, no.1, pp.235–240, Jan. 2004.

[9] P. Kovintavewat, I. Ozgunes, E.M. Kurtas, J.R. Barry, and S.W. McLaughlin, "Generalized partial responsetargets for perpendicular recording with jitter noise," IEEE Trans. Magn., vol.38, no.5,

pp.2340–2342, Sept. 2002.
[10] X. Yang and E.M. Kurtas, "Signal and noise generation for magnetic recording channel simulations," Coding and Signal Processing for Magnetic Recording Systems, ed. B. Vasic and E.M. Kurtas, pp.61-1–6-20, CRC Press LLC, 2005.
[11] S. Stupp, A. Baldwinson, P. McEwen, M. Crawford, and T. Rogers, "Thermal asperity trends," IEEE Trans. Magn., vol.35, no.2, pp.752–757, March 1999.
[12] M.F. Erden and E.M. Kurtas, "Baseline wander compensation for perpendicular recording," IEEE Trans. Magn., vol.40, no.4, pp.3114–3116, July 2004.
[13] X. Hu and B.V.K. Vijaya Kumar, "Evaluation of low-density parity-check codes on perpendicular magnetic recording model," IEEE Trans. Magn., vol.43, no.2, pp.727–732, Feb. 2007.
[14] Y. Okamoto, H. Osawa, H. Saito, H. Muraoka, and Y. Nakamura, "Performance of PRML systems in perpendicular magnetic recording channel with jitter-like noise," J. Magn. Magn. Mater., vol.235, no.1-3, pp.259–264, Oct. 2001.

Yupin Suppakhun received the B.S. degrees in Science Industrial Education in 1992 and M.S. degrees in Electrical Engineering in 1999 from King Mongkut's Institute of Technology Ladkrabang, Bangkok, Thailand. She is an Assistant Professor in the Department of Information Technology, Faculty of Industrial Technology and Management, King Mongkut's University of Technology North Bangkok Prachinburi Campus. She has been accepted as qualified recipient for scholarship under The Commission on Higher Education Staff Development Project for the Joint Ph.D. Program in Engineering at King Mongkut's Institute of Technology Ladkrabang, Bangkok, Thailand. She is currently with the Department of Electrical and Electronic Engineering, Ehime University as a Visiting Researcher. Her current research interest is in signal processing in digital recording system.

Pornchai Supnithi received the B.S. degree in Electrical Engineering from University of Rochester, Rochester, New York, USA, in 1995. M.S. degree in Electrical Engineering from University of Southern California, Los Angeles, California, USA in 1997 and Ph.D. in Electrical Engineering from Georgia Institute of Technology, Atlanta, Georgia, USA in 2002. He has work experience with INTELSAT, Washington, DC in 1995, Intellicom, Inc., Fremont, CA in 1997, and Calimetrics, Inc., Alameda, CA in 2000–2001. He is currently an Associate Professor in the Telecommunications Engineering Department, KMITL, Bangkok, Thailand. His research interests are in the area of scintillation modeling, error correction control and equalization and soft decoding/iterative decoding applied to recording channels, satellite channels and mobile wireless channels.

Yoshihiro Okamoto received the B.E. and M.E. degrees in electronic engineering from Ehime University, Matsuyama, Japan, in 1983 and 1985, respectively, and Dr.Eng. degree from Osaka University, Osaka, Japan in 1993. From 1985 to 1990, he worked for Sharp Corporation. In 1990, he joined the faculty of engineering, Ehime University. Presently, he is a Professor in the Department of Electrical and Electronic Engineering, Faculty of Engineering, Ehime University. During 1996 to 1997, he was a Visiting Research Associate at the School of Electronic, Communication and Electrical Engineering at the University of Plymouth, UK. His current research interest is in signal processing in digital recording system. Dr. Okamoto is a member of the Institute of Electrical and Electronic Engineering, the Institute of Image Information and Television Engineers of Japan and Magnetic Society of Japan.

Yasuaki Nakamura received his B.E., M.E. degrees in Electrical and Electronic Engineering from Ehime University, Matsuyama, Japan in 2001 and 2003, respectively and Dr.Eng. degree from Ehime University in 2008. He is presently a Assistant Professor in the Department of Electrical and Electronic Engineering and Computer Science, Graduate School of Science and Engineering, Ehime University. His research interests include error correcting code and signal processing for magnetic recording channel.

Hisashi Osawa received the B.E. and M.E. and Dr.Eng. degrees from Osaka University, Osaka, Japan in 1966, 1968 and 1971, respectively. From 1973 to 1974 he was a Research Associate in the Department of Electrical Communication Engineering, Osaka University. In 1974 he joined the Department of Electrical and Electronic Engineering of Ehime University, Matsuyama, Japan, where he was an Associate Professor from 1974 to 1988 and a Professor from 1988 to 2008. Since 2008 he has been with Institution for Collaborative Relations, Ehime University, where he is currently a Professor Extraordinary. During 1987 to 1988, he was a Visiting Scientist at the Department of Electronic and Electrical Engineering of King's College London, University of London. He has previously worked in the areas of signal detection and optical communications. His current research interest is in signal processing for high density recording. He received the Fujo Frontier Prize from the Institute of Image Information and Television Engineers in 2000 and the MSJ Outstanding Research Award from the Magnetics Society of Japan in 2008.

ITC-CSCC2008

The 23rd International Technical Conference on Circuits/Systems, Computers and Communications

Conference Abstracts

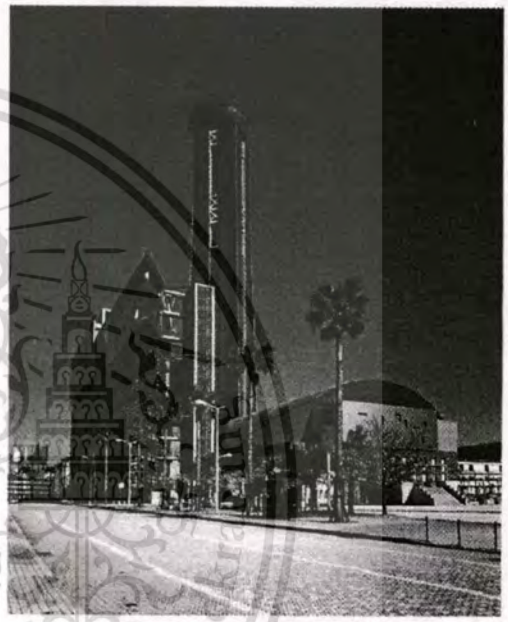

Kaikyo Messe Shimonoseki

Kaikyou Messe
Shimonoseki,
Yamaguchi, Japan
July 6-9, 2008

Sponsored by

* The Institute of Electronics, Information and Communication Engineers (IEICE), the Engineering Sciences Society
* The Institute of Electronics Engineers of Korea (IEEK)
* The Electrical Engineering/Electronics, Computer, Telecommunications and Information Association, Thailand

Cosponsored by

* Yamaguchi University, Japan

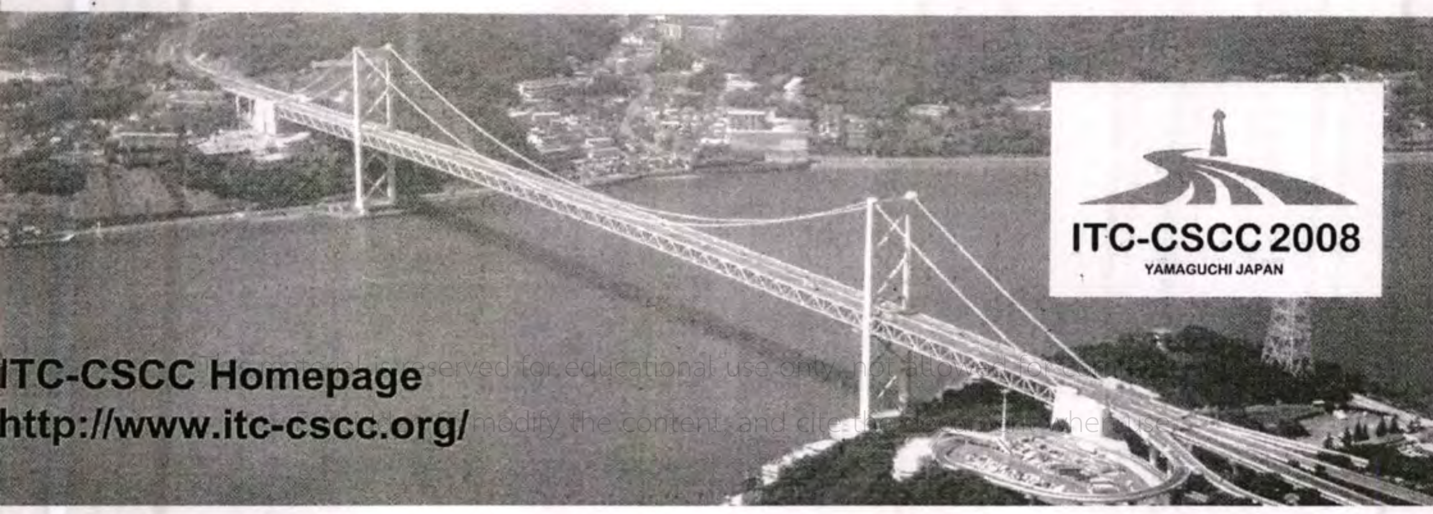

ITC-CSCC 2008
YAMAGUCHI JAPAN

ITC-CSCC Homepage
http://www.itc-cscc.org/

The Performance Comparison Between DC-Full and DC-Attenuation Partial-Response Targets in Perpendicular Magnetic Recording Channel

Yupin Suppakhun[1], Pornchai Supnithi[2]
[1,2] Faculty of Engineering and Research Center for Communications and Information Technology(ReCCIT)
King Mongkut's Institute of Technology Ladkrabang
3 Moo 2 Chalongkrung Rd., Ladkrabang, Bangkok, Thailand, 10520.
E-mail: [1]s9060001@kmitl.ac.th, [2]ksupornc@kmitl.ac.th

Abstract: In this paper, we investigate the performance of perpendicular recording channel for dc-full and dc-attenuation partial response targets under the environment of electronics noise and jitter noise. We compare the performance of partial-response maximum-likelihood (PRML) and noise-predictive maximum–likelihood (NPML) detector for both types of targets. The NPML system is more suited for dc-attenuation targets, whereas the dc-full targets are suited to PRML system at low jitter noise.

1. Introduction

In order to achieve high-density recording, the development of the signal processing schemes matching the perpendicular magnetic recording (PMR) channel is desired. Partial-response maximum-likelihood (PRML) and noise-predictive maximum–likelihood (NPML) detector which are signal processing technique for to day hard disk drive.

In this paper, we investigate the performance of partial-response maximum-likelihood (PRML) and noise-predictive maximum–likelihood (NPML) detector for high density perpendicular magnetic recording (PMR) channel with the environment of electronics noise and media noise. The performance of perpendicular recording channel is consider with dc-full and dc-attenuation targets types. In previous work, perpendicular magnetic recording with PRML detector for dc-full targets give higher performance than the dc-attenuation targets[1]. We report the BER performance of NPML system with dc- attenuation targets can be improved more than to PRML system while the dc-full targets suited to PRML system because can to received nearly gain as the complexity of the viterbi detector is not increased at low jitter noise. The next section of this paper, we overview the read-back system model, targets types of PMR, the NPML system and related parameters. The simulation results and discussions are then illustrated in Section 3. The conclusion is described in Section 4 and the references are in Section 5.

2. Read-back System Model

The read-back system block diagram for the perpendicular magnetic recording is shown in Fig. 1.

The binary random sequences $a_k \in \{\pm 1\}$ are input of the channel, where k represents the discrete time index, $k = 1 \ldots K$ (K is total number of transmitted bits). A data input sequence with bit period T is filtered by ideal differentiator (1-D) to form a transition sequence $b_k \in \{-2, 0, 2\}$, where $b_k = \{\pm 2\}$ corresponds to a positive and negative transition, and $b_k = \{0\}$ corresponds to the absence of transition. The sequence b_k passing through the channel is convolved with the transition response.

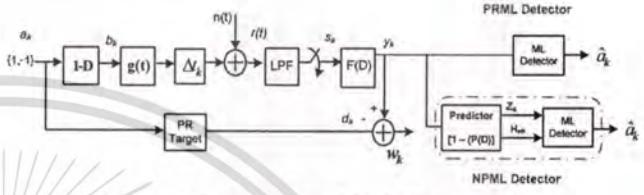

Figure 1. The read-back system block diagram

The transition response for perpendicular recording can be written as[2].

$$g(t) = erf\left(\frac{2t\sqrt{ln2}}{PW50}\right) \quad (1)$$

where $erf(.)$ is an error function defined as $erf(x) = \frac{2}{\sqrt{\pi}} \int_0^x e^{-z^2} dz$, and $PW50$ determines the pulse width of the derivative of $g(t)$. The recorded normalized density is defined by $ND = PW50/T$. The noise in PMR can be model as a mixture of additive white Gaussian noise (AWGN) with two-sided power spectral density $No/2$ and medis noise,assume to be transition jitter dominated. We apply a jitter noise modeled as a random shift in the transition position, which has a Gaussian distribution function with zero mean specified as a percentage of T and $|\Delta t_k| \le T/2$. Hence the read-back signal $r(t)$ can be expressed as

$$r(t) = \sum_{k=-\infty}^{\infty} b_k g(t - kT + \Delta tk) + n(t) \quad (2)$$

where $n(t)$ is additive white Gaussian noise (AWGN), and Δt_k is transition jitter noise

The read-back signal $r(t)$ is filtered by a Butterworth low-pass filter with cutoff frequency at $1/2T$, which is sampled at a symbol rate. Its function is to eliminate out-off-band noise.

The detection process is composed of two components. The first component is a noise predictive filter that reduces distortion (noise) from equalized signal. The second component is the viterbi detector based on trellis of the PR targets with adjusted trellis to the output of the noise predictor.

2. 1 Noise-Predictive Maximum-Likelihood (NPML) Detector

Let y_k be output data sequence of the PR equalizer at instant k. The finite impulse response(FIR) filter has the polynomial of the PR targets in the form of

$$F(D) = (1 + f_1 D + f_2 D^2 + ... + f_N D^N) \quad (3)$$

where the f_i $(i = 1,2,...,N)$ is the coefficients of the filter. The equalized output is

$$y_k = a_k + \sum_{i=1}^{n} f_i a_{k-i} + w_k \quad (4)$$

where w_k is the colored noise sequences at the output of equalizer. The power of the colored noise component can be reduced by noise prediction. The NPML system uses a predictor with N-coefficients. Given the transfer polynomial of the FIR noise predictor filter is $P(D) = (p_1 D + p_2 D^2 + ... + p_N D^N)$ or, equivalently, $E(D) = [1 - P(D)]$ denotes the transfer polynomial of the predictor error filter, then the whitened noise component e_k from the predictor can be computed by

$$\begin{aligned} e_k &= w_k - \hat{w}_k \\ &= w_k - \sum_{i=1}^{N} w_{k-i}\, p_i \quad , \end{aligned} \quad (5)$$

where the noise predicted sample $\hat{w}_k$ can be defined as

$$\hat{w}_k = \sum_{i=1}^{N} w_{k-i}\, p_i \quad (6)$$

The length N coefficients of a noise predictor filter are determined by solving the system of well-known normal equation given by [3]

$$R_{ww}(i) = \sum_{j=1}^{N} p_i R_{ww}(i-j), \qquad i = 1,2,...,N \quad (7)$$

where R_{ww} is the autocorrelation function, which can be written in the matrix form as

$$\underbrace{\begin{bmatrix} r_{ww}(1) \\ r_{ww}(2) \\ \vdots \\ r_{ww}(N) \end{bmatrix}}_{\mathbf{r}} = \underbrace{\begin{bmatrix} R_{ww}(0) & R_{ww}(1) & \cdots & R_{ww}(N-1) \\ R_{ww}(1) & R_{ww}(0) & \cdots & R_{ww}(N-2) \\ \vdots & \vdots & \ddots & \vdots \\ R_{ww}(N-1) & R_{ww}(1) & \cdots & R_{ww}(0) \end{bmatrix}}_{\mathbf{R}} \underbrace{\begin{bmatrix} p_1 \\ p_2 \\ \vdots \\ p_N \end{bmatrix}}_{\mathbf{p}}, \quad (8)$$

where **R** represents the square matrix, p_i is determined by

$$\mathbf{p} = \mathbf{R}^{-1}\mathbf{r} \quad (9)$$

where $\mathbf{p} = [p_1\ p_2 \ldots p_N]$ and

$$\mathbf{r} = [R_{ww}(1)\ R_{ww}(2) \ldots R_{ww}(N)]^T .$$

The NPML detection results from the embedding the noise prediction/whitening process into the branch metric computation of the viterbi detector. The output of noise predictor error filter Z_k to viterbi detector can be computed by

$$z_k = y_k + \sum_{i=1}^{n} p_i y_{k-1} \quad (10)$$

or in D domain is

$$Z_k = (y_k)[1 - P(D)] \quad (11)$$

and

$$H_{eff}(D) = H(D)[1 - P(D)] \quad (12)$$

where $H_{eff}(D) = (1 - g_1 D - g_2 D^2 - \ldots - g_{N+V} D^{N+v})$ represents the transfer polynomial of effective targets which corresponds to noise predictor error filter, where the g_i $(i = 1,2,...,N)$ is the N-tap coefficients of the effective targets, v is the memory of PR targets and $H(D)$ is partial response targets, then the viterbi detector uses a state trellis with the number of state 2^{N+v}.

The branch metric of the NPML detector for effective targets samples corresponding to a transition from state p to state q takes the form

$$\lambda_k(p,q) = \left| Z_k - \hat{O}_k(p,q) \right|^2 \quad (13)$$

where $\lambda_k(p,q)$ represents the branch metric cost from state p to state q, and $\hat{O}_k$ is noiseless channel output from effective targets ($H_{eff}(D)$) defined as

$$\hat{O}_k = a_k * H_{eff} \quad (14)$$

where * denotes the convolution operator.

3. Simulation Results and Discussions

In this section, we present BER simulation results for two targets types for PMR system, and investigate the BER performance in PRML detector and NPML detector. In the simulations, the received sequence S_k is equalized by 21-tap finite impulse response(FIR) filter calculated to minimize the mean-square error (MMSE) of the equalizer output and targets response such that y_k resembles d_k. We process each sector consisting of 4096 information bits and let the parameter of normalized recording density (ND) = 2.5, media jitter noise(J2) various 10% 30% and 50%. The noise predictive filter (NP_Tap) is 4 tap. The average BER from the results are plotted versus the SNR(dB). The dc-attenuation targets polynomials are (2 3 0 -1) and (5 6 0 -1), while the dc-full targets are (1 6 7 2) and (4 6 4 2). We compare the performance of PRML and NPML detector at different target types.

In Fig. 2, the BER performance of PRML detector at different targets types between dc-attenuation targets(5 6 0 -1), (2 3 0 -1) and dc-full targets (1 6 7 2), (4 6 4 2) with 10% jitter noise is shown. We can see that the dc-full targets achives than dc-attenuation targets.

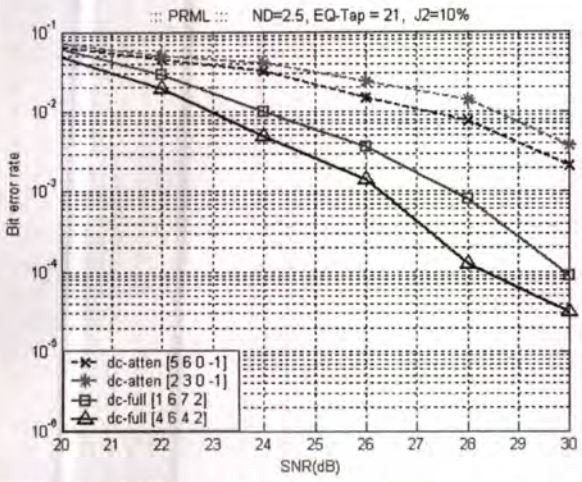

Figure 2. PRML performance between dc-attenuation targets(5 6 0 -1), (2 3 0 -1) and dc-full targets (1 6 7 2), (4 6 4 2)

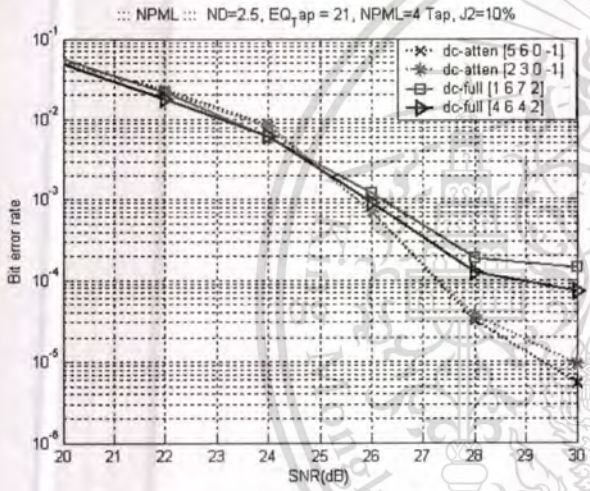

Fgure 3. NPML performance between dc-attenuation targets (5 6 0 -1), (2 3 0 -1) and dc-full targets (1 6 7 2), (4 6 4 2)

In Fig. 3, the BER performance of NPML detector at different targets types between dc-attenuation targets (5 6 0 -1), (2 3 0 -1) and dc-full targets (1 6 7 2), (4 6 4 2) versus the system performance is shown. We can see at higher SNR, the dc-attenuation targets achieves better performance than dc-attenuation targets. For the example, at BER $\approx 1\times10^{-4}$, the dc-attenuation targets (5 6 0 -1) have gain more than dc-full targets (4 6 4 2) about 1.8 dB at the jitter noise is 10% and noise predictor is 4 tap.

In Fig. 4, the BER performance of PRML and NPML detector base on dc-full targets (1 6 7 2) at percentages jitter noise various 10% 30% 50% and NP_Tap = 4 tap. We can see at BER $\approx 8\times10^{-4}$, the NPML have gain more than PRML about 1.8 and 1.4 dB at the jitter noise is 10% and 50% sequentially.

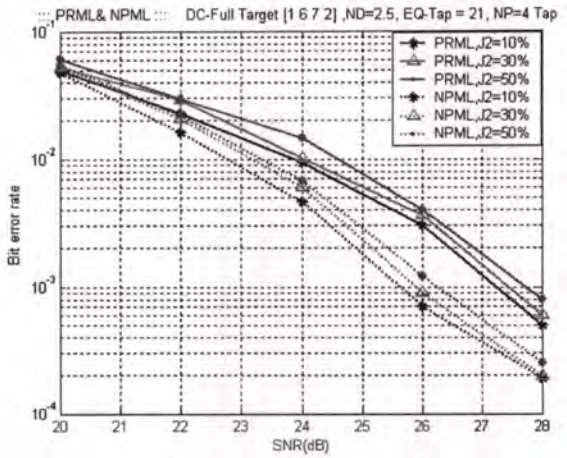

Figure 4. PRML and NPML performance of percentages jitter noise various base on dc-full targets (1 6 7 2)

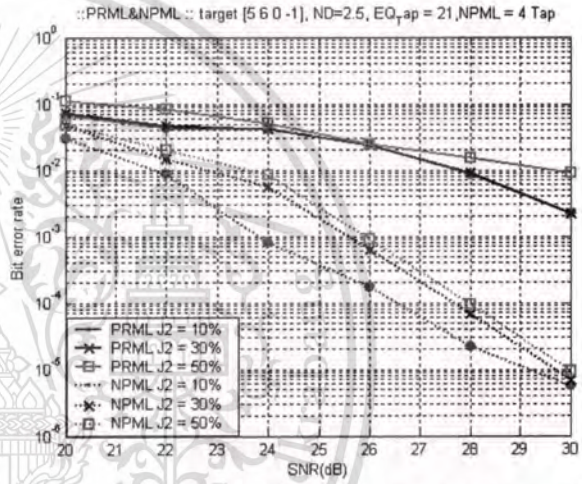

Figure 5. PRML and NPML performance of percentages jitter noise various base on dc-attenuation targets(5 6 0 -1)

In Fig. 5, the BER performance of PRML and NPML detector base on dc-attenuation targets (5 6 0 -1) with transition jitter noise of 10% 30% and 50%. We found that the NPML detector achieves better performance than PRML detector.

4. Conclusions

We investigate using PRML and NPML detector partial response targets types appropriate for high density perpendicular magnetic recording (PMR) channel with the environment of electronics noise and jitter noise. From the simulation results, The bit error rate(BER) performance of NPML system with dc-attenuation targets is better than that of PRML system, while the dc-full targets is more suited to PRML system at low jitter noise. However, with media-noise-dominant model, the NPML detector achieves higher improvement gian over PRML detector at hight SNR.

5. References

[1] M. Madden, M. Oberg, Z. Wu and R. He, "Read Channel for Perpendicular Magnetic Recording", *IEEE Trans. on Magnetics*, Vol. 40, No. 1, Jan. 2004, pp. 241-246.

[2] P. Kovintavewat, I. Ozgunes, E. Kurtas, J. R. Barry and S. W. McLaughlin "Generalized Partial Response Targets for Perpendicular Recording with Jitter Noise", *IEEE Trans. on Magnetics*, Vol. 38, Issue 5, Sep. 2002, pp. 2340-2342.

[3] J. D. Coker, E. Eleftheriou, R. L. Galbraith, and W. Hirt, "Noise-predictive maximum likelihood detection", *IEEE Trans. on Magnetics*, Vol. 34, No. 1, Jan. 1998, pp.110-117.

[4] J. Lee, and J. Lee "A Simplified Noise-Predictive Partial Response Maximum Likelihood Detection Using M-Algorithm for Perpendicular Recording Channel", *IEEE Trans. on Magnetics*, Vol. 41, Issue 2, Feb. 2005, pp. 1064-1066.

[5] Isatake Kaitsu and et al. "Ultra High Density Perpendicular Magnetic RecordingTechnology", *FUJITSU Sci.Tech. J.*, Vol. 42, Issue 1, Jan. 2006, pp. 122-130.

The 1st International Data Storage Technology Conference

DST-CON 2008

THAILAND - *The paragon of the world's HDD manufacturing*

Miracle Grand Convention Hotel
Bangkok, Thailand

April 21-23, 2008

Organized by

National Electronics and Computer Technology Center (NECTEC)
I/U CRC in HDD Component
I/U CRC in HDD Advanced Manufacturing
Data Storage Technology and Applications Research Center (D*STAR)

Sponsored by

WD Western Digital · Seagate · FUJITSU · hard drive by HITACHI

ID-52

Title: Effect of Cutoff Frequency of Lowpass Filter on the Performance of Perpendicular Magnetic Recording Systems

Author: [1]Yupin Suppakhun
[2]Pornchai Supnithi

Affiliation: Faculty of Engineering, Research Center for Telecommunications and Information Technology (ReCCIT) and Research Center in Data Storage Technology and Applications (D*STAR) King Mongkut's Institite of Tecnology Ladkrabang, Bangkok, Thailand

Email: [1]s9060001@kmitl.ac.th,
[2]ksupornc@kmitl.ac.th

Abstract: *In this paper, the effect of cutoff frequency of the front-end low-pass filter on the performance of perpendicular recording channel is investigated. With positive and negative deviation from the nominal value, the partial–response maximum–likelihood (PRML) system shows more degradation by the positive deviation than the negative one. The noise-predictive maximum–likelihood (NPML) system shows the results otherwise.*

Effect of Cutoff Frequency of Lowpass Filter on the Performance of Perpendicular Magnetic Recording Channel

Presented in 1st Data Storage Technology Conference (DST-CON 2008)

Yupin Suppakhun[1], Pornchai Supnithi[2]

Abstract

In this paper, the effect of cutoff frequency of the front-end low-pass filter on the performance of perpendicular recording channel is investigated. With positive and negative deviation from the nominal value, the partial -response maximum-likelihood (PRML) system shows more degradation by the positive deviation than the negative one. The noise-predictive maximum-likelihood (NPML) system shows the results otherwise.

Introduction

Current magnetic recording system employs perpendicular media , thus the transition response is vastly different from the longitudinal media with existent dc component. The front-end components in the read channel chip consists of variable gain amplifier (VGA), amplitude asymmetry correction, thermal asperity (TA) detection and correction and low-pass filter. The low-pass filter has a function of suppressing the out-of-band noise. Its coefficients, cut off frequency, frequency boost factor among others can be adapted for each media and read-write system so that bit error rate (BER) can be optimized. In this paper, we aim to investigate the influence of the cutoff frequency deviation to the system performance, in particular, the PRML and NPML detector in the environment of electronics noise and jitter noise. In Section 2, we overview the readback system model, the NPML system and related parameters. The simulation results and discussions are then illustrated in Section 3. The conclusion is described in Section 4 and the references are in Section 5.

Readback System Model

The readback system block diagram for the perpendicular magnetic recording is shown in Figure 1.

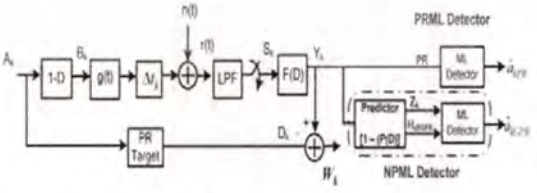

Figure 1. The readback system block diagram

*Faculty of Engineering, Research Center for Telecommunications and Information Technology(ReCCIT) and Research Center in Data Storage Technology and Applications (D*STAR) King Mongkut's Institite of Tecnology Ladkrabang, Bangkok, Thailand,*
**corresponding author; e-mail: s9060001@kmitl.ac.th[1], ksupornc@kmitl.ac.th[2]*

The binary random sequences $a_k \in \{\pm 1\}$ are input of the channel, where k represents the discrete time index, $k = 1...K$ (K is total number of transmitted bits). A data input sequence with bit period T is filtered by ideal differentiator $(1-D)$ to form a transition sequence $b_k \in \{-2,0,2\}$, where $b_k = \{\pm 2\}$ corresponds to a positive and negative transition, and $b_k = \{0\}$ corresponds to the absence of transition. The sequence b_k passing through the channel is convolved with the transition response.

The transition response for perpendicular recording can be written as(Kovintavewat et al., 2002).

$$g(t) = erf\left(\frac{2t\sqrt{ln2}}{PW50}\right) \quad (1)$$

where $erf(.)$ is an error function defined as $erf(x) = \frac{2}{\sqrt{\pi}}\int_0^x e^{-z^2} dz$, and $PW50$ determines the pulse width of the derivative of $g(t)$. The recorded normalized density is defined by $ND = PW50/T$, hence, the readback signal $r(t)$ can be expressed as

$$r(t) = \sum_{k=-\infty}^{\infty} b_k g(t - kT + \Delta tk) + n(t)$$

where $n(t)$ is additive white Gaussian noise (AWGN) with two-sided power spectral density $No/2$, and Δt_k is jitter noise modeled as a random shift in the transition position, which has a Gaussian distribution function with zero mean and variance $\sigma_j{}^2$,where σ_j isspecified as a percentage of T and $|\Delta t_k| \le T/2$.

The readback signal $r(t)$ is filtered by a Butterworth lowpass filter with cutoff frequency at $1/2T$, which is sampled at a symbol rate. Its function is to eliminate out-off-band noise.

The detection process is composed of two components. The first component is a noise predictive filter that reduces distortion(noise) from equalized signal. The second component is the Viterbi detector based on trellis of the PR target with adjusted trellis adjusted by output of the noise predictor.

Noise-predictive maximum likelihood (NPML) detector

Let y_k be output data sequence of the PR equalizer at instant k. The finite impulse response(FIR) filter has the polynomial of the PR target in the form of $F(D)=(1 + f_1D + f_2D^2 +...+f_ND^N)$, where the $fi(i = 2,...,N)$ is the coefficients of the filter. The equalized output is

$$y_k = a_k + \sum_{i=1}^{n} f_i a_{k-i} + w_k \quad (3)$$

where w_k is the colored noise sequences at the output of equalizer. The power of the colored noise component can be reduced by noise prediction. The NPML system uses a predictor with N-coefficients. Given the transfer polynomial of the FIR noise predictor filter is $P(D)=(1 + p_1D + p_2D^2 +...+p_ND^N)$ or, equivalently, $E(D) = [1-P(D)]$ denotes the transfer polynomial of the predictor error filter, then the whitened noise component e_k from the predictor can be computed by

$$e_k = w_k - \hat{w}_k = w_k - \sum_{i=1}^{N} w_{k-i}\, p_i \quad , \quad (4)$$

where the noise predicted sample $\hat{w}_k$ can be defined as

$$\hat{w}_k = \sum_{i=1}^{N} w_{k-i}\, p_i \quad (5)$$

The coefficients of a noise predictor filter are determined by solving the system of well-known normal equation given by and variance $\sigma_j{}^2$, where σ_j is

$$R_{ww}(i) = \sum_{j=1}^{N} p_i R_{ww}(i-j), \qquad i = 1,2,...,N \qquad (6)$$

where R_{ww} is autocorrelation function, which can be written in the matrix form as

$$\underbrace{\begin{bmatrix} R_{ww}(1) \\ R_{ww}(2) \\ \vdots \\ R_{ww}(N) \end{bmatrix}}_{\mathbf{r}} = \underbrace{\begin{bmatrix} R_{ww}(0) & R_{ww}(1) & \cdots & R_{ww}(N-1) \\ R_{ww}(1) & R_{ww}(0) & \cdots & R_{ww}(N-2) \\ \vdots & \vdots & \ddots & \vdots \\ R_{ww}(N-1) & R_{ww}(1) & \cdots & R_{ww}(0) \end{bmatrix}}_{\mathbf{R}} \underbrace{\begin{bmatrix} p_1 \\ p_2 \\ \vdots \\ p_N \end{bmatrix}}_{\mathbf{p}}, \qquad (7)$$

where R represents the square matrix, p_i is determined by

where $\mathbf{p} = [p_1\ p_2 \ldots p_N]$ and

$\mathbf{r} = [R_{WW}(1)\ R_{WW}(2) \ldots R_{WW}(N)]^T$.

The NPML detection results from the embedding the noise prediction/whitening process into the branch metric computation of the Viterbi detector. The output of noise predictor error filter Z_k to viterbi detector in D domain term is

$$Z_k = (y_k)[1\text{-}P(D), \qquad (9)$$

and

$$H_{eff}(D) = (H(D))[1\text{-}P(D)], \qquad (10)$$

where $H_{eff}(D) = (1 - g_1 D - g_2 D^2 - \ldots - g_N + {}_V D^{N+v}$ represents the transfer polynomial of effective target which corresponds to noise predictor error filter, where the gi ($i = 1, 2,...,N$) is the N-tap coefficients of the effective target, v is the memory of PR target and $H(D)$ is partial response target, then the viterbi detector uses a state trellis with the number of state 2^{N+v}.

The branch metric of the NPML detector for effective target samples corresponding to a transition from state p to state q takes the form

$$\lambda_k(p,q) = \left| Z_k - \hat{O}_k(p,q) \right|^2 \qquad (11)$$

where $\lambda_k(p,q)$ represents the branch metric cost from state p to state q, and $\hat{O}_k$ is noiseless channel output from effective target ($H_{eff}(D)$) defined as

$$\hat{O}_k = a_k * H_{eff} \qquad (12)$$

Where * denotes the convolution operator.

Simulation Results and Discussions

In this section, we present BER simulation results for various percentage of cutoff frequency (%Wn) on infinite impulse response(IIR) low pass filter, and investigate the BER performance in PRML detector and NPML detector at DC-Attenuation target (5 6 0 -1). In the simulations, the received sequence S_k is equalized by 21-tap finite impulse response(FIR) filter calculated to minimize the mean-square error (MMSE) of the equalizer output and target response such that y_k resembles d_k. We process each sector consisting of 4096 information bits and let the parameter of normalized recording density (ND) = 2.5, media jitter noise(J2) = 10%. and noise predictive filter (NP_Tap) = 4 tap. The average BER from the results are plotted versus the SNR(dB). The percentages of cutoff frequency that deviates from the nominal value 1/2T may be positive or negative. For example, with +/-10% deviation, Wn = 110 and Wn = 90, respectively , with +20%

deviation, Wn = 120, and with -30% deviation, Wn = 70. In Figure 2, the NPML detector at different percentages cutoff frequency versus the system performance is shown. We can see that the performance degrades as %Wn changes, for example at BER = 2×10^{-4} with Wn = 70, there is an error loss of 1.2 dB compared with the case when the cutoff frequency is at 1/2T (Wn = 100).

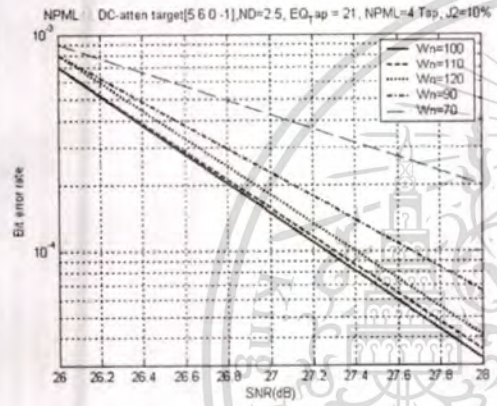

Figure 2. NPML performance of percentages cutoff frequency various base on DC-attenuation target(5 6 0 -1)

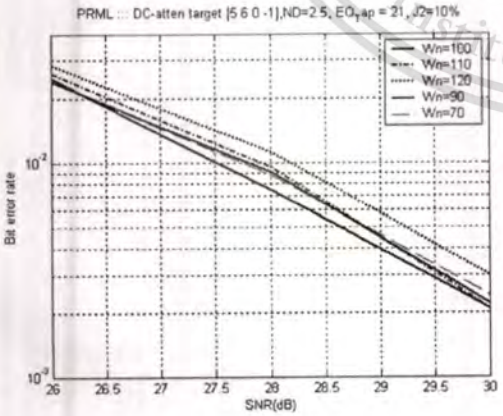

Figure 3. PRML performance of percentages cutoff frequency various base on DC-attenuation target(5 6 0 -1)

In Figure 3 the BER performance of PRML detector system affected by %Wn is shown. The performance degrades more with positive deviation from nominal cut frequency compared with the negative one. For example, at BER = 3×10^{-3} with Wn = 120, there is an error loss of 0.6 dB compared with the nominal cutoff frequency.

Conclusions

We have investigated the effect of cutoff frequency percentage various of LPF in perpendicular magnetic recording channel model in terms of the BER performance of PRML and NPML detector for DC-attenuation PR target. From the simulation results, the NPML performance is affected by the negative deviation of cutoff frequency more than the positive one. On the contrary, the PRML performance is affected by the positive deviation of cutoff frequency more than the negative one.

References

Kovintavewat, P., Ozgunes, I., Kurtas, E., Barry, J. R and McLaughlin, S. W. 2002. "Generalized Partial Response Target for Perpendicular Recording with Jitter Noise", *IEEE Trans. on Magnetics*, Vol. 38, Issue 5, Sep. pp. 2340-2342.

Lee, J. and Lee, J. 2005. "A Simplified Noise-Predictive Partial Response Maximum Likelihood Detection Using M-Algorithm for Perpendicular Recording Channel", *IEEE Trans. on Magnetics*, Vol. 41, Issue 2, Feb. pp. 1064-1066.

Madden, M., Oberg, M., Wu, Z. and He, R. 2004. "Read Channel for Perpendicular Magnetic Recording", *IEEE Trans. on Magnetics*, Vol. 40, No. 1, Jan., pp. 241-246.